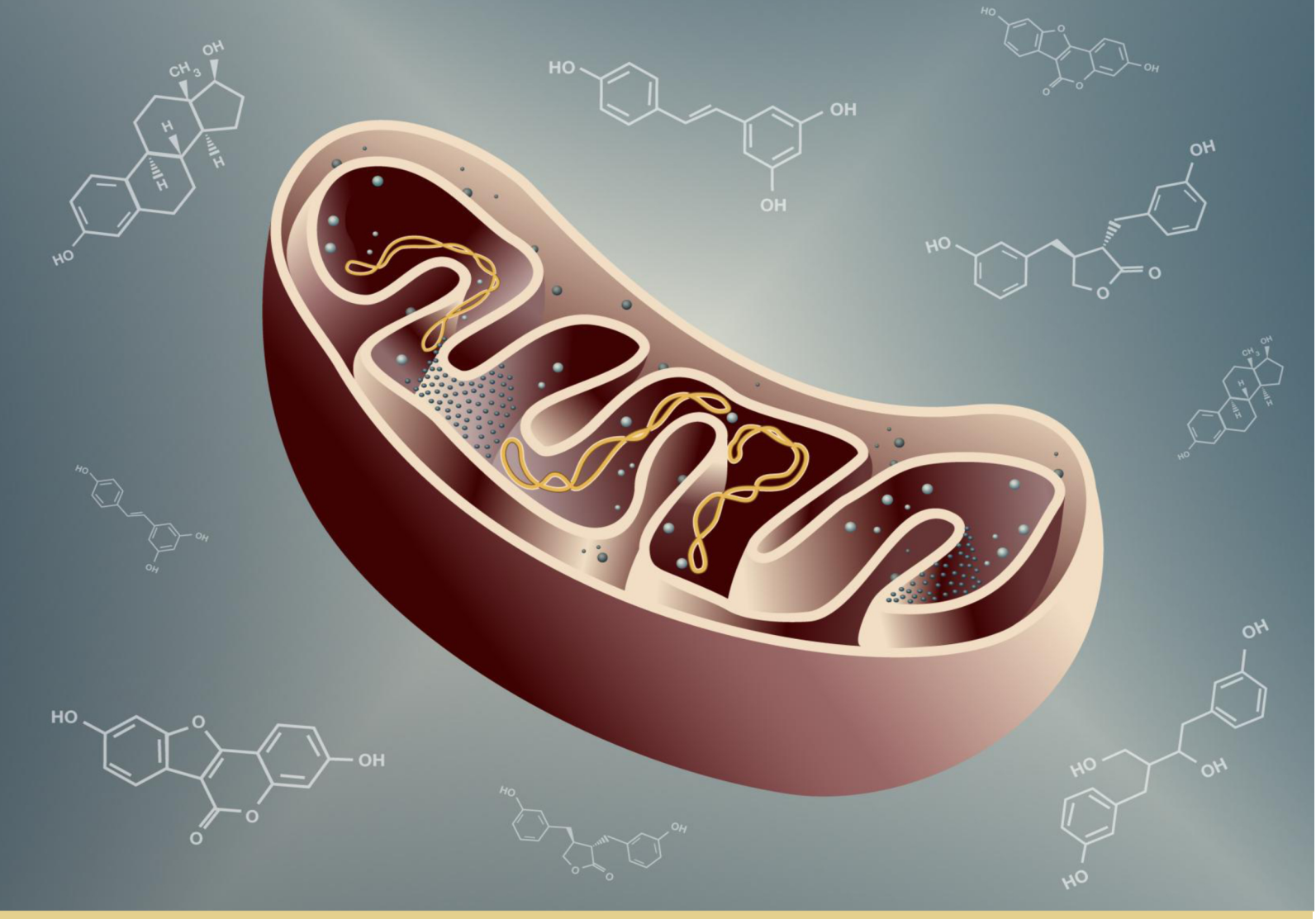

Ana Carolina dos Santos Moreira

PHYTOESTROGENS AS ALTERNATIVE TO THE HORMONE REPLACEMENT THERAPY: MITOCHONDRIAL AND CELLULAR INTERACTIONS

Tese de Doutoramento na área científica de Biociências, especialidade Toxicologia, orientada pela Doutora Maria Sancha Santos e pela Doutora Vilma Sardão Oliveira e apresentada ao Departamento de Ciências da Vida da Faculdade de Ciências e Tecnologia da Universidade de Coimbra.

Setembro de 2013

· U C ·

Universidade de Coimbra

Phytoestrogens as Alternative to the Hormone Replacement Therapy: Mitochondrial and Cellular Interactions

Ana C. Moreira, BSc, MSc

Tese apresentada à Faculdade de Ciências e Tecnologia da Universidade de Coimbra com vista à obtenção do grau de Doutor em Biociências, especialidade em Toxicologia.

Thesis presented to the Faculty of Sciences and Technology of the University of Coimbra as requirement for the PhD degree in Biosciences, specialty of Toxicology.

Coimbra, September 2013

Cover Illustration Credit: Marta Vargas
imartavargas@gmail.com
www.martavargas.com

This work was conducted at Center for Neuroscience and Cell Biology, Department of Life Sciences, University of Coimbra, Portugal, under the supervision of Doctor Maria Sancha Santos and Doctor Vilma Sardão Oliveira, at the Department of Anatomy, Microbiology and Pathology, University of Minnesota, Medical School, Duluth, MN, USA, under the supervision of Doctor Jon Holy and Doctor Vilma Sardão Oliveira and at the College of Pharmacy, University of Minnesota, Duluth, MN, USA, under the supervision of Doctor Bjoern Bauer and Doctor Anika Hartz.

The work presented in this dissertation was supported by a PhD fellowship from the Portuguese Foundation for Science and Technology (FCT) to the author (SFRH/BD/33892/2009), by a research grant to Doctor Maria Sancha Santos (PTDC/AGR-ALI/108326/2008), by the institutional grant PEst-C/SAU/LA0001/2013-2014 to the CNC and by the University of Minnesota, College of Pharmacy startup funding to Doctors Bjoern Bauer and Anika Hartz.

Agradecimentos/Acknowlegdments

Um trabalho de Doutoramento nunca é um trabalho solitário e, por isso, chega o momento de agradecer às pessoas e instituições que permitiram a realização desta tese.

À Fundação para a Ciência e Tecnologia, instituição com a qual tantas vezes reclamamos, mas que no fundo é aquela de que todos dependemos, agradeço o financiamento do projecto PTDC/AGR-ALI/108326/2008 que permitiu desenvolver as minhas experiências e a bolsa SFRH/BD/33892/2009 que me permitiu fazer o que mais gosto durante 4 anos. Ao BEB, Programa Doutoral em Biologia Experimental e Biomedicina do Centro de Neurosciências e Biologia Celular (CNC), pela escolha, pelo suporte, pelos grandes momentos de aprendizagem e discussão científica. Agradeço ao Departamento de Ciências da Vida da Universidade de Coimbra e ao CNC as condições necessárias à realização do meu trabalho.

Às minhas orientadoras, pelo papel importante que tiveram na condução do meu doutoramento e pela sua dedicação ao meu trabalho:

À Doutora Maria Sancha Santos, agradeço a presença, o optimismo, a segurança, mas sobretudo a confiança prestada a cada dia, os ensinamentos das mais variadas técnicas, a constante ajuda e as longas horas em que me acompanhou no laboratório. Agradeço as boas discussões em que pude crescer. A minha gratidão é enorme.

À Doutora Vilma Sardão Oliveira, agradeço o estímulo e a liberdade cedida para o desenvolvimento das minhas experiências, assim como a exigência e o querer que, em cada dia, eu fosse melhor que no anterior. Agradeço o tempo e a persistência para que eu evoluísse a cada passo deste doutoramento. Obrigada pelo desafio e novas metas em vários momentos deste trajecto. Muito obrigada!

Ao Doutor Paulo Jorge Oliveira, apesar de nunca ter sido oficialmente sua aluna, foi sempre extremamente dedicado ao meu trabalho. Ao Doutor Paulo, agradeço ter deixado a porta aberta do seu laboratório, me ter recebido e me ter proporcionado tanto como aos seus alunos, quer nas actividades no nosso laboratório, quer fora deste, assim como me permitiu trabalhar nas suas colaborações. Agradeço, muito em especial, o seu tempo ao meu doutoramento, quer no dissipar de muitas dúvidas, quer na correcção desta tese. Muito obrigada!

I am thankful to Dr. Jon Holy for accepting me so nicely in his lab in 2010.

To Doctors Anika Hartz and Bjoern Bauer, for the time, guidance and dedication to my PhD Project, as also for the exceptional discussions and shared knowledge that made my time in Dultuh an exceptional experience. Thank you very much for the amazing months spent in your laboratory. I extend my acknowledgments to Emma, Britt and Kevin, for the amazing time spent with you, for all the help and friendship. I special thanks to Andrea, for the

interrupted help, for the activities we made together, for your time, for the smiles and the hugs, for making me feel home, while we were both abroad.

À Ana Maria Silva, pela dedicação inesgotável. A Ana foi a pessoa com quem mais discuti o meu trabalho, a quem mais expus as minhas dúvidas, a quem desabafei as minhas frustrações. Muito obrigada por tudo em todas as horas. O que sinto pela Ana enquanto pessoa e cientista, é profunda admiração. A ti, Anokas, do fundo do meu coração, o meu Muito Obrigado.

A Ana Branco, por me ter ensinado tanto e com tanta clareza. Agradeço a sinceridade, a liberdade de me deixar errar quando cheguei ao laboratório, agradeço as ajudas sempre que precisei. Agradeço-te os momentos de discussão, em que entrámos dentro de células e pensámos como fôssemos um dos mecanismos. Agradeço-te, sobretudo, a amizade que comigo construíste.

Ao Gonçalo Pereira, agradeço os conselhos informáticos e os ensinamentos estatísticos. Obrigado pelas horas de partilha de saber.

À Cátia Diogo, pelas boas sobremesas que tanto alegraram as nossas tardes e, sobretudo, pela ajuda sempre que pedida.

Agradeço os meus colegas do grupo de Toxicologia Mitocondrial e Doença por me terem proporcionado realizar o meu trabalho em bom ambiente. Agradeço em especial aos que se tornaram amigos ao longo dos últimos anos:

Ao João Monteiro, por fazer da melhor ciência, por me ensinar muito e me dar sempre bons conselhos.

Ao Sandro Pereira, pelo carinho e atenção com que sempre me tratou.

À Filipa Carvalho que com a sua calma e frieza, fez sempre um esforço enorme para que fosse pragmática e objectiva. Agradeço os momentos de amizade, os longos jantares, as boas conversas, as constantes surpresas boas e a ajuda crucial nas figuras.

À Telma Bernardo, pela companhia a bordo do intercidades, pelo carinho e preocupação comigo em cada momento. Pelos longos telefonemas e o recorrente: “Então, como estamos?”.

À Rute Loureiro, pela maneira de ser, pela verdade em cada expressão, pela dedicação à ciência, pelos bons momentos, longas conversas, e desabafos mútuos em que podemos solidificar a nossa amizade.

À Inês Barbosa, porque apesar de nos conhecermos desde os 12 anos, ter comigo construído uma amizade em Duluth. Nunca me esquecerei das vezes, em que com graus negativos (e neve, muiiiiitttaaa neve) na rua, foste a casa cozinhar para mim, e voltaste para jantarmos juntas. Foi preciso nos encontrarmos num lugar distante e isolado para vivermos momentos tão marcantes que nos tornaram amigas.

À Susana Pereira, pelo companheirismo e optimismo especialmente ao longo dos últimos três anos. Pela partilha de momentos marcantes e pela viagem a Chicago.

Ao Filipe Duarte, pelas boas conversas nos corredores da Zoologia, pela amizade e pela cordialidade.

Ao Ludgero Tavares, pelas risadas à segunda-feira no balanço do fim de semana desportivo. Agora a sério, apesar de nunca ter trabalhado directamente contigo, reconheço-te um enorme sentido de grupo, luta pela justiça e igualdade entre todos.

Ao Professor António Moreno, para mim personifica os conceitos: sabedoria e generosidade. É raro encontrar alguém, extremamente ocupado, com tanta disponibilidade e gosto em transmitir conhecimentos. Cada minuto de conversa ou discussão consigo foi um minuto de aprendizagem intensa.

À Doutora Paula Moreira, pelo seu contributo e presença sempre que lhe pedi ajuda. Pela disponibilidade e partilha de saber. Estendo os agradecimentos ao seu grupo pela ajuda sempre que solicitada e pelos ensinamentos, em especial ao Renato e Cristina. Um agradecimento dedicado à Sónia Correia, cujo convívio no laboratório e boa disposição (a alegria constante), entre outros, fizeram com que nos tornássemos amigas pessoais.

À Doutora Raquel Seiça e ao Doutor Romeu Videira, pelas boas discussões ao longo do trabalho.

Aos funcionários do Departamento de Ciências da Vida, em especial à D. Paula, pela simplicidade, bom humor e dedicação que atendeu sempre aos meus pedidos de última hora e cujo trabalho, tantos dias, facilitou o meu.

À Professora Isabel Paiva, por me motivar para a Ciência em cada uma das suas aulas, por ser Professora a tempo inteiro. Alargo este agradecimento ao David e à Cláudia que acompanham a minha vida desde esse tempo.

To Marian that was much more than my landlady, she is a friend and her place was home during my stays abroad, thank you for the delicious dinners and intense conversations. I am glad I met you!

Aos meus amigos, que felizmente são muitos e bons, por estarem presentes. Em especial, ao João Costa, à Marisa Baptista, Sara Lemos, Vera Francisco, Cláudio Roque e Paula Banca que partilham comigo o gosto pela ciência, a ânsia por querer saber mais e as frustrações dos dias menos fáceis. É bom ter-vos por perto.

À minha madrinha Prazeres Henriques e à minha amiga Paula Oliveira, que me conhecem desde o dia 19 de Junho de 1985 e sempre acompanharam o meu crescimento, participaram na minha educação, mas mais que isso, e mais importantemente, nos últimos anos têm sido uma rede de suporte sem falhas, o que me permitiu estar mais segura e estar ausente na certeza que as minhas pessoas não ficariam sós. Muito Obrigado.

Ao Pedro, por ter estado presente nestes últimos anos, pela calma, pela paciência, pelo carinho com que sempre me tratou. Muito obrigado por me mostrares (tantas vezes) que posso contar contigo.

Ao Marco, pela presença, por me dizer o que pensa sem filtros, por me fazer crescer, por me desafiar, pela enorme ajuda sempre que pedi, e mesmo, quando não pedi.

Ao Raúl, que é dos meus amigos mais recentes e dos que vive mais longe, mas nem por isso está distante ou ausente. Obrigado por teres dado sempre tudo, sem pedir nada em troca. Obrigado por estares sempre connosco. Estendo os agradecimentos à família que é minha também, mas noutro lugar.

À Mary e ao Bruno, por serem amigos excelentes, amigos de tanta partilha e de tão boas conversas, por tudo o que temos em comum e o que não temos, que cada vez mais sustenta a nossa amizade. Por serem genuínos e por estarem sempre por perto.

À Marianinha por estar sempre comigo, por me entender, por me ouvir e por me compreender, por toda a força e todo o carinho, mesmo quando os dias não são fáceis. Ter-te sempre a meu lado, dá-me confiança e uma alegria que me comove.

À Tânia por ser assim: por me mostrar que os dias têm tanto tempo quanto o que lhe quisermos dar, por me mostrar que não importam distâncias, nem diferenças horárias, nós somos amigas em cada instante. Obrigada amiga por trazeres muita cor à minha vida e só bons momentos. Ter-te por perto, é das minhas maiores sortes.

Ao Paulo e Rita Oliveira, que são os meus amigos de sempre, desde o meu dia zero, não me lembro de um único momento importante em toda a minha vida, que não tenham estado presentes. Obrigada por estarem sempre por perto.

Aos meus amigos de palmo e meio que na sua presença, nos seus sorrisos, berros e babas, tornam este caminho mais fácil de percorrer: Lucas, Martim, Maria Rita, Maria Pêpê e o mais pequenino David.

À minha família, toda sem excepção, são eles o *state of art* da Ana Carolina e são eles que fazem o que eu sou hoje, em especial ao meu Tio Quim, pela serenidade, por ser um agente unificador, pelo orgulho que tem em mim e por ser o elemento da nossa família que mais motiva para o conhecimento.

MUITO em especial, às minhas pessoas que são um quarteto fantástico:

Ao meu pai, força de trabalho, por me mostrar que nenhum motivo, nem ninguém nos pode magoar, enquanto a nossa dignidade e vontade de fazer mais e melhor, se mantiverem. O meu pai pode não entender o que é isto de um doutoramento, mas sem os seus impulsos, eu nunca teria chegado aqui.

À minha mãe, por me ter motivado sempre para eu fazer o que queria, mesmo quando os caminhos eram difíceis de percorrer. Por ser um exemplo de trabalho e sobretudo de

integridade, por nunca baixar os braços e nunca me deixar baixar os meus. Por ser uma pessoa maravilhosa, por querer sempre que eu viva mais e melhor, por me incentivar, por ser a melhor pessoa que eu conheço.

Ao meu irmão, melhor presente que eu tive na vida. Nada, nem ninguém consegue entender esta relação se não tiver um João, como eu tenho este. É das pessoas mais diferentes de mim, mas que melhor me consegue mostrar o caminho a seguir. O passado que (só nós) partilhamos é o principal suporte de cada nova etapa.

Ao Vítor, meu colega de escola, meu amigo, meu melhor amigo, meu namorado, e hoje, meu marido. Tanto se tem passado ao longo destes 13 anos e tu foste/és o pilar mais sólido e o porto mais seguro. Sem a tua paciência, paz e tranquilidade tudo seria mais difícil. Obrigada por teres feito de cada chegada a casa, o grande momento do meu dia e dos meus longos silêncios, momentos de compreensão. Obrigada por seres a minha casa.

Por decisão do autor as secções escritas em Português nesta tese, não seguem a ortografia do Acordo do Segundo Protocolo Modificativo do Acordo Ortográfico da Língua Portuguesa, aprovado pela Resolução da Assembleia da Republica, nº 35/2008 e ratificado pelo Decreto do Presidente da República nº 52/2008, de 29 de Julho de 2008.

À minha mãe, por tudo

“It always seems impossible until it's done.”

Nelson Mandela

Published work

Part of the work presented in this thesis is already published or submitted to international peer-reviewed scientific journals or published as book chapter, as follows:

Ana C. Moreira, Ana M. Silva, Maria S. Santos, Vilma A. Sardão (**2013**), *Phytoestrogens as Alternative Hormone Replacement Therapy in Menopause: what is Real, what is Unknown*, Submitted.

Ana C. Moreira, Ana M. Silva, Maria S. Santos, Vilma A. Sardão, **(2013)** *Resveratrol Affects Differently Rat Liver and Brain Mitochondrial Bioenergetics and Oxidative Stress in vitro: Investigation of the Role of Gender*, Food and Chemical Toxicology, 53, 18-26.

Ana C. Moreira, Nuno G. Machado, Telma S. Bernardo, Vilma A. *Sardão,* Paulo J. Oliveira (**2011**) *Mitochondria as a biosensor for drug-induced toxicity – is it relevant?*, ISBN 978-953-307-443-6.

Table of Contents

List of figures

List of Tables

Abbreviations used

Δψ – Mitochondrial transmembrane electric potential

ADP – Adenosine diphosphate

AF-2 – Activation function 2

AIF – Apoptosis-inducing factor

AMP – Adenosine monophosphate

ANT – Adenosine nucleotide translocator

ATP – Adenosine triphosphate

ATPase – ATP synthase

Aβ – Amyloid beta

Ca^{2+} – Calcium ions

CAT – Catalase

CK – Creatine kinase

CNS – Central nervous system

CoA – Coenzyme A

Coum – Coumestrol

COX – Cytochrome c oxidase

COX2 – Cyclooxygenase-2

Cyp D – Cyclophilin D

Cu^{2+} – Copper

DPN – Diarylpropionitrile

ER – Estrogen Receptor

ETC – Electron transport chain

EtOH – Ethanol

FADD – Fas-associated protein with death domain

FCCP – Trifluorocarbonylcyanide phenylhydrazone

FELASA – Federation for Laboratory Animal Science Associations

FSH – Follicle-stimulating hormone

GPR – G protein-coupled receptor

GLUT-1 – Glucose transporter-1

GOT – Glutamic-oxaloacetic transaminase

GPT – Glutamate pyruvate transaminase

GPx – Glutathione peroxidase

GSH – Reduced gluthathione

H_2O_2 – Hydrogen peroxide

HRT – Hormone replacement therapy

Hsp 90 – Heat shock protein 90

IL1β – Interleukin 1 beta

IMM - Inner mitochondrial membrane

KO – Knockout

LH – Luteinizing hormone

MAPK – Mitogen-activated protein kinase

MDA – Malondialdehyde

Mn^{2+} – Manganese

MPTP – Mitochondrial permeability transition pore

mRNA – Messenger RNA

mtDNA – Mitochondrial DNA

NO – Nitric oxide

NRF-1 – Nuclear respiratory factor 1

$O_2^{\bullet -}$ – Superoxide anion

$^{\bullet}ONOO^-$ – Peroxynitrite

OVX – Ovariectomy/Ovariectomized

OXPHOS – Oxidative phosphorylation

P4 – Progesterone

PDH – Pyruvate dehydrogenase

PE – Phytoestrogens

PGC – Peroxisome proliferator-activated receptor gamma coactivator

PI3K – Phosphoinositol 3- kinase

PT – Permeability transition

PPT – Propyl pyrazole triol

RAM – Rapid uptake mode

RCR – Respiratory control ratio

Resv – Resveratrol

RNS – Reactive nitrogen species

ROS – Reactive oxygen species

ROT – Rotenone

SMAC/Diablo – Second mitochondria-derived activator of caspases

SOD – Superoxide dismutase

TFAM – Mitochondrial transcription factor A

TNFα – Tumor necrosis factor alpha

VCD – 4-vinylcyclohexene diepoxide

VDAC – Voltage-dependent anion channel

Vit E – Vitamin E

Zn^{2+} – Zinc

Abstract

The symptoms associated with menopause, which result from hormonal changes observed during this period, are most of the times disquieting for women. These hormonal variations lead to an increased incidence of different medical conditions such as hot flashes, cardiovascular diseases and osteoporosis, among others. Hormone replacement therapy (HRT), based in 17β-estradiol (E2), is conventionally administered to menopausal women in order to overcome the symptoms associated with menopause. However, HRT has some side effects, such as increased risk of breast cancer. Phytoestrogens (PE), plant-derived compounds that structurally mimic E2, have been suggested as alternatives to HRT. Due to their molecular resemblance with E2, PE can have estrogenic and/or antiestrogenic activity. Nevertheless, the risk and benefits of PE in women's health are not yet well established. The main purpose of this project was to identify PE with low toxicity but able to attenuate some symptoms associtated to menopause, with a special focus on hot flashes.

An initial screening of all selected PE (enterolactone, enterodiol, resveratrol and coumestrol) was performed by using isolated mitochondrial fractions from brain and liver and cells in culture. We observed that coumestrol and resveratrol reduced mitochondrial lipid peroxidation and that the latter decreased ATP synthase activity and competitively inhibited complex I of the mitochondrial respiratory chain. The antioxidant effects of coumestrol were also observed on the HepG2 cell line, reducing mitochondrial superoxide anion generation in the presence of the complex I inhibitor rotenone.

Following the "impaired glucose delivery" hypothesis for hot flashes, we then investigated the role of E2 and PE in GLUT-1 expression at the blood-brain barrier (BBB). The GLUT-1 content increased in brain microvessels after six hours of incubation with E2. We observed that this modulation of GLUT-1 expression occurred through ERα signaling. From the PEs tested, only coumestrol increased GLUT-1 expression similarily to E2.

We then evaluated the effects of coumestrol *in vivo* by using two menopausal rodent models: ovariectomy and 4-Vinylcyclohexene diepoxide (VCD) treatment. Our data showed that coumestrol, as E2, increased mitochondrial function by increasing complex I activity, state 3 and respiratory control ratio (RCR) in brain. Furthermore, coumestrol administration in ovariectomized (OVX) rats reduced oxidative stress and temperature variations in OVX rats measured in a 6 hours span, an approach to indirectly evaluate hot flashes.

In conclusion, the results obtained from this thesis showed that although some of the PE had benefits in menopausal models, they also showed mitochondrial toxicity, while others had no effects for the parameters analyzed. On the other hand, coumestrol demonstrated the lowest toxicity *in vitro* and *in vivo*, especially regarding mitochondrial function. Also, coumestrol modulated GLUT-1 expression similarly to E2 and decreased the temperature variation in

ovariectomized rats.

The data highlight the need to identify PE-mediated toxicity in several target organs, namely regarding mitochondrial alterations. This should be important when proposing a widespread use of PEs in HRT.

Key Words: Phytoestrogens, Menopause, Mitochondria, Blood-Brain Barrier, Toxicology

Resumo

Os sintomas associados à menopausa são na maioria dos casos desconfortáveis para as mulheres. As alterações hormonais observadas neste período podem aumentar a incidência de condições patológicas tais como doenças cardiovasculares, osteoporose, afrontamentos, entre outros. A terapia de substituição hormonal (TSH), baseada em 17β-estradiol (E2), é normalmente administrada às mulheres na menopausa para ultrapassar os sintomas associados a este período. Contudo, a TSH tem alguns efeitos secundários, nomeadamente o risco aumentado de cancro da mama. Fitoestrogénios (FE), compostos naturais que são estruturalmente semelhantes a E2, têm sido sugeridos como alternativa à TSH. Devido à sua semelhança com E2, os FE podem ter actividade estrogénica ou anti-estrogénica. Não obstante, os riscos e benefícios dos FE na saúde da mulher não estão ainda bem estabelecidos. O principal objectivo deste projecto foi identificar FE com baixa toxicidade mas, simultaneamente, capaz (es) de atenuar alguns sintomas conhecidos da menopausa, com especial ênfase para os afrontamentos.

Um *screening* inicial foi efectuado com os FE seleccionados (enterolactona, enterodiol, resveratrol e coumestrol) usando fracções mitocondriais de cérebro e fígado, assim como células em cultura. Observámos que o coumestrol e o resveratrol reduziram a peroxidação lipídica mitocondrial. Adicionalmente, verificou-se que o resveratrol diminuiu a actividade da ATP sintase e inibiu competitivamente o complexo I da cadeia respiratória mitocondrial. Os efeitos antioxidantes do coumestrol foram também verificados na linha celular HepG2, reduzindo a geração do anião superóxido mitocondrial na presença de rotenona, um inibidor do complexo I.

Tendo por base a hipótese de “transporte deficiente de glucose”, que pretende explicar os mecanismos moleculares dos afrontamentos, investigámos em seguida a função do E2 e dos FE na expressão de GLUT-1 na barreira hematoencefálica (BHC). Com efeito, foi possível verificar que o conteúdo em GLUT-1 aumentou nos capilares do cérebro seis horas após a incubação com E2. Nós verificámos que esta modulação da expressão de GLUT-1 ocorre a via sinalização ao nível do receptor de estrogénio alfa. Dos FE testados, apenas o coumestrol aumentou a expressão de GLUT-1 de maneira semelhante a E2.

Seguidamente, avaliámos os efeitos do coumestrol *in vivo*, através do recurso a dois modelos de rato para a menopausa: a ovariectomia e o tratamento com diepóxido 4-Vinilciclohexeno. Os nossos resultados mostraram que, tanto o coumestrol como o E2, melhoram a função mitocondrial, aumentando a actividade do complexo I, a respiração ao nível do estado 3 e o índice de controlo respiratório no cérebro. Além disso, a administração de coumestrol em ratos fêmea ovariectomizados reduziu o stress oxidativo e as variações de temperatura medidas durante 6h, sendo este último um processo de avaliação de

afrontamentos.

Em conclusão, os resultados obtidos nesta tese mostram que, apesar de alguns FE terem apresentado benefícios em vários indicadores relacionados com a menopausa, mostraram também toxicidade mitocondrial, enquanto outros dos FE testados não mostraram qualquer efeito nos parâmetros analisados. Por outro lado, o coumestrol demonstrou possuir a menor toxicidade *in vitro* e *in vivo*, com especial enfoque para a função mitochondrial. O coumestrol modulou a expressão de GLUT-1 de forma similar ao E2, reduzindo a variação de temperatura em ratos fêmea ovariectomizados.

Os resultados destacam a necessidade de identificar a toxicidade mediada por FE em diferentes órgãos alvo, nomeadamente ao nível da mitocondria. Neste âmbito, o estudo toxicológico é importante quando se propõe o uso indiscriminado de FE na TSH.

Palavras-Chave: Fitoestrogénios, Menopausa, Mitocôndria, Barreira Hematoencefálica, Toxicologia

Por decisão do autor o resumo desta tese, não segue a ortografia do Acordo do Segundo Protocolo Modificativo do Acordo Ortográfico da Língua Portuguesa, aprovado pela Resolução da Assembleia da Republica, nº 35/2008 e ratificado pelo Decreto do Presidente da República nº 52/2008, de 29 de Julho de 2008.

1. General Introduction

The women's reproductive stage is tightly controlled by autocrine, paracrine and endocrine factors, which regulate female development, especially the maturation of the ovarian follicle, ovulation, luteinisation and endometrium remodelling. Healthy women are expected to spend in average 36 years in a reproductive life span. However, with the increase of life expectancy, women spend one-third of their lifetime under menopause, which represents an infertile stage in their lives. The hormonal alterations that occur during menopause, such as the decrease in 17β-estradiol (E2) and the increase in follicle-stimulating hormone (FSH), trigger several alterations in the body, illustrated by the increased risk for the development of several pathologies.

Although being a natural process, the transition to menopause is a challenge for the majority of the women and an estradiol/progesterone (P4)-based therapy (hormone replacement therapy, HRT) is normally used to overcome or to avoid physiological alterations associated with menopause. However, several problems are associated with HRT, justifying the need for possible therapeutic replacement. In this scenario, phytoestrogens (PEs) gain great importance due to their chemical resemblance to E2. Even though, their use is not free of debate. This is a clearly relevant topic in medicinal research since the use of these compounds is increasing.

1.1 The role of estrogens during a woman's life span

Estrogens are a class of steroid hormones, which generate and regulate the oestrous and menstrual cycle. Estrogens are mainly produced in the theca interna cells of ovaries resulting from the conversion of cholesterol to androstenedione or testosterone, being subsequently aromatized to estrone and estradiol in granulosa cells [1] (Fig.1). Estrogens can also be produced in the corpus luteum and placenta [2] or in non-traditional sources including adrenal glands, adipose tissue, brain and breast [3]. Estrogens promote the development and maintenance of the female reproductive system and of the secondary sexual characteristics. The latter include breast development, typical female body proportions, distribution of subcutaneous adipose tissue and the characteristic estrogen-dependent alterations in the female genital tract [4].

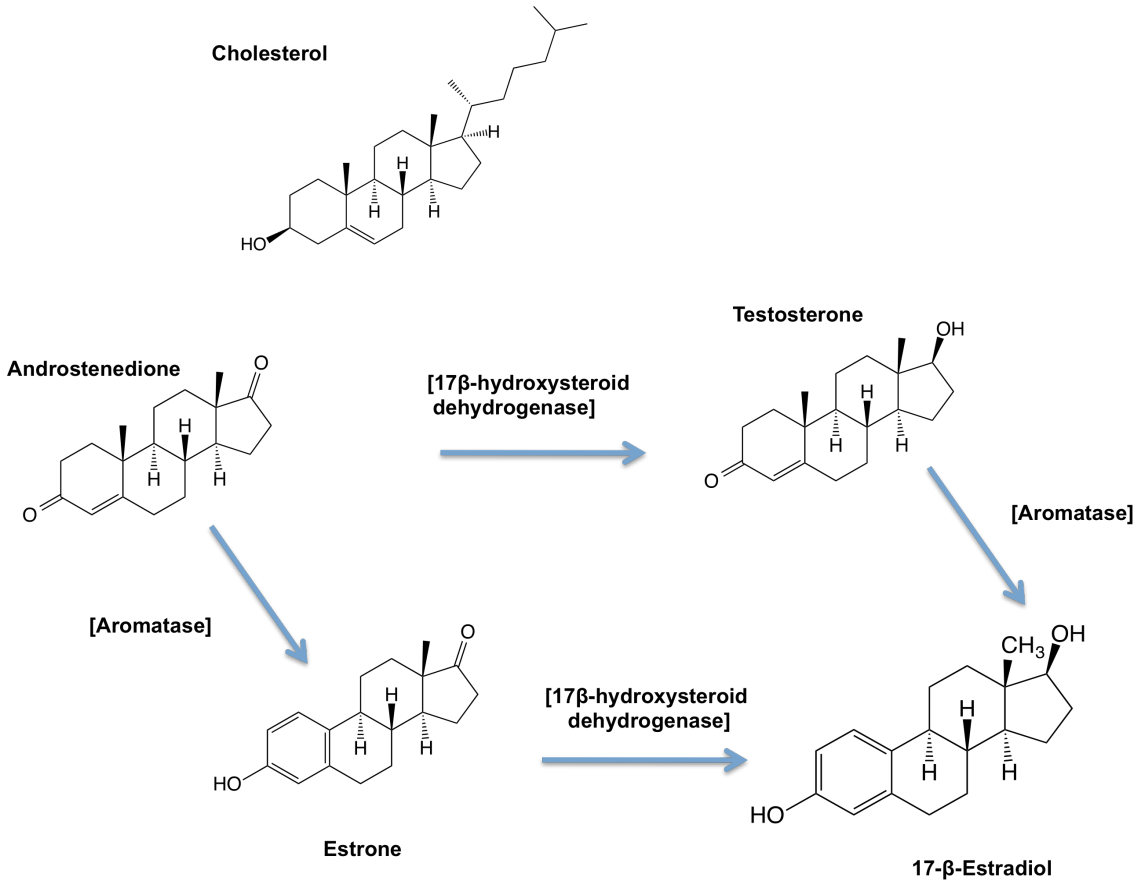

Figure 1: Estradiol production in the ovary.
Although sources of E2 include fat, adrenal glands, and breast, ovaries are the main source of this hormone for women. Estradiol is produced in the granulosa cells through the aromatization of androstenedione that is produced in theca cells from cholesterol. The figure also shows the enzymes that partipate in the process (in square brackets).

Estradiol is the main estrogen in the human body and is primarily produced in the ovarian follicle, sustaining a production of E2 as high as 700 µg daily, depending on the phase of the menstrual cycle [5, 6]. The intracellular effects of estrogens are mainly mediated by estrogen receptors (ER) that regulate the transcription of target genes through binding to specific DNA target sequences called ER-responsive elements [7]. Estrogen receptors play both genomic and non-genomic functions [8], with the magnitude and tissue-specific effects being mediated by two distinct ER subtypes: α and β, as well as by multiple co-regulators.

The activities of an extensive number of ER-interacting proteins converge to grant several functionalities to ERs, including the activation and repression of transcription, the integration of intracellular signalling pathways and the control of cell cycle [8]. Both ERs subtypes are widely expressed in both genders, with ERα being predominant in the mammary gland and in the uterus and ERβ having an augmented role in the central nervous system, heart, immune system, urogenital tract, bones, kidneys and lungs. At the sub-cellular level, both ERα and β are present in the cytoplasm and nucleus, with 2% of the ER pool being associated with the cellular membrane [9]. E2 induces the transcription of its own receptors and stimulates the

biosynthesis of progesterone receptors, which are required for progesterone effects. In opposition, progesterone and progestin, a synthetic compound with similar functions as progesterone, inhibit the transcription of ER when bound to the respective receptors, inducing an anti-estrogenic effect [10, 11].

The genomic activity of estrogens is mediated by the ERs, while their non-genomic activity is mediated only by ERs present in the plasma membrane. After the activation by E2 or estrogen-like compounds, ERs form ERα/ERβ homodimers or heterodimers and bind with high affinity to estrogen response elements in promoters, introns, or 3' untranslated regions of target genes. A G protein-coupled receptor (GPR), GPR30, has been proposed to mediate ER-α and ERβ-independent signalling pathways induced by E2 [12, 13], responding to E2 in the plasma membrane or in the endoplasmastic reticulum [14]. Also, E2 interacts with G-proteins, the p85 subunit of phophoinositol-3-kinase (PI3K), with the tyrosine-protein kinase Src and caveolin-1, contributing to regulate PI3K/AKT and MAP kinases [15]. The amplitude of the estrogen actions is vast and committed with several cellular functions, thus the menopausal-related decrease of estrogens is a challenge at the cellular, tissue and whole body level.

1.2 Menopause

The symptoms associated with menopause are mostly uncomfortable for women and affect their emotional and social lives. Most of the symptoms originate from hormonal changes resulting from the decline in estrogens [16]. The menopausal transition is initiated by fluctuations in the menstrual cycle, comprising a rise in FSH following a decrease in both estrogen and progesterone. The final menstrual period, medically confirmed after twelve months of amenorrhea [17, 18], sets the initial stages of menopause. The transition to menopause is a complex but physiological process usually synergizing with the effects of aging and other social adjustments, all contributing to a decrease in life quality [17].

On average, menopause occurs when women are about 51.4 years old [19]. Women that smoke may have an accelerated ovarian aging which can anticipate the menopausal transition by two years [20]; this may be also observed in women with low social and economic status [21] resulting in lower life quality. Other conditions may affect the age at which women have their final menstrual period: the age of menarche, ethnic origin, body mass index and family health history [22]. Menopause can also be induced by chemotherapy [23] and radiation [24], which increase follicular atresia and apoptosis or result from surgery, through the mechanical removal of ovaries, the main estradiol source [25].

Circulating hormones during the menopausal transition were initially thought to decrease in a linear fashion, but in fact, circulating FSH concentrations increase progressively during the

menopausal transition [26]. This does not occur due to decreased estradiol production, which usually occurs during late menopausal transition [27], but instead due to decreased ovarian inhibin secretion [28]. Inhibin and activin, produced by the granulosa cells in the antral and dominant follicles, are proteins that have a role in the menopausal transition [28, 29]. Inhibin A increases during the luteal phase while inhibin B increases during the follicular phase, with both events inhibiting pituitary FSH secretion. In opposition, activins are a class of proteins that stimulate pituitary FSH release [30]. By the late reproductive stage, inhibin B decreases while FSH increases.

During the menopause transition, inhibin A concentrations decline, while increasing in perimenopausal women. This hormone variation may promote an increase of FSH secretion and a simultaneous decrease in estradiol production. Similarly to estradiol and FSH, activin and inhibin regulate the menstrual cycle and the menopausal transition [28] (Table 1).

Table 1: Women's reproductive life span

	Menarche	Reproductive Age	Perimenopause	Posmenopause
Hormones	Normal FSH, E2 activins and inhibins	Normal FSH, E2, activins and inhibins	Increasing FSH and activin A and decreasing E2 and inhibin B	Increasing FSH Low E2
Age	9-15 years	16-40 years	41- late 50's	60's and further
Reproductive stage	Low	High	Low	Absent
Menstrual cycle	Irregular to regular	Regular	Irregular	Absent

Time frame representative of Women's reproductive life span, beginning with menarche and ending with menopausal transition. The table shows the influence of endocrine hormones on the menstrual cycle (adapted from [16, 17, 31])

Although the main characteristics of menopause are related with the hormonal changes occurring in women, a single hormone end-point measurement is not useful for predicting the menopausal phase due to the large hormone fluctuation during this period [30]. Thus, the symptoms that appear during this period are an important tool in the characterization of the menopausal transition.

1.2.1 Menopausal symptoms

Body weight gain, fatigue and hot flashes are some of the symptoms that appear during the menopausal transition [17]. Hot flashes, a vasomotor symptom, are manifested as spontaneous sensations of warmth on the chest, neck and face, usually associated with palpitations, resulting from estrogen withdrawal [32]. By persisting for several years, hot flashes interfere with daily activities or regular sleep and are considered a classical menopausal symptom. Hot flashes are often accompanied by skin flushing and sweating followed by a sensation of cold as the core body temperature drops [33].

Vasomotor symptoms clearly compromise the quality of life and health status since most of these episodes are associated with anxiety, irritation, panic, decreased work efficacy and disturbances of regular activities performed by women, sometimes leading these to seek medical help [34]. Hot flashes vary in length and intensity, although the mechanisms responsible are not entirely known. It is possible that reduced estrogen levels induce a decrease in endorphin concentrations in the hypothalamus, which augments the release of norepinephrine and serotonin. Those neurotransmitters lower the set point in the thermoregulatory nucleus, and trigger an inappropriate heat loss [35]. Another hypothesis considers that hot flashes result from a decrease of Glucose Transporter-1 (GLUT-1) expression in the blood-brain barrier (BBB), a consequence of diminishing estradiol levels. The lower expression of GLUT-1 in the BBB results in decreased delivery of glucose to the brain. The lower neurobarrier response to metabolic stimulation during estrogen reduction and a consequent vascular reaction is then observed [36]. Besides hot flashes, other menopausal symptoms such as vaginal dryness, itching and dyspareunia resulting from low levels of estrogen and androgen can also be experienced by women [37]. Reduced vaginal blood flow and vaginal secretions, alterations in vaginal fluid pH from acid to neutral can also alter women sexual behaviour [38]. This mainly occurs due to the fact that the vaginal epithelium becomes thinner and friable, shortening the vagina, which becomes narrower and less elastic [39]. Along with these symptoms, several others are associated with the menopause transition including head and back aches and stress [17]. Several clinical conditions also have an increased incidence with menopause, such as cardiovascular diseases [40] and osteoporosis [41, 42]. The risk of cardiovascular disease markedly increases after women enter menopause [31]. Before that period, women have a lower risk than men of the same age due to higher circulating levels of high density proteins (HDL), occurring when estrogen levels are elevated in the woman's body [43, 44]. Increased osteoporosis is often associated with menopausal estrogen deficiency, since this induces a deregulation of bone remodelling, with bone reabsorption being accelerated and bone formation being decreased [45]. In order to overcome the menopausal symptoms, HRT therapy has been administered to menopausal and perimenopausal women.

1.3. Hormone replacement therapy

It is estimated that from 2030, 47 million women will be undergoing menopause each year [46, 47]. Bearing in mind the burden of menopause-associated symptoms, a combination of estrogens with synthetic progesterone had been used and is known as the classic hormone replacement therapy (HRT), available and administered since the 1940's [48].

1.3.1 Estradiol-based therapy

Physiologically, follicles are lost due to follicular atresia. Even if some remain in postmenopausal women, those are less sensitive to gonadotropin stimulation. Postmenopausal decline in ovarian E2 induces a decrease in the negative feedback in the pituitary glands, resulting in the secretion of FSH and luteinizing hormone (LH). Most of the symptoms present during menopause result from estrogen deficiency, simultaneous with high levels of LH or gonadotropin releasing hormone [30]. As previously referred, the most common therapy administered to women in menopause is a combined therapy of E2 and P4, constituting the classical HRT [30, 49, 50]. Both P4, produced in the corpus luteum, and progestins act on the uterus endometrium, converting it from a proliferative to a secretory tissue [51]. These hormones are effective in the attenuation of hot flashes [51, 52].

Hormone replacement therapy inhibits the aging-related bone loss that occurs during menopause. Women under HRT have a lower risk of vertebral and hip fracture [53], a lower incidence of cardiovascular diseases [54, 55], as well as a reduction of vasomotor symptoms and a delay in the onset of Alzheimer's disease [56]. The vasoprotective and anti-oxidative effects are also responsible for some beneficial effects of estrogens in the brain. In fact, estrogens have been shown to be potentially preventive against neurodegenerative diseases through multiple mechanisms including reactive oxygen species (ROS) scavenging, up-regulation of antioxidant systems, as well as by preventing degeneration of the mitochondrial electron transport chain (ETC) [57].

However, some controversies regarding the administration of HRT to menopausal women exist. For years, it was almost a dogma that cardiovascular disease was prevented in women undergoing HRT, which was supported by the beneficial effects of estrogen on metabolic risk factors [58, 59]. However, the Women's Health Initiative (WHI) showed that HRT resulted in an increased incidence of stroke [60] and venous thromboembolism [61]. The results from the previous 2002 WHI study also showed that estrogen-based HRTs have negative effects on post-menopausal women [62], including a significant increase in the incidence of breast cancer, heart diseases, pulmonary embolism and vascular dementia in a group of postmenopausal women aged over 65 years old. In agreement, HRT was shown to increase the incidence of endometrial cancer and breast cancer [63], as well as gallbladder [64] and ovarian disease [65].

Results from different sources indicate that the use of HRT needs to be carefully assessed and an analysis of risks and benefits of the therapy should be done by the clinician for each individual woman, specially to those who have higher risk of breast cancer. Clearly, the possible problems associated with HRT in a sub-population in women may expedite the replacement of estrogens by other safer molecules.

1.4 Phytoestrogens

Phytoestrogens (PE), a group of plant-derived chemicals, are a popular alternative to estrogens/progesterone therapy [66]. Due to their similar chemical structure to the principal mammalian estrogen, E2, it is thought that PE can replace estrogens during HRT. Several studies have focused on their potential clinical use and influence on the regulation of cellular pathways [67]. The interest in the use of PE stems from epidemiologic studies that suggest a decreased risk of breast cancer, lower incidence of menopausal symptoms and osteoporosis in women from countries with high PEs consumption, namely through soy-based diets [68, 69]. Several PE have antioxidant properties through hydrogen/electron donation via hydroxyl groups, acting as free radical scavengers and inhibiting the development of coronary heart disease and some types of cancer [70].

1.4.1 Phytoestrogens: structure, origin and metabolism

Phytoestrogens are classified in four main distinct classes: isoflavones, lignans, coumestans and stilbenes (Fig. 2). Isoflavones, originated from soy and soy derivatives are the most common PEs with genistein and daidzein being the most abundant and studied [71]. This class of PEs may also be found in clover and alfalfa [72]. Lignans are the most prevalent PEs in nature, comprising a large variety of individual structures in plants. Many non-toxic lignans are constituents of human diet, being present in high levels in oilseeds, in flaxseed, in grains such as wheat, rye, and oat and in various types of berries. Both isoflavonoids and lignans are stored in plants predominantly as glycosides in vacuoles [73]. Lignans yield metabolites with estrogen activity such as enterodiol and enterolactone through the metabolism of intestinal bacteria (Fig. 2) like *Peptostreptococcus productus*, *Eggerthella lenta* or *Atopobium*, among others [74, 75] from secoisolariciresinol and matairesinol, respectively. Non-metabolized plant lignans can also be found in human urine indicating that they can be absorbed from the intestine as aglycones [76]. Coumestans and stilbenes are less abundant in the diet and thus have also been less studied [71]. Coumestrol is a coumestan found in clover and alfalfa sprouts and in lower concentrations in lima bean and sunflower seeds, among other sources [77, 78]. Resveratrol is the most studied stilbene, being present in grapes, peanuts and cranberries. Resveratrol is metabolized in the intestine and liver by enzymes as β-glucuronidase and sulfatase, however, its non-metabolized form is also active [79]. Although there are some authors that do not consider resveratrol as a phytoestrogen, the finding that resveratrol has estrogenic activity expanded the spectrum of known dietary phytoestrogens [80].

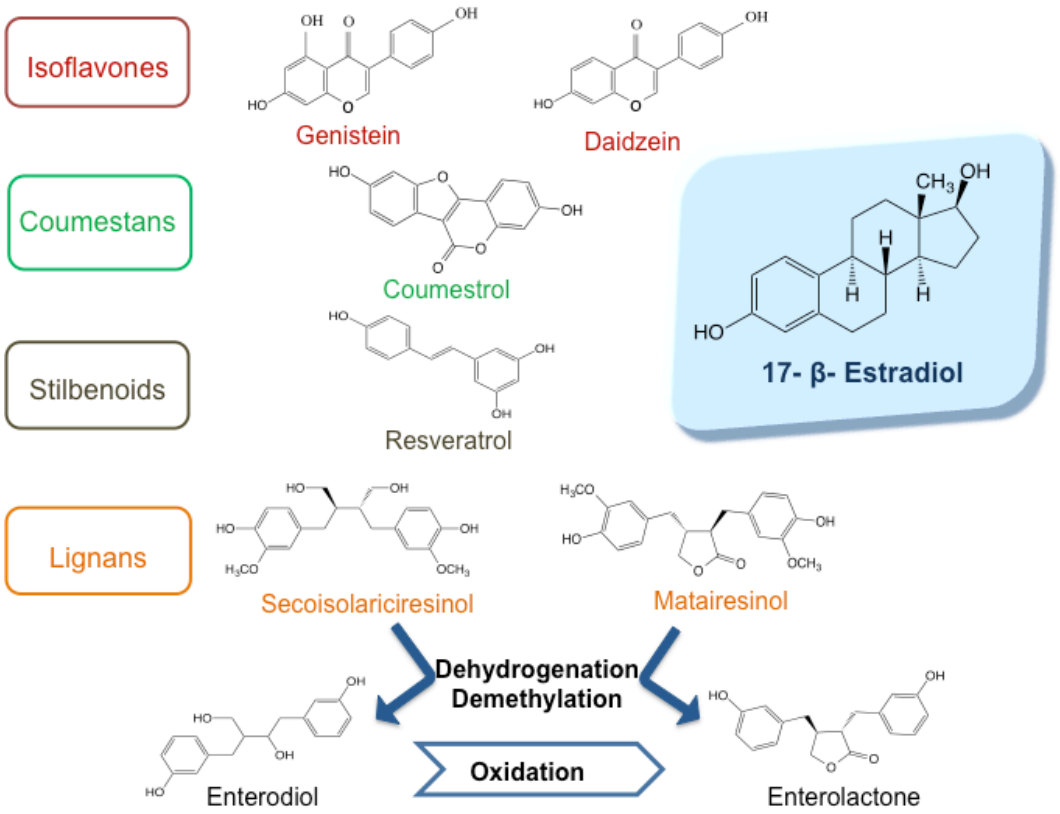

Figure 2: Different classes of phytoestrogens.
Isoflavones, lignans, coumestans and stilbenes are the different classes of PEs presenting a chemical structure similar to the main female estrogen, estradiol. These compounds are metabolically active, with the exception of secoisolariciresinol and matairesinol that are first converted to enterodiol and enterolactone by the intestinal flora.

1.4.2 Estrogenic activity

Phytoestrogens have a phenolic ring that is a prerequisite for binding to estrogen receptors and a molecular weight similar to E2, acting as agonists or antagonists of ERs. The effects of PEs at the cellular and molecular levels are influenced by many factors, including concentration, receptor status, presence or absence of endogenous estrogens and the target tissue [81].

Phytoestrogens' dual performance of estrogenic/anti-estrogenic activity may influence their direct effects on cells. The most popular PE, study- and consumption-wise, genistein, is effective as an agonist of both ER for concentrations lower than 10 μM, with anti-estrogenic properties being observed for higher concentrations [82, 83].

Phytoestrogens can bind either to ERα or ERβ, although these compounds appear to have a higher affinity for ERβ [84]. However, the estrogenic potency of PEs varies within the particular group and the tissue in study [85]. The presence of a correctly positioned phenolic ring and also the distance between the two opposing phenolic oxygens in isoflavone structure is similar to that of E2. This similitude allows isoflavones to bind to the ER, effectively displacing E2 [86], which may help to explain how PEs protect against breast cancer, since ERβ signalling inhibits mammary cell growth [87]. Nevertheless, it is still not

defined whether isoflavones competitively displace estradiol by binding to the primary site in the ER, or whether isoflavones bind to a secondary site in the receptor, altering the binding pocket for E2 [85, 86].

The recruitment of co-regulatory molecules may be important in determining the biological function of PEs. Particularly, isoflavones appear to selectively trigger ERβ transcriptional pathways, especially leading to gene expression repression. This affinity for the ERβ results in the exposure of activation function-2 (AF-2) on the surface of ERβ, which has greater affinity for certain co-regulators [86]. Phytoestrogens also have differential activity on several ER associated-signalling pathways. For example, Akt phosphorylation is normally secondary to ERα activation, being upregulated by genistein and daidzein in ER-positive breast cancer cell lines, while resveratrol has an inhibitory effect on the phosphorylation of Akt [88]. Furthermore, in ER-negative cell lines, resveratrol and daidzein activate Akt while genistein inhibits its activation [89]. As already described, PEs generally have a lower affinity to ER than E2. The affinity to estrogen receptors depends on the tissue in study although must be stressed that the estrogenic affinity of several PEs is still unknown.

In brain, the affinity of the majority of PEs to the ER is not yet defined. Genistein has an affinity of 4% and 87% for the ERα and ERβ, respectively, while daidzein has an affinity of 0.1% and 0.5% to the same receptors, when compared with E2. On the other hand, the binding affinity of coumestrol is 20% and 140% of E2, respectively to ERα and ERβ [90]. Although coumestrol is one of the PEs with a higher affinity for the ER, thus presenting a high estrogenic activity [91], its effects as a hormone-like compound are far from being understood. In ovarian cells, the binding affinity of resveratrol to estrogen receptors is 7,000 times lower than E2 [92] (Table 2).

The interaction of PEs with the most recently described ER, GPR30, and their consequent binding affinity have not been described thus far. Novel insights into this new binding partner may help in understanding the different signalling pathways and the cell fates arising downstream from the ER.

1.4.3 Biologic effects during menopause

The use of PEs as an alternative to HRT resulted from observations that several symptoms or pathologies associated with menopause and with low estrogen content [93] were partly prevented.

Moreover, in an epidemiologic study of dietary lignan intake and breast cancer, a higher lignan intake was associated with lower risks of that type of cancer [94]. Relatively to menopause-associated symptoms, PEs have shown satisfactory results regarding a decreased incidence of hot flashes and night sweats [95]. In this section, the effects of PEs

in menopause-related conditions are discussed. On the other hand, epidemiological studies show that Asian populations have a lower incidence of prostate cancer in comparison with the Western World, which has been suggested to result from higher consumption of PEs in Asia, and the importance that diet is believed to play in cancer [96].

Table 2: Estrogenic affinity of some phytoestrogens as compared with E2

Estrogens	ERα % to E2	ERβ % to E2	Tissue
E2	100	100	
Genistein	4	87	Brain
Daidzein	0.1	0.5	Brain
Coumestrol	20	140	Brain
Resveratrol	0.01	0.01	Ovary
Enterolactone	N.D.	N.D.	N.D.
Enterodiol	N.D.	N.D.	N.D.

The estrogenic affinity of PEs for each estrogen receptor is dependent on the tissue and agonist concentration. Despite the fact that there are clear voids in the current knowledge, it is generally accepted that PEs have lower estrogenic affinity than E2. Adapted from [90, 92].

1.4.4 Menopausal classic symptoms and phytoestrogens

The effect of PEs in the attenuation of hot flashes is still far from being fully determined. However, some studies suggest that isoflavones can relieve vasomotor symptoms. Episodes of hot flashes and night sweats were demonstrated to be less frequent and weaker in women with higher consumption of isoflavones [97-100]. Isoflavones attenuate bone loss in premenopausal women, increasing bone density and decreasing the bone turnover resorption markers [101]. The role of many PEs on other previously reported menopausal symptoms is still untested.

1.4.5 Cancer

Increased incidence of breast and endometrial cancer is associated with menopause, mainly due to HRT [63]. This said, the effects of PEs on cancer incidence and progression are of critical importance when investigating the potential use of those compounds as a safe and viable alternative to HRT.

The effect of PEs on cell cycle regulators and transcription factors is relevant since many novel synthetic agents aimed at inhibiting pathways and proteins up-regulated by ER activation are under development [85]. It is important to emphasise that, despite the fact that there have been numerous and extensive studies on the mechanisms of PEs, there is no clear evidence whether PEs are chemopreventive or actually contribute to increased cell transformation and proliferation.

Several isoflavones have potential anti-tumor effects by modulating genes controlling cell-cycle progression. Genistein inhibits the activation of the nuclear factor kappa-light polypeptide gene enhancer in B-cells (NF-κB), regulating a signaling pathway that is implicated in the balance between cell survival and programmed cell death (apoptosis). Antioxidant and antiangiogenic properties of genistein have also been demonstrated [102-104]. Genistein treatment inhibits human mammary epithelial cell growth, increases the expression of tumor suppressor genes and decreases the expression of two tumor promoting genes: p21 and p16 [105]. In accordance, genistein and daidzein inhibited the proliferation of three different breast cancer cell lines [106]. Genistein promotes mobilization of copper leading to pro-oxidant signalling and consequent cell death; this is particularly relevant for an anticancer therapy since tumour cells have increased copper content [107]. Controversially, it has also been suggested that soy-based supplements may decrease the efficacy of breast cancer treatment with aromatase inhibitors [108]. A clinical study showed that a 6-month intervention of mixed soy isoflavones in healthy, high-risk adult Western women did not reduce breast epithelial proliferation, suggesting a lack of efficacy for breast cancer prevention and a possible adverse effect in premenopausal women [109]. On the other hand, daidzein and its metabolite equol induced apoptosis in MCF-7 breast cancer xenografts in rodents, suggesting its use as a core structure for the design of new drugs for cancer therapy [110]. Although isoflavones have agonistic and antagonistic estrogenic effects, these PEs, similarly to lignans, also induce differentiation and inhibit angiogenesis, cell proliferation, tyrosine kinase, and topoisomerase II, thus preventing tumor growth [111]. High serum enterolactone levels were previously associated with a reduced incidence of breast cancer in healthy women [112]. Enterodiol and enterolactone showed a higher inhibition of MCF-7 breast cancer cells growth than their precursors, secoisolariciresinol and matairesinol [113], suggesting that the parent compounds are less active in terms of cancer cell cytotoxicity. Resveratrol inhibits cell proliferation, reduces reactive oxygen species and induces apopotosis through cycle arrest in hepatocellular carcinoma cells [114]. Resveratrol also suppresses human metastatic lung and cervical cancer through the inhibition of NF-kB transactivation [115]. Regarding the anti-cancer therapy of PEs, the type of tumor and host determine the final effect of each specific PE on cancer cells.

1.4.6 Cardiovascular diseases

The decrease of E2 levels during menopause has been associated with the development of cardiovascular diseases [31, 116]. Several PEs have been demonstrated to be cardioprotective during the transition to menopause, by reducing the levels of cholesterol in plasma [117]. Genistein shows pharmacological cardioprotection after ischemic post-conditioning, involving the activation of the estrogen receptor, of PI3K/Akt and preservation of mitochondrial function, showing to be as cardioprotective as E2 at lower concentrations

[118]. The consumption of soy also decreases the arterial pressure in postmenopausal women, which is accepted to be preventive towards the development of heart disease [119]. Genistein also inhibits the activity of inducible nitric oxide sythase (iNOS) and increases the endothelial form activities in an isoproterenol-induced cardiac hypertrophy model in male Wistar rats of 10-12 weeks old [120], resulting in a protective cardiac phenotype in this animal model. This PE has been also shown to increase the cAMP/PKA pathway in a *db/db* diabetic mouse model, reducing the vascular inflammation related with diabetes [121]. The consumption of soy may also have a role in delaying atherosclerosis and the risk of cardiovascular diseases that is associated with the loss of ovarian function and consequent estrogen deficiency in menopause [122]. Due to its antioxidant proprieties, resveratrol has been studied in the context of cardiovascular diseases. Accordingly to that, resveratrol prevented the development of insulin resistance, increased mitochondrial biogenesis and improved vascular function in mice at a dose of 4g/kg of food consumed [123, 124].

1.4.7 Neurodegenerative diseases

Due to estrogen withdrawal, women are more prone to develop neurodegenerative disorders such as Alzheimer's disease [125, 126] and the possible benefits of PEs are also extensive to the Central Nervous System (CNS). The PE alpha-zearalanol was previously shown to effectively antagonize beta-amyloid-induced oxidative damage in cultured rat hippocampal neurons [127]. Daidzein treatment resulted in decreased apoptosis in the brains of D-galactose-treated mice, characterized by an increase in Bcl-2 mRNA and a decrease in the expression of the caspase-3, making it a potential candidate for neuropharmaceutical therapy [128]. By increasing the expression of the anti-apoptotic protein Bcl-xL, a high soy diet reduced cell death induced by an experimental stroke in adult ovariectomized female Sprague-Dawley rats [129]. The therapeutic effects of PEs were also observed on Parkinson's and Alzheimer's disease. In a Parkinson's disease mouse model, genistein prevented the loss of neurons through the increase of Bcl-2 gene expression [130]. In a model of Alzheimer's disease, genistein prevented the effects of beta amyloid (Aβ) plaques, including the increase of inflammatory mediators such as cyclooxygenase 2 (COX2), iNOS and interleukin 1 beta (IL1β), as well as the tumor necrosis factor alpha (TNFα) [131]. Furthermore, acute genistein treatment has been suggested to be useful in improving memory deficits associated with the loss of ovarian function [132].

1.4.8 Other therapeutic applications

Phytoestrogens have also been shown to prevent hepatic alterations, which may also have a role in menopause-associated complications. Coumestrol was described to have beneficial effects on lipid and glucose metabolism of HepG2 cells, independently of its estrogenic activity as well as in ovariectomized rats [133, 134]. Daidzein was demonstrated to afford

hepatic protection against oxidative damage in a d-galactosamine rat model, being this effect mediated by an increased superoxide dismutase activity [135]. An anti-diabetic effect in type-2 diabetes in C57BL/KsJ *db/db* mice was previously observed by using genistein and daidzein, with both compounds increasing glucose and lipid metabolism [136].

1.5 Aging, menopause and mitochondrial function

1.5.1 Mitochondrial physiology

Mitochondria are the metabolic center of the cell. Besides energy production, mitochondria are responsible for several other functions including steroid synthesis, calcium homeostasis, regulation of apoptosis signaling and regulation of the redox potential. Within a cell, the distribution of the mitochondria is unequal depending on the cellular energetic or metabolic demand [137]. The overall shape of the mitochondrial network results from an equilibrium between fusion and fission events [138], which allow the exchange of organelle contents such as membrane lipids, proteins, ions, metabolites and even mitochondrial DNA (mtDNA) [139], as well as to provide a steady-state for the electrochemical gradient [140].

In the present section, some important roles of the mitochondria that are critical for the experimental context of this thesis are revised.

1.5.1.1 ATP and metabolites

Most of the metabolic reactions in cells are powered by the hydrolysis of adenosine triphosphate (ATP) to adenosine diphosphate (ADP). In order to maintain the bioenergetic homeostasis and consequently cellular integrity and regular function, ATP must be constantly produced from the conversion of dietary fats and carbohydrates to reducing equivalents in the living cell [141]. Mitochondria are considered the powerhouses of the cell, due to a variety of important energy-producing metabolic pathways in their interior. Pyruvate is formed in the cytosol as an end product of glucose metabolism (glycolysis) and can be converted to lactic acid under anaerobic conditions. Under aerobic conditions, pyruvate is converted to acetyl coenzyme A (acetyl-CoA) by pyruvate dehydrogenase (PDH) in the mitochondrial matrix [142]. Acetyl-CoA enters the Krebs cycle, being oxidized to generate several intermediates, including NADH and succinate. Other intermediates of the Krebs cycle are also important in several metabolic pathways, such as in the biosynthesis of heme groups and amino acids [143]. Mitochondria can also be involved in the β-oxidation of fatty acids [144]. The end product of this pathway is, once again, acetyl-CoA, which is then used in the Krebs cycle. NADH and succinate, are both oxidized by the ETC, ultimately leading to ATP synthesis, in a process known as oxidative phosphorylation (OXPHOS) [145, 146]. The electrons derived from reduced substrates are transferred through several multi-protein complexes (mitochondrial complexes I to IV), downward their redox potentials. The energy

derived from electron transfer is used to pump protons across the inner mitochondrial membrane (IMM) at complexes I, III and IV, creating an electrochemical gradient between both sides of the IMM. This electrochemical gradient is a proton-motive force driving the re-entry of protons towards the matrix through complex V (ATP synthase), coupled to ATP synthesis [142, 147, 148]. The ATP produced is then exported from mitochondria by the ADP/ATP translocator (ANT). The final electron acceptor in the mitochondrial respiratory chain is molecular oxygen, which is reduced via a sequential four-electron transfer to water in complex IV (cytochrome c oxidase, COX). However, some of the electrons transferred across the mitochondrial ETC can perform a single electron reduction of molecular oxygen. This phenomenon occurs continuously even under physiological conditions leading to formation of superoxide anion ($O_2^{\bullet -}$) that will be discussed in the next section.

1.5.1.2 Reactive oxygen species

Among the reactive molecules produced within a living cell, reactive oxygen species (ROS) are a widely studied example. There are several components in mitochondria which have the capacity to produce ROS [149], including ubiquinone-binding sites in complex I (site IQ) and complex III (site IIIQo), glycerol 3-phosphate dehydrogenase, the flavin moiety in complex I (site IF), the electron transferring flavoprotein:Q oxidoreductase which participates in fatty acid beta-oxidation, and pyruvate and 2-oxoglutarate dehydrogenases [150], as well as monoamine oxidase in the outer membrane [151]. Mitochondrial complexes I and III account for a significant proportion of intracellular ROS formation due to the CoQ cycle that occurs in those sites, although complex I is considered the major contributor [152]. The mitochondrial ETC contains several redox centers, which can react with molecular oxygen. As a result, a small amount of electrons leaks from complex I and complex III, performing a one-electron reduction of molecular oxygen that gives rise to superoxide anion ($O_2^{\bullet -}$). Approximately 1-2% of the oxygen consumed during OXPHOS under physiological conditions is converted into this byproduct [153].

Superoxide anion produced by the respiratory complex I is released in the mitochondrial matrix being spontaneously or via the manganese superoxide dismutase (MnSOD) transformed into hydrogen peroxide (H_2O_2). In turn, $O_2^{\bullet -}$ generated by complex III can be released in both sides of the IMM, although in the inter membrane space (IMS), the dismutation into H_2O_2 is achieved via a Cu/Zn-dependent SOD (Cu/ZnSOD). Hydrogen peroxide can be converted to water in the mitochondrial matrix by catalase (CAT) or glutathione peroxidase (GSH). The H_2O_2 produced can also diffuse in the cytosol and trigger the activation of some transcription factors and various enzymatic cascades [154]. Mitochondrial thioredoxin, glutaredoxin and even cytochrome *c* are other relevant ROS scavengers (as reviewed elsewhere [155]).

General oxidative stress arises when an imbalance in the redox steady-state occurs and the ROS production exceeds the capacity of the cell for detoxification. Moreover, some new theories have described the notion of localized oxidative stress. These observations suggest that disruption of redox-dependent coordination in organelles results in cellular toxicity. The improved understanding of the compartmentalized nature of oxidative stress may help on the compression of the oxidative redox signaling modulation [156]. If H_2O_2 reacts with a reduced transition metal (Fe^{2+} or Cu^{2+}) or $O_2^{\bullet-}$, it can be further reduced to a highly reactive and toxic hydroxyl radical ($^{\bullet}OH$) by a Fenton or Haber-Weiss reaction [157]. Although very short-lived, $^{-\bullet}OH$ can damage cellular macromolecules including proteins, lipids and nucleic acids. The oxidation of proteins can inactivate and target them for degradation; oxidative damage of DNA causes single and double strand-breaks, crosslink with other molecules and base modifications, while lipid oxidation can generate membrane alterations. As described above, mtDNA represents a critical target of oxidative damage since it does not contain any protective histones and it is located in proximity to the production site of ROS [145]. Once damaged, mtDNA can indirectly amplify oxidative stress since transcription of critical mitochondrial proteins is defective, leading to a vicious cycle of ROS production and eventually triggering cell death. Oxidative stress has been related with aging [158] and with some disorders such as cancer and diabetes [159].

Reactive nitrogen species (RNS), including nitric oxide ($^{\bullet}NO$) and peroxynitrite ($ONOO^-$), can also contribute for a regulation of mitochondrial function [160] as well as for increased mitochondrial damage during pathological conditions [161]. Although elevated ROS production can promote cell damage, lower amounts of ROS may act as signaling molecules, leading cell adaptation to stress. [150]. A large number of reports have suggested that mitochondrial ROS are of great importance and critical for cellular homeostasis [162-165].

1.5.1.3 Calcium and mitochondrial physiology

Calcium ions (Ca^{2+}) control different cellular processes, including muscle contraction, gene expression, energy metabolism and the balance between cell death/survival [166]. If cytosolic calcium concentration reaches over basal values, the regulation of cellular processes is hindered. Several are the cellular mechanisms of Ca^{2+} regulation, with mitochondria having an important role [167]. Calcium handling by mitochondria is considered a physiological process of extreme importance. Mitochondrial Ca^{2+} uptake (either through the calcium uniporter or through the alternative RAM pathway – rapid uptake mode) was demonstrated to control cell metabolism, cell survival and intracellular Ca^{2+} signaling [166]. The accumulation of Ca^{2+} within mitochondria allows the regulation or activation of matrix Krebs cycle dehydrogenases and increases the electron flow along the ETC, adjusting the ATP production to follow the requirements of the cell [168-170]. On the other hand,

mitochondrial Ca^{2+} overload associated with an increase in the generation of ROS promotes the sustained opening of the called mitochondrial permeability transition pore (MPTP) [171].

The term mitochondrial permeability transition (MPT) was first described in 1976 by Hunter and colleagues [172], and it results in alterations on the permeability of the inner mitochondrial membrane. Since its discovery, several were the attempts to define the structure of the MPTP, but this subject is still controversial [173-176]. The role of VDAC (voltage dependent anion channel) and ANT as pore components was not confirmed although they can be regulators of the MPTP [174, 177]. Recently, by identifying that cyclophilin D, a regulator of MPTP, binds to F_oF_1 ATP synthase, it was suggested that ATP synthase dimers form channels with electrophysiological properties similar to the MPTP [178]. The MPTP is described as an abrupt increase of the mitochondrial inner membrane permeability to solutes with a molecular mass inferior to 1.5 kDa. In the low conductance mode, the MPTP is permeable to small ions such as Ca^{2+}, and can promote Ca^{2+} release transmitting calcium signaling from one mitochondrion to another. The high conductance form may lead ultimately to cellular death [179], since the opening of the MPTP may result in the release of cytochrome *c* and other pro-apoptotic factors (such as the AIF and SMAC/Diablo), [180] from mitochondria, leading to activation of the apoptotic signaling pathway [181].

1.5.1.4 Tissue-specific differences in mitochondrial function

Mitochondrial function tightly controls the cellular adaptation to environmental and physiological cues, responding to alterations in energy demand and substrate delivery. In this regard, several studies reported tissue-dependent differences in the OXPHOS machinery [182-184]. Mitochondrial morphology is irregular and less compacted by tissue architecture in the liver and kidney, while in heart and skeletal muscle, mitochondria have a regular shape with well-defined cristae. In neurons, mitochondria are preferentially distributed along the axons, with few mitochondria concentrated around the nucleus. Similarly, kidney mitochondria concentrate on the tubules. By measuring endpoints of mitochondrial function (respiratory chain complexes activity, respiratory state 3, citrate synthase and protein content) in distinct tissues, three groups can be distinguished considering the similarities in mitochondrial morphology: (1) skeletal muscle and heart, (2) brain, (3) liver and kidney [182].

The parameters ADP/O (or P/O) and RCR are of importance in mitochondrial studies and also to cluster different tissues. The ADP/O is a ratio between the nmoles of ADP phosphorylated per natoms of oxygen consumed during that process – this parameter measures the phosphorylation efficiency of the mitochondrial preparation. The RCR (respiratory control ratio) measures the coupling between substrate oxidation and ADP phosphorylation. Regarding the phosphorylative system, the ADP/O ratio is slightly different

in each tissue in the presence of complex I substrates. However, when mitochondrial function is sustained with the complex II substrate succinate, no tissue dependent differences are observed [183]. The authors suggest that complex I is the energy conservation site, in charge of the rate dependent regulation of the mitochondrial energy conservation efficiency, excluding the dependence of the catalytic efficiency of the ATP synthase on the respiratory fluxes. Brain mitochondria show the lowest OXPHOS efficiency [183], which might be explained by limited antioxidant defense [185, 186]. The tissue-specific differences found with complex I substrates can explain the tissue specific effects of different compounds on mitochondrial function [187, 188]. For instance, the organ with the highest COX activity found per cell is the heart, which is justified the high energy demand of that tissue [189].

The differences observed regarding the mitochondrial function result from the requirements of each tissue ranging from a primarily biosynthetic role in liver to an energy metabolism oriented tissue in heart.

1.5.1.5 Mitochondrial liability, safety assessment and drug development

Mitochondria are indeed, the crossroad for many cellular pathways, which explains the growing number of publications dealing with the mitochondrial role in cell life and death [142]. As a result of the increased efforts focusing on the role of mitochondria in a variety of human disorders such as cancer, neurodegenerative and cardiovascular diseases, obesity and diabetes, “mitochondrial medicine” emerged as a whole new field of biomedical research. Based on the recent developments in this field, a large effort is underway to understand how different molecules regulate or damage mitochondrial function, with the ultimate goal to improve human health.

Two distinct and important mechanisms/endpoints by which drugs may inhibit mitochondrial function can be considered: a) direct interference with mitochondrial respiration/ATP synthesis (inhibition of respiratory complex activity, damage by ROS production, uncoupling activity, MPT induction) and b) inhibition of mtDNA synthesis. Regardless of the initial trigger, inhibition of ATP synthesis and bioenergetic failure of the tissue are severe manifestations of mitochondrial impairment. Some xenobiotics can lead mitochondria to an irreversible bioenergetic collapse via formation of the MPTP leading to the release of pro-apoptotic factors such as cytochrome *c*, AIF and Smac/Diablo [180]. Drugs that alter the normal balance between pro-apoptotic and anti-apoptotic proteins can also induce mitochondrial failure and eventually cell death [190]. Additional information for drug safety, as well as for toxicity assessment, may be achieved by the use of targeted approaches, affinity for overexpressed/subexpressed mitochondrial proteins during different pathologies, or selective mitochondrial accumulation of delocalized lipophilic molecules with positive charge and with

different redox actions [142, 191].

Nevertheless, further investigation in these endpoints or guidelines for molecular mechanisms of mitochondria-drug interaction will be needed for a better understanding of the mechanism of action involved in mitochondrial toxicity, allowing an improvement in the safety assessment of xenobiotics with relevant human exposure. Resulting from this concern, several high-throughput techniques have been used to test and screen drug candidate safety on mitochondrial function [192] and are used to improve basic knowledge in compounds-associated toxicity.

1.5.1.6 Toxicity of phytoestrogens

Despite the general positive effects of PEs, it is important to be aware that excessive PEs consumption may lead to adverse health effects. Furthermore, not all PEs are able to improve women's quality of life after menopause. For this reason, future studies with PEs must help define the safest dietary levels and clarify the mechanism of health risks and/or therapeutic action involved. Interestingly, prenatal exposure to genistein resulted in transgerational effects on the progeny. This particular study showed that fetus exposure to genistein affects fetal erythropoiesis and gene expression as well as DNA methylation of hematopoietic cells. Pregnant mice, consuming doses of soy below the range of human consumption normalized per weight, showed genistein accumulation in the fetus [193]. In agreement with this study, genistein inhibited testosterone secretion in fetal Leydig cells during early fetal development, suggesting that for concentrations comparable with human consumption, genistein can affect the development and function of the male reproductive system [194, 195]. Furthermore, resveratrol concentrations, which were previously shown to have potential anticancer activity and afford cardiac and antioxidant protection, caused a decrease in the final body weight, increased the levels of creatinine, alkaline phosphatase, alanine aminotransferase and albumin, and reduced hematocrit and red cell counts. In addition, resveratrol increased white cell counts and induced significant renal lesions, including severe nephropathy, when administered by *gavage* to male and female rats [196]. Moreover, relevant alterations on hepatic gene expression (down-regulation of the hepatic markers CaBP9K and IGFBP1 mRNA) were caused by genistein, again raising a cautionary note on the possible toxic effects of that class of compounds [197].

Phytoestrogens can also alter mitochondrial function, even at doses observed *in vivo* in the plasma [198]. Genistein induces the MPT through an increase in ROS production by the mitochondrial complex III [199]. Resveratrol, genistein and quercetin inhibit the enzymatic activity of mitochondrial F_oF_1-ATPase/ATP synthase, compromising ATP synthesis in isolated preparations of brain and liver mitochondria [200] (Fig. 3).

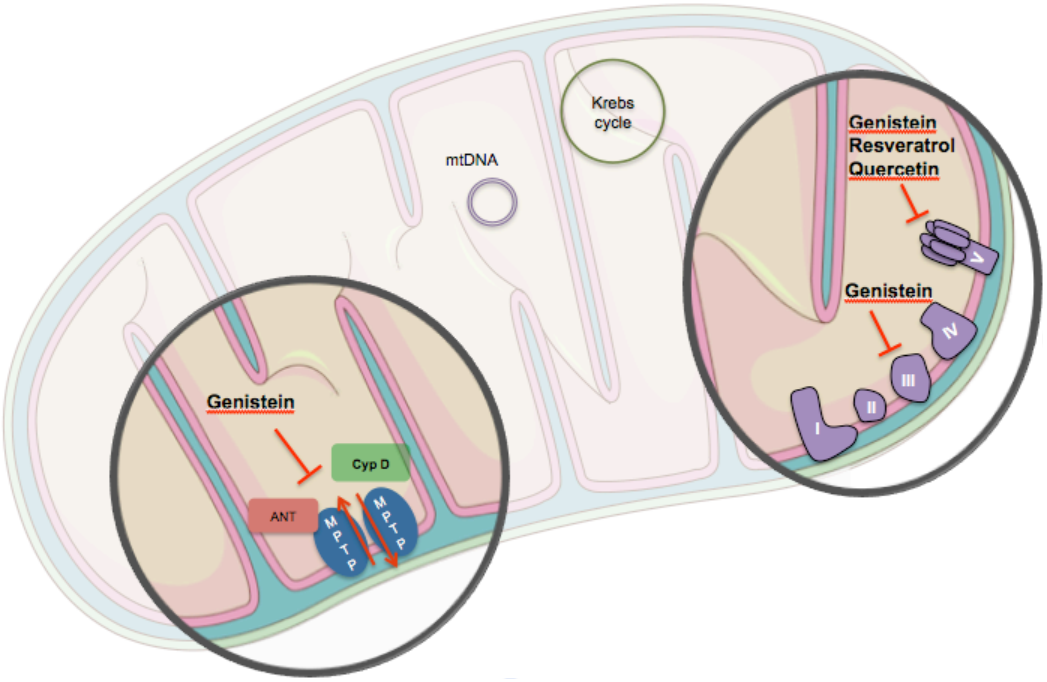

Figure 3: Mitochondrial effects of phytoestrogens.
Genistein induces the mitochondrial permeability transition possibly by augmenting ROS production by mitochondrial complex III. Resveratrol, genistein and quercetin inhibit the enzymatic activity of mitochondrial FoF1-ATPase/ATP synthase. Legend: I, II, III, and IV - mitochondrial electron transport complexes; V - F_oF_1-ATPase/ATP synthase; ANT – adenine nucleotide translocator; Cyp D – cyclophilin D; MPTP – mitochondrial permeability transition pore; mtDNA – mitochondrial DNA.

The previously described studies showing the benefits of PEs, their effectiveness and safety are still under debate, especially regarding their effects during pregnancy. Since several side effects were already described above, the transgenerational impact of PEs [193-195] is something that should be taken into account for the consumption of those compounds during pregnancy.

1.6 Aging and mitochondrial (dys) function

Life span is regulated by complex interactions of genetic and metabolic factors. The role of mitochondrial function as a determinant in aging has been extensively explored. Mitochondrial function decline plays a role in the aging process [201]. Several lines of study suggest that certain molecular and cellular changes lead to progressive disruption of mitochondrial energy metabolism [202]. The free radical theory of aging postulates that oxidative stress is a determinant factor that limits longevity [203, 204]. Increased oxidative stress promoted by higher production of ROS is considered an important factor linking mitochondrial dysfunction with aging. Aged mammalian mitochondria have decreased ability to produce ATP through OXPHOS, thereby altering cellular homeostasis. In the brain, the impaired mitochondrial function during aging results from lower rates of electron transfer from complex I to complex IV [205]. An impairment on complex I function was also observed and suggested to be due to oxidation of cardiolipin [206]. Also, cytochrome *c* oxidase activity,

mitochondrial transmembrane electric potential and state 3 respiration are decreased in brain mitochondria of aged animals [207]. During aging, the increase in the production of H_2O_2 is one of the most ubiquitous occurring events [208, 209]. The increased oxidative stress damages mitochondrial components, such as lipids and proteins, and induce accumulation of mutations on mtDNA, turning into a vicious cycle that induces a larger ROS production, ATP depletion and cell death [210]. If a mutated mtDNA molecule is replicated, the error propagates and may cause a deficit in cell respiration and OXPHOS. The unbalance in cell homeostasis may result in tissue dysfunction and consequently, aging. In terms of mitochondrial morphology, some alterations have been observed with aging, including increased size of mitochondria and decrease in the number of mitochondrial cristae [211].

1.6.1 Aging and menopause: animal models and alterations in mitochondrial function

Regardless the profound impact of menopause on women's health, animal models that mimic the natural progression through perimenopause and into the postmenopausal stages are currently absent. Ovariectomy (OVX), or surgical removal of the ovaries, is the most common animal model for studying the mechanisms that underlie menopause. Although widely used, the OVX model is problematic with regard to reproducing the effects of natural menopause. OVX produces a rapid cessation of ovarian function, dissimilar from the gradual decline that occurs in perimenopause. Moreover, the postmenopausal ovary continues to produce low levels of androstenedione [212], which is not produced in rodents after surgical removal of the ovaries. A chemically induced mouse model for peri- and postmenopause has been developed using the chemical 4-vinylcyclohexene diepoxide (VCD). This chemical is used in the manufacture of flame-retardants, insecticides and rubber tires [213] and selectively destroys ovarian small preantral follicles after repeated daily dosing in mice and rats [214]. The mechanism of VCD is apparently caused by the acceleration of the natural process of atresia (apoptosis) through follicle-specific pathways. No necrotic changes in ovarian tissue or changes in gene expression that cannot be attributed to ovarian failure were observed [212, 215-217]. Due to the selectivity of its effects, VCD has been used to cause premature ovarian failure after repeated daily dosing in rodents [214, 218]. After the destruction of preantral follicles, the estrous cycle length in VCD-treated animals increases as well as FSH levels [219]. This rodent model successfully reproduces human perimenopause and postmenopause, based in estrous acyclity and fluctuating, followed by low levels of estrogen [214, 220, 221].

Previous studies demonstrated that VCD causes a 40% and 81% destruction of primordial follicles in rats in comparison with control after 15 and 30 day of treatment [213, 216], respectively. A VCD model was also associated with increased oxidative stress, which also occurs in this period of women's life [222, 223]. For the past years, VCD has been used to

model menopausal transition in rodents and minimal toxicological effects have been observed. However, some literature reports the emergence of tumours [224, 225].

Table 3: Comparison between OVX and VCD models

Models	Species	Vantage (s)	Disadvantage (s)
OVX	• Rat • Mouse • Dog	• Widely used in research	• Rapid cessation of ovarian function • Ovary removal
VCD	• Rat • Mouse	• Selectively destroy preantral follicles of ovary • No tissue removal	• No studies comparing with OVX model • Chemical may have extra ovary effects

Ovariectomy is the classical model to study menopause in animals. However, it only occurs in 13% of women and excludes the menopausal transition since it is based in the removal of the ovaries. VCD appears to be a closer model to what actually occurs in women [214, 226, 227].

Additionally, unlike OVX animals, the VCD-treated animal retains residual ovarian tissue, mimicking natural menopause. Besides, less of 13% of women undergo surgical ovariectomy. The great majority of women undergo a transitional hormone variation and estradiol withdrawal [226] (Table 3).

The alteration of mitochondrial function in low-estrogen models is far from being understood, with only some reports available. In OVX rats, an increase in the expression of VDAC, adenine nucleotide transporter (ANT) and cytochrome *c* was observed, suggesting an age-dependent alteration in mitochondrial energetics [228]. It has been shown that E2 supplementation can revert the observed alterations including increased TNF-alpha, Fas ligand, Fas death receptor and Fas associated domain (FADD), as well as increased intrinsic pathway-linked caspase 9 and with extrinsic pathway-linked caspase 8, besides augmented caspase 3 activity [229]. Beyond the increase of the pro-apoptotic proteins t-Bid and Bax, Liou and collaborators suggested that E2 can prevent cell death signaling in heart from OVX rats [229]. The myocardial architecture in an OVX rat model was altered with the appearance of large interstitial spaces, increased number of cardiac fibrosis and apoptotic cells [230]. In accordance, a decreased content of cytochrome *c* in mitochondria, simultaneously with increased cytosol levels, were observed in the liver of OVX rats [231]. In addition, increased nitric oxide (NO) levels were also detected. Livers from OVX rats showed a higher content in malondialdehyde (MDA) and a decrease in mitochondrial superoxide dismutase (MnSOD) and catalase (CAT) expression [232], (Fig. 4), suggesting alterations of mitochondrial function resulting from increased ROS. The consequent decrease in ATP levels may affect plasma membrane ATPases and disturb ionic and redox homeostasis, possibly resulting in cell death [231, 233, 234]. Alterations in the expression of antioxidant defenses was also demonstrated in brain endothelial cells from OVX rats as shown by a decreased MnSOD transcripts and glutamate-cystein ligase modulatory subunit [235].

A link between mitochondrial dysfunction and menopause has been described in a perspective of estrogen impact on Alzheimer's disease. This is relevant since surgically induced early menopause may increase cognitive vulnerability. In agreement, estrogen replacement may decrease cognitive deficits even though the link between age at menopause and Alzheimer risk has still to be defined [236]. The role of ovarian hormones E2 and P4 on cerebral endothelium has also been demonstrated. Kemper and colleagues showed that ovariectomy decreases mitochondrial biogenesis and alters mitochondrial function, as observed by decreasing mtDNA/nuDNA ratio and ATPase 1α subunit [235]. Moreover, a decrease in PGC-1β, NRF1 and TFAM, transcription factors related with replication of mtDNA and expression of mitochondrial genes was also observed [235].

The role of depressed mitochondrial function during menopause is far from being completely understood and some of the conclusions presented so far are based on aging-related alterations of mitochondrial function and are also based on the effects of E2 replacement on OVX rats.

Our group suggested that menopause leads to cardiac mitochondrial dysfunction and decreased in fatty acid β-oxidation. It was proposed that this leads to fatty acid accumulation in the cytosol, promoting lipotoxicity, which may justify the higher risk of cardiovascular disease in menopausal women [31]. Nevertheless, this remains to be determined in OVX or VCD models.

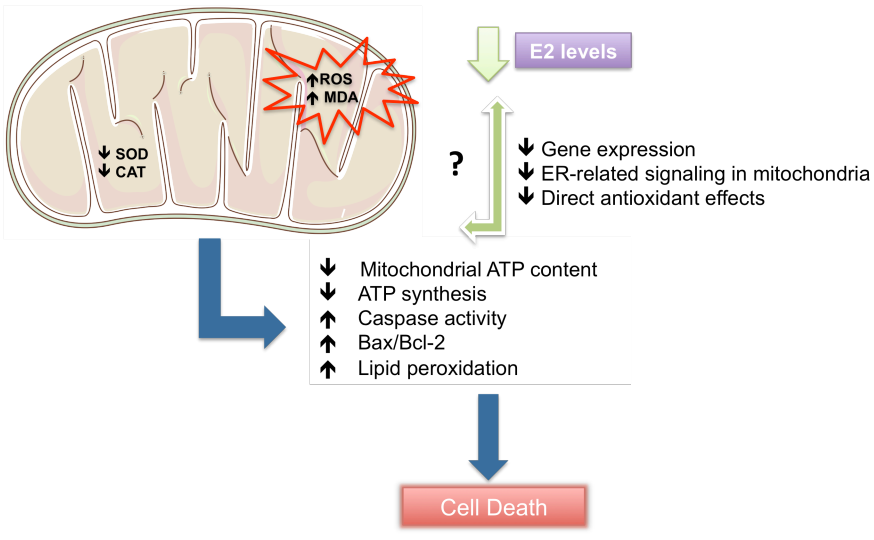

Figure 4: Mitochondrial alterations during menopause.
In animal models for menopause, a decrease in superoxide dismutase and catalase and an increase in ROS formation and on MDA content, are observed. A pro-oxidant environment activates caspase-signaling pathways. The link between circulating E2 and the decrease in mitochondrial function is not clear but decreased gene expression or ER-signaling on mitochondria may be explanations for this deficit. Legend: CAT- catalase, ER- estrogen receptor, MDA- malondialdehyde, ROS- reactive oxygen species, SOD – superoxide dismutase,

2. Aims of the present thesis

Phytoestrogens are natural compounds found in several edible plants [71, 237]. The evaluation of risks and benefits of PE is crucial to determine if those compounds can be used by menopausal women in the context of a safe and effective HRT. One particular aspect of drug-induced toxicity is the degeneration of the mitochondrial fraction, which can limit the clinical use of several new molecules or lead to the withdrawn from the market of currently used drugs [238]. Thus, the main objective of this thesis was to identify PEs with antioxidant properties and low toxicological effects (namely on mitochondria) and with the capacity to improve several end-points of estrogen deficiency in biological models. We hypothesize that one or more PEs with low mitochondrial toxicity can mimic E2 in improving the investigated phenotypes resulting from estrogen deficiency in several *in vitro* and *in vivo* models (Fig. 5).

For this purpose, the following experimental aims were pursued in this thesis:

1. Evaluate the possible *in vitro* mitochondrial toxicity of selected PE in isolated mitochondrial fractions from brain and liver. The purpose of this aim is to identify mitochondrial toxicity and/or antioxidant capacity of the tested PEs. Isolated mitochondria from brain and liver were used as biological models. The effects of PEs on mitochondrial bioenergetic parameters as well as on lipid peroxidation were evaluated.

2. Moreover, the use of cell lines was intended to increase the complexity of the systems in study and to exclude the highest resistance to the use of the classical HRT, the increased risk of breast cancer development. In order to test antioxidant protection in a more complex system, we used the HepG2 cell line that exhibits many of the features of normal liver cells, such as polarity based on the existence of several basolateral and apical poles [239, 240]. This cell line is widely used to screen the toxicity of new chemicals [241]. These cells have a similar phenotype to human hepatocytes and can activate or detoxify xenobiotics, reflecting the metabolism of xenobiotics in the human body better than other conventional *in vitro* assays [242, 243]. With this cell line we compared the proliferation rate and the antioxidant effects of one selected PE, using E2 as a control.

The most discussed side effect of HRT is the increased risk of developing breast cancer. MCF-7 and MDA-MB-231, estrogen-dependent and estrogen-independent human breast carcinoma cells, respectively, as well as human immortalized normal breast MCF-12A cells were used as models for breast cancer and normal cells. In these cell lines, the role of PE and E2 on cell proliferation was evaluated. The aim for this specific part is the selection of a PE presenting low toxicity on normal cells and not increasing (or inhibiting) the proliferation of breast cells.

3. Hot flashes may result from a decrease of GLUT-1 expression in BBB, being a probable link between decreased E2 and women sense of warmth [36]. The third goal of this work was to investigate whether selected PEs increase GLUT-1 expression at the BBB, following the "impaired glucose delivery hypothesis of menopausal hot flashes" previously described on the introductory chapter of this thesis [36, 244]. With this in mind, the role of E2 on GLUT-1 expression and the signalling mechanism behind its modulation were studied *ex-vivo* with ER agonists and *in vivo* with E2 administration in ER knockout mice for each receptor α and β (C57BL/6 background). Our hypothesis is that PE (s), similarly to E2, modulate GLUT-1 expression at the BBB. Brain microvessels were also isolated and exposed to E2 or PE (s) and capillaries membranes were isolated to evaluate GLUT-1 content.

4. The last goal was to determine if E2 and a selected PE would be beneficial for liver and brain mitochondrial function in two menopause rodent models: OVX and the VCD-chemical induced models. As female rats do not experience menopause, ovariectomy is generally considered as a model for menopause in animals. The temperature of these animals was also recorded as an approach to evaluate hot flashes in OVX rats. At this point, the hypothesis postulated was that the similarity to E2, was able to reduce temperature variations in OVX rats. Additionally to this menopausal surgical model, and after evaluating the eventual mitochondrial toxicity of 4-venylcyclohexene diepoxide – VCD (an environmental toxicant that progressively induces ovarian atresia resulting in a reduction of E2 production) administration in Wistar female rats, an additional *in vivo* study was performed based in this same chemically-induced model for menopause. Again, E2 was compared with selected PE in terms of mitochondrial function.

With these lines of study, we proposed a deeper understanding of the eventual risks / benefits of PE consumption, highlighting the PE effects. Some end-points can be measured in menopausal models, including based in alteration of mitochondrial function.

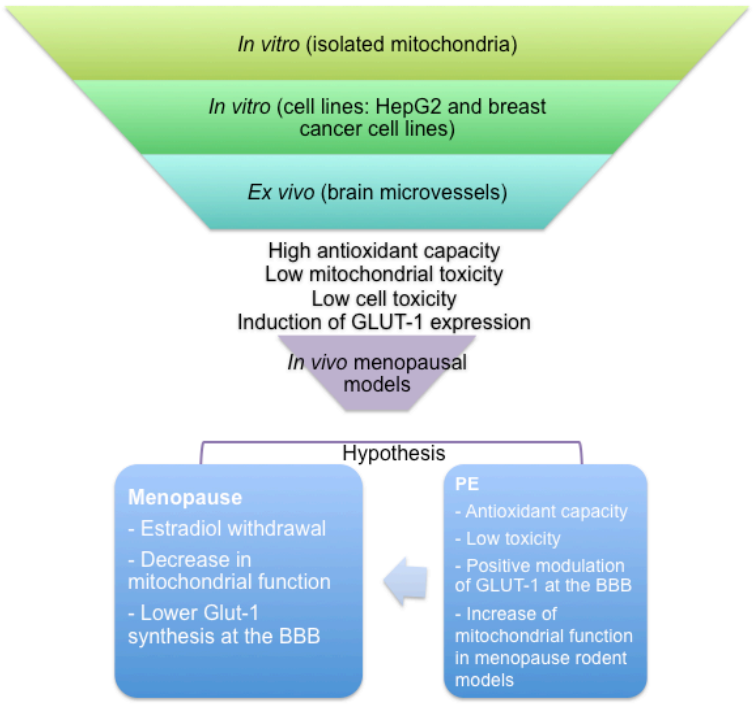

Figure 5: Scheme of the proposed work for this thesis.
After an initial screening *in vitro* on the toxicity of phytoestrogens, the role of these compounds on GLUT-1 expression was evaluated. The selected compound was further used in *in vivo* studies to verify its toxicity and to evaluate its effect in temperature variations in OVX rats.

3. Material and Methods

3.1 Chemicals

All chemicals used in this work of the highest analytical grade are from Sigma Aldrich Co (St. Louis, MO), unless specified in each section. Resveratrol, enterodiol, enterolactone, coumestrol and E2 were prepared in DMSO, with the final volume used being lower than 0.1% (v/v). Aqueous solutions were prepared in ultrapure water (Milli-Q Biocel A10 with pre-treatment via Elix 5, Millipore, Billerica, MA, USA). Non-aqueous solutions were prepared in ethanol. In this case, the final volume used was always lower than 0.1% (v/v). For *in vivo* experiments, 4- venycyclohexene diepoxide was prepared in sesame oil and E2 and coumestrol were prepared in ethanol dissolved in corn oil tocopherol stripped (MP Biomedicals, Santa Ana, CA, USA).

3.2 *In vitro* mitochondrial studies (Chapter 4.1)

3.2.1 Animals

Male and female Wistar rats (8-12 week old) from our animal colony (Center for Neuroscience and Cell Biology, University of Coimbra) were housed in type III-H cages (Tecniplast, Italy) with irradiated corn cob grit bedding (Scobis Due, Mucedola, Italy), following environmental requirements with *ad libitum* access to food (4RF21, Mucedola, Italy) and water and maintained at constant temperature (22 ºC) and humidity with a 12h light/dark cycle. Animal handling and sacrifice followed the procedures approved by the Federation of European Laboratory Animal Science Associations (FELASA). The author of this PhD thesis is credited by FELASA (category C) for animal experimentation.

3.2.2 Mitochondrial fraction preparation

Mitochondria were isolated through standard methods performed in our laboratory [245-247]. The liver was quickly removed and the tissue was homogenized in ice-cold homogenization buffer containing 250 mM sucrose, 5 mM Hepes (pH 7.2), 0.5 mM EGTA and 0.1% defatted bovine serum albumin. Cellular suspension is centrifuged at 746 x *g* in a Sorvall Evolution RC, SS-34 rotor (Thermo Scientific Inc., Rockford, IL, USA) and the supernatant is used for further centrifugations. The mitochondrial pellet was obtained by gradient centrifugation at 11,950 x *g* in a Sorvall Evolution RC, SS-34 rotor (Thermo Scientific Inc., Rockford, IL, USA) washed twice and suspended in washing buffer (250 mM sucrose, 10 mM HEPES pH 7.4) [248]. Brain mitochondria were isolated using a previously published method [249], through the use of 0.02% digitonin to release mitochondria from the synaptosomal fraction. The whole brain, except the cerebellum, was immediately removed, washed and homogenized at 4ºC in 10mL of isolation medium (225 mM mannitol, 75 mM sucrose, 5 mM Hepes, 1 mM EGTA, 1mg/ml defatted BSA, pH 7.4) containing 5 mg of the bacterial protease, Subtilisin A, type VIII from *Baccilus licheniformis*, (Sigma, St Louis, MO). Single brain homogenates were

brought to 30 ml and then centrifuged at 746 x *g* (Sorvall RC-5B Refrigerated Superspeed Centrifuge) for 5 min. The pellet was resuspended in 10 ml of the isolation medium containing 0.02% digitonin and centrifuged at 11,950 x *g* for 10 min. The pellet was then resuspended in 10ml of resuspension medium (225 mM mannitol, 75 mM sucrose, 5 mM Hepes, pH 7.4) and centrifuged again at 11,950 x *g* for 5 min. Finally, the mitochondrial pellet was resuspended in about 200 µl of resuspension medium. The mitochondrial suspensions were incubated with the compounds in study for three minutes previous the experiments' begin.

3.2.3 Mitochondrial protein quantification

Mitochondrial protein was determined by the Biuret method [250]. This method is based in the chemical reaction of an alkaline solution of cooper with the polypeptide chain followed by a reduction of Cu^{2+} to Cu^{+}. The reaction was initiated by the addition of 2 mL of biuret reagent to 20 µl (for liver fractions) or 10 µl (for brain fractions) of sample and 10% of deoxycholic acid (DOC). After 15 min of incubation at room temperature the resulting color was read at 540 nm in a Spectronic 21 spectrophotometer (Bausch & Lomb, NY, USA). A calibration curve with BSA standards ranging from 0.5 to 2.0 mg/ml was performed.

3.2.4 Mitochondrial respiration

Oxygen consumption was measured polarographically with a Clark-type oxygen electrode, connected to a recorder in a thermostated water-jacketed closed chamber with magnetic stirring. The reactions were performed at 30 ºC in 1 ml of standard respiratory medium with 1 mg of liver or 0.5 mg of brain mitochondrial protein. For liver mitochondria, the reaction medium used was composed by 130 mM sucrose, 50 mM KCl, 2.5 mM KH_2PO_4, 5 mM Hepes and 2 mM $MgCl_2$; for brain mitochondria, the reaction medium was composed of 100 mM sucrose, 100 mM KCl, 2 mM KH_2PO_4, 5 mM Hepes and 0.01 mM EGTA (pH 7.4). State 2 respiration was initiated with 5 mM glutamate/2.5 mM malate (mitochondrial complex I substrates) and state 3 respiration by adding 125 nmol ADP to the mitochondrial fractions. Respiration rates were obtained assuming an oxygen concentration of 236 nmol O_2/ ml in the experimental medium at 30 ºC [251]. The respiratory state 2 (oxygen consumption before ADP addition – v2), state 3 (oxygen consumption in the presence of ADP – v3), state 4 (oxygen consumption after ADP phosphorylation- v4) and the respiratory control ratio (RCR = state 3/state 4) were calculated according to Chance and Williams [252]. The ADP/O ratio is expressed as the ratio between the amount of ADP added and the oxygen consumed during v3.

For the assessment of direct effects of resveratrol and estradiol over complex I or II, mitochondrial preparations were frozen in liquid nitrogen and kept at -80 ºC. At the day of the experiments, the preparations were frozen-thawed and sonicated on ice. Oxygen

consumption was measured by using a Clark-type oxygen electrode in 1ml of reaction medium, using 0.8 or 1.0 mg protein for brain and liver preparations, respectively. The direct effects of E2 and resveratrol on complex I-sustained respiration were obtained by using NADH as a substrate, while direct effects on complex II-sustained respiration were assessed in the presence of 5 mM of succinate plus 2 μM rotenone. KCN was added at the end of the experiments to confirm oxygen consumption through complex IV. K_M was determined using the initial rate of oxygen consumption versus the concentration of NADH in the presence of the compounds, according to Lineweaver-Burk plots.

3.2.5 Mitochondrial transmembrane electric potential

The mitochondrial transmembrane electric potential (ΔΨm) was indirectly measured, evaluating the transmembrane distribution of the lipophilic cation tetraphenylphosphonium (TPP^+) by using a selective electrode prepared as previously described by Kamo *et al.* [253], having a $Ag/AgCl_2$ — saturated electrode as reference. TPP^+ uptake was measured from the decrease in its concentration in the medium as sensed by the electrode [254]. Mitochondria (1 or 0.5 mg protein/ml, for liver or brain, respectively) were incubated in the standard reaction medium supplemented with 3 μM TPP^+ at 30 ºC, before energization with 5 mM glutamate/2.5 mM malate. After a steady-state distribution of TPP^+ was reached (after about 1 min of recording), 125 nmol ADP was added and ΔΨm fluctuations recorded. Each tested compound was pre-incubated with the mitochondrial fractions for 3 minutes before ADP addition. Several parameters were obtained, including the maximum ΔΨm, the ADP-induced depolarization (corresponding to the depolarization induced by the addition of ADP) and lag phase (the time needed for complete ADP phosphorylation to ATP). No correction was made to the passive binding of TPP^+ to the mitochondrial membranes because the objective of our experiments was to show changes in potential rather than absolute values.

3.2.6 Lipid peroxidation evaluation

Lipid peroxidation was evaluated following oxygen consumption using a Clark-type electrode (Yellow springs instruments model 5371, OH, USA) in a glass chamber with magnetic stirring, at 30 ºC. Mitochondria (1 mg and 0.8 mg for liver and brain, respectively) were pre-incubated for three minutes with the test-compounds or vehicle in 1 ml of medium containing 175 mM KCl and 10 mM Tris-Cl (pH 7.4), supplemented with 2 μM rotenone to avoid mitochondrial respiration induced by endogenous respiratory substrates. The alterations in O_2 tension were recorded in a potentiometric chart and oxygen consumption estimated assuming an oxygen concentration of 236 nmol O_2/ml at 30 ºC. Membrane lipid peroxidation was initiated by adding 1 mM adenosine diphosphate (ADP)/0.1 mM Fe^{2+} as oxidizing agents. Controls (basal levels) in the absence of ADP/ Fe^{2+} were performed under the same conditions. Lipid peroxidation was also evaluated by measuring thiobarbituric acid reactive

species (TBARS) generation according to a modified procedure [255, 256]. Aliquots of mitochondrial suspension were obtained 10 min after the addition of ADP/ Fe^{2+} and added to 0.5ml of ice-cold 40% trichloroacetic acid. Two ml of aqueous thiobarbituric acid (0.67%) was then added to samples. The mixtures were heated at 90 ºC for 10 min, cooled in ice and centrifuged at 850 x *g* for 10 min. The supernatant fractions were collected and the absorbance read at 530 nm in a Spectronic 21 spectrophotometer (Bausch & Lomb, NY, USA). The amount of TBARS formed was calculated using a molar extinction coefficient of 1.56×10^{-5} mol^{-1} cm^{-1} and expressed as nmol TBARS/mg protein [247, 255].

3.2.7 Hydrogen peroxide generation

Hydrogen peroxide (H_2O_2) generated by the respiratory chain was measured fluorimetrically using a modification of a previously described method [257]. Briefly, mitochondria (0.5 mg protein for brain and 1.0 mg protein for liver) were incubated in 1.5 ml of phosphate buffer, pH 7.4, containing 0.1 mM EGTA, 5 mM KH_2PO_4, 145 mM KCl, 30 mM Hepes, 0.1 mM homovalinic acid and 6 U/ml horseradish peroxidase. After 15 min, the reaction was stopped with 0.5 ml cold stop solution (0.1 mM gycine, 25 mM EDTA, pH 12) The compound in test was incubated for three minutes with the mitochondrial fractions. The reactions were initiated by adding 5 mM glutamate / 2.5 mM malate or 5 mM succinate as substrates. Rotenone and antimycin were used as complex I and complex III inhibitors. The fluorescence was measured at 312 nm as excitation and 420 nm as emission wavelengths in a Victor X3 Multilabel reader (Perkin Elmer, Waltham, USA). Hydrogen peroxide levels were calculated using a standard curve of H_2O_2, freshly prepared. The standards and the samples were incubated under the same conditions.

3.2.8 Glutathione peroxidase (GPx) activity measurement

GPx activity was determined spectrophotometrically at 340 nm according to the method of Flohe and Gunzler [258]. Briefly, the activity of GPx was measured after 5 min incubation of 200 µL from each sample in the dark with 0.5 mM phosphate buffer (0.25 M KH_2PO_4, 0.25 M K_2HPO_4 and 0.5 mM EDTA, pH 7.0), 0.5 mM EDTA, 1 mM GSH, and 2.4 U/mL glutathione reductase. The quantification occurred after the addition of 0.2 mM NADPH and 1.2 mM tert-butyl hydroperoxide and was measured at 30 ºC with continuous magnetic stirring, for 5 min, in a Jasco V560 UV/VIS spectrophotometer (Jasco Corp., Japan). The measurements were made against blanks prepared in the absence of NADPH. GPx activity was determined using the molar extinction coefficient 6220/M/cm [259] and expressed as nmol/min/mg protein.

3.2.9 Glutathione levels measurement

Mitochondria (0.2 mg protein for brain or liver mitochondria/assay) were deproteinized in 1.5 mL phosphate buffer (100 mM NaH_2PO_4/5 mM EDTA, pH 8) and 0.5 mL H_3PO_4 2.5%,

sonicated and centrifuged at 4º C and 108,726 x *g*, during 30 min. Supernatants were stored at -80 º C until glutathione determination. GSH and GSSG levels were determined with fluorescence detection (350 nm excitation, 420 nm emission) measured in Perkin Elmer LS 55 - Luminescence Spectrometer after the reaction of the supernatants from deproteinized mitochondria with o-phthaldehyde (OPT). GSH was determined after incubation of 100 µL supernatant with 1.8 mL phosphate buffer and 100 µL OPT, during 15 min. For GSSG content, 500 µL supernatant was incubated during 15 min, with 200 µL N-ethylmaleimide (NEM) before measurement. Finally 140 µL of the mixture was incubated with 1.76 mL NaOH (100 mM) and 100 µL OPT, during 15 min [260]. The GSG and GSSG contents were determined from comparisons with a linear GSG and GSSG standard curves, respectively.

3.2.10 Monitoring of phosphorylation rate

To investigate the effects of E2 and resveratrol on phosphorylation rates, external pH was measured. Mitochondria (1.5 mg protein) were suspended in 1.5 ml of the medium containing of 125 mM sucrose, 65 mM KCl, 2.5 mM $MgCl_2$, 2 mM KH_2PO_4, 0.5 mM Hepes, pH 7.2, 5 mM glutamate, 2.5 mM malate (pH 7.2). Phosphorylation was indirectely monitored using a pH electrode by measuring the pH increase associated with ATP synthesis by mitochondria, as previously described [248]. The phosphorylation was initiated by adding ADP 375 nmol to a mitochondrial suspension containing complex I substrate.

3.2.11 Complex I activity

The maximal activity of mitochondrial complex I [261] was assessed in disrupted mitochondrial preparations after three cycles of freezing/thawing. One hundred and ninety microlitres of reaction medium (25 mM KH_2PO_4, 5 mM $MgCl_2$, pH 7.5, 300 µM KCN), supplemented with 4 µM antimycin A, 3 mg/ml BSA, 60 µM coenzyme Q1, 160 µM DCPIP and 10 µg protein/ml of brain or liver mitochondria were transferred to a 96-well plate. One µM of Complex I inhibitor rotenone or 5 µl EtOH (vehicle) was added to the respective wells. Enzymatic activity of brain and liver preparations was measured through a decrease in absorbance of DCPIP after the addition of 100 µM fresh-prepared NADH in a Victor X3 plate reader (Perkin Elmer, Waltham, USA) at 600nm. Enzyme activity was calculated by using the slope during the linear phase (15 cycles). Specific complex I activity was calculated through the difference with the basal activity in the presence of rotenone.

3.3 Cell culture studies (Chapter 4.1.4)

3.3.1 Cell culture

Four distinct cell lines were used in this study. Two human breast cancer cell lines: MDA-MB-231 and MCF-7 (ATCC, Barcelona, Spain), one immortalized normal-like human breast cell line, MCF-12A (ATCC, Barcelona, Spain) and the human hepatoma HepG2 cell line (gently

supplied by Dr. Carlos Palmeira, CNC, Coimbra) The cell lines were cultured as monolayer, at 37 ºC in a humidified incubator with 5% CO_2, in the following culture media (Table 4).

Table 4: Culture media for the cell lines used in the present thesis

MDA-MB-231	DMEM:high glucose,1.5g $NaHCO_3$, 1% penicillin/streptomycin, 10% FBS	DMEM high glucose phenol red free, 1% AA, 10% Charcoal Stripped FBS
MCF-7	DMEM:high glucose, 1.5g $NaHCO_3$, 1% penicillin/streptomycin, 0.01 mg/ml human recombinant insulin, 10% FBS,	DMEM high glucose phenol red free, 1% AA, 0.01 mg/ml human recombinant insulin, 10% Charcoal Stripped FBS
MCF-12A	1:1 mixture of DMEM Ham's F12 medium, 20 ng/ml Human epidermal growth factor, 100 ng/ml cholera toxin, 0.01 mg/ml bovine insulin and 500 ng/ml hydrocortisone, 95%; penicillin/streptomycin, 5% FBS	1:1 mixture of DMEM Ham's F12 phenol red free, 20 ng/ml Human epidermal growth factor, 100 ng/ml cholera toxin, 0.01 mg/ml bovine insulin and 500 ng/ml hydrocortisone, 95%; 5% Charcoal Stripped FBS
HepG2	DMEM:high glucose, 1% penicillin/streptomycin, 10% FBS	N.A.

Low estrogen media was obtained by the use of charcoal stripped FBS instead of regular FBS and by the use of phenol red free DMEM. The removal of those two components is essential due to their estrogenic activity [262, 263].

3.3.2 Cell density assay evaluation

For analysis of cell density in the presence of regular FBS-medium or FBS-charcoal stripped-medium, we used the previously described sulforhodamine B (SRB) assay [264]. Cells in regular media were plated at 5,000 cells/ml in 48-well plates. Twelve hours later, the media was replaced by regular or low estrogen media and, every 24h, the cell media was removed. Cells were washed in PBS and ice-cold methanol supplemented with 1% acetic acid was added to each well. The same protocol was performed in the presence of different concentrations of E2 and coumestrol. Cells were fixed for at least one hour at -20 ºC and allowed to dry. After that, 250 µL of 0.05% SRB in 1% acetic acid solution was added to each well and incubated for 1h at 37 ºC. The wells were then washed with 1% acetic acid solution and allowed to dry. The amount of SRB attached to the cells protein was read after solubilization in 10 mM Tris pH 10 solution, at 545 nm in a Victor X3 plate reader (Perkin Elmer, Waltham, USA).

3.3.3 Evaluation of oxidative stress by MitoSox and 5-(and-6)-chloromethyl-2', 7'-dichlorodihydrofluorescein diacetate (CMH_2DCFDA)

HepG2 cells were seeded at 40,000 cells/ml and treated with the test compounds for 24h. Cells in PBS containing 5 mM glucose were incubated with 2.7 µM Mitosox (Invitrogen, Madrid, Spain) for 15 min at 37 ºC in the dark and fluorescence read at 510/580 nm emission/excitation wavelengths, respectively. In order to evaluate the global oxidative stress in the cells, HepG2 were incubated with 13 µM CMH_2DCFDA in PBS containing 5 mM glucose and the kinetic of fluorescence emission was read during 30 minutes at 495/520 nm

emission/excitation wavelengths, respectively, in a Victor X3 plate reader (Perkin Elmer, Waltham, USA).

3.3.4 Protein analysis by Western blotting

Cells were collected after treatment with cell lysis buffer (Cell Signaling, Danvers, MA, USA) supplemented with 1 mM DTT, 100 µM PMSF and protease inhibitor cocktail (containing 1 g/ml of leupeptin, antipain, chymostatin and pepstatin). After denaturation at 95 ºC for 5 min in Laemmli buffer (from BioRad, CA, USA), equivalent amount of proteins (20 or 30 µg) were separated by electrophoresis on 8% or 12% SDS-polyacrylamide (Bio-Rad, CA, USA) (SDS-PAGE) gels during 1 hour at 30 mA/gel at room temperature and electrophoretically transferred to a polyvinylidene difluoride (PVDF) membrane at 100 V during 90 min at 4 ºC. Membranes were blocked in 5% non-fat milk or 2% BSA in Tris Buffered Saline with Tween 20 (TBST) for one hour at room temperature, depending on the antibodies used, and incubated with primary antibodies overnight (Table 5). Membranes were then washed three times with TBST and incubated with secondary antibodies for one hour at room temperature. After 3 washes with TBST for 5 minutes each, membranes were incubated with the ECF detection system (from Amersham, GE Helthcare, Carnaxide, Portugal) and imaged with a Versa Doc device (Bio-Rad, CA, USA) or with an UVP, Biospectrum 500 Imaging System (UVP, Upland, CA, USA). Densities of each band were calculated with Quantity One Software (Bio-Rad, CA, USA). Membranes were also stained with Ponceau reagent to confirm equal amount of protein loading in each lane.

Table 5: List of primary antibodies used in this part of this work

Primary Antibody	Dilution	Host specie	Company	Company code
ER α	1:250	Rabbit	Abcam	ab2746
ER β	1:1,000	Rabbit	Abcam	ab3577
SOD 2	1:1,000	Rabbit	Abcam	ab13533
HSP 90	1:1,000	Rabbit	Cell Signaling	4877
GPx	1:1,000	Rabbit	Abcam	ab22604

Antibodies were prepared in 1% milk in TBST.

3.3.5 Mitochondrial transmembrane polarization and morphology by vital epifluorescence microscopy

MDA-MB-231, MCF-7 and MCF-12A cell lines were plated on glass-bottom dishes and cultured in regular or low estrogen media. Twenty-four hours after cells were incubated with 100 nM tetramethylrhodaminemethylester (TMRM) during 30min at 37 ºC in the dark. After the incubation period, media was replaced by Krebs solution (1 mM $CaCl_2$, 132 mM NaCl, 4 mM KCl, 1.2 mM Na_2HPO_4, 1.4 mM $MgCl_2$, 6 mM glucose, 10 mM HEPES, pH 7.4).

Epifluorescence images were obtained using the Metamorph software on Nikon Eclipse TE2000U microscope (Nikon, Melville, USA).

3.4 *Ex-vivo* studies in a blood-brain barrier model (Chapter 4.2)

3.4.1 Animals

Animal procedures were carried out by trained personnel and performed in accordance with Association for Assessment and Accreditation of Laboratory Animals (AAALAC) regulations and the US Department of Agriculture Animal Welfare Act. Animal protocols were approved by the Institutional Animal Care and Use Committees of the University of Minnesota, USA (Protocol #1007A86652). Male Wistar rats (8-10 weeks of age, average weight 250g) were also purchased from Charles River Laboratories (Portage, MI, USA). Male and female ERKO-α (estrogen receptor α-deficient, B6.129-Esr1tm1Ksk N10), ERKO-β (estrogen receptor β-deficient, B6.129-Esr2tm1Unc N9), and wild-type mice (C57BL/6 background) were a generous gift from Dr. Kenneth Korach (National Institute of Environmental Health Sciences (NIEHS), NC, USA). Mice were 10 weeks old with an average body weight of 20 g for females and 25 g for males.

3.4.2 Brain capillary isolation

Brain capillaries were isolated from rats and mice according to a previously published protocol [265]. . Briefly, for each preparation, 10 rats or 20 mice were sacrificed by CO_2 inhalation and decapitated. Brains were harvested, dissected and homogenized in ice-cold PBS buffer (2.7 mmol/L KCl, 1.46 mmol/L KH_2PO_4, 136.9 mmol/L NaCl, 8.1 mmol/L Na_2HPO_4, 0.9 mmol/L $CaCl_2$, and 0.5 mmol/L $MgCl_2$ supplemented with 5 mmol/L D-glucose, 1 mmol/L sodium pyruvate, pH 7.4). The homogenate was mixed with Ficoll (final concentration 15%) and centrifuged at 5,800 x g for 20 min at 4 ºC. After resuspending the pellet in 1% BSA, the capillary suspension was passed over a glass bead column. Capillaries adhering to the glass beads were collected by gentle agitation in 1% BSA. Capillaries were then washed with PBS and used for experiments.

3.4.3 Immunofluorescence

Freshly isolated rat brain capillaries adhering to glass cover slips were fixed for 15 min with 3% paraformaldehyde 0.2% glutaraldehyde at room temperature. After washing with PBS, samples were permeabilized for 30 min with 0.1% (v/v) Triton X-100 in PBS and blocked with 1% BSA in PBS. Capillaries were incubated for 1 h at 37 ºC with the primary antibody to GLUT-1. After washing with 1% BSA, capillaries were incubated for 1h at 37ºC with the corresponding Alexa Fluor® 488-conjugated secondary IgG (1:1000, 2 mg/mL; Invitrogen, Eugene, OR, USA). Negative controls were incubated with secondary antibody alone. Nuclei were counterstained with 5 mg/mL propidium iodide for 15 min. GLUT-1 staining was

visualized using a Nikon C1 confocal laser scanning microscope (Nikon C1, Nikon TE2000 inverted microscope, 40x/1.3 NA oil objective, 488 nm (Argon laser), 543 nm (HeNe laser; Nikon Instruments, Melville, NY, USA).

3.4.4 Protein expression semi-quantification by Western blot

Brains were homogenized in lysis buffer (Sigma) containing complete protease inhibitor (Roche, Mannheim, Germany). Homogenized samples were centrifuged at 10,000 x g for 15 min; denucleated supernatants were used as brain and capillary lysates. Crude membrane fractions from capillaries were obtained by the centrifugation of denucleated supernatants at 100,000 x *g* for 90 min. Pellets of crude plasma membranes were resuspended in buffer and protein concentrations were determined. Western blots were performed using the Invitrogen NuPage Bis-Tris electrophoresis and blotting system (Invitrogen, Carlsbad, CA, USA). After protein transfer, blotting PVDF membranes were blocked and incubated with primary antibody to GLUT-1 (1:1,000, 1 µg/mL) or β-actin (1:1,000, 1 µg /mL). Membranes were washed and incubated with horseradish peroxidase-conjugated ImmunoPure secondary IgG (1:15,000; Pierce, Rockford, IL, USA) for one hour. Proteins were detected using SuperSignal West Pico Chemoluminescent Substrate (Pierce). Bands were visualized and recorded using a BioRad Gel Doc 2000 gel documentation system (BioRad, Hercules, CA, USA). Densitometric analysis of GLUT-1 band intensity and digital analysis of the molecular weight were performed with QuantityOne 1-D v4.6.5 software (BioRad). Data were normalized to β-actin loading controls. Molecular weight marker RPN800 used in the same run was from GE Healthcare (Piscataway, NJ, USA).

3.5 *In-vivo* studies (Chapter 4.3)

3.5.1 Experimental design

For the present thesis two distinct, *in vivo* protocols were performed:

I. Mitochondrial effects of E2 and coumestrol on ovariectomized (OVX) female rats.

II. Mitochondrial effects resulting from a chemical-induced model of menopause – 4-vinylcyclohexene diepoxide, VCD and mitochondrial effects of E2 and coumestrol in a chemical induced model of menopause.

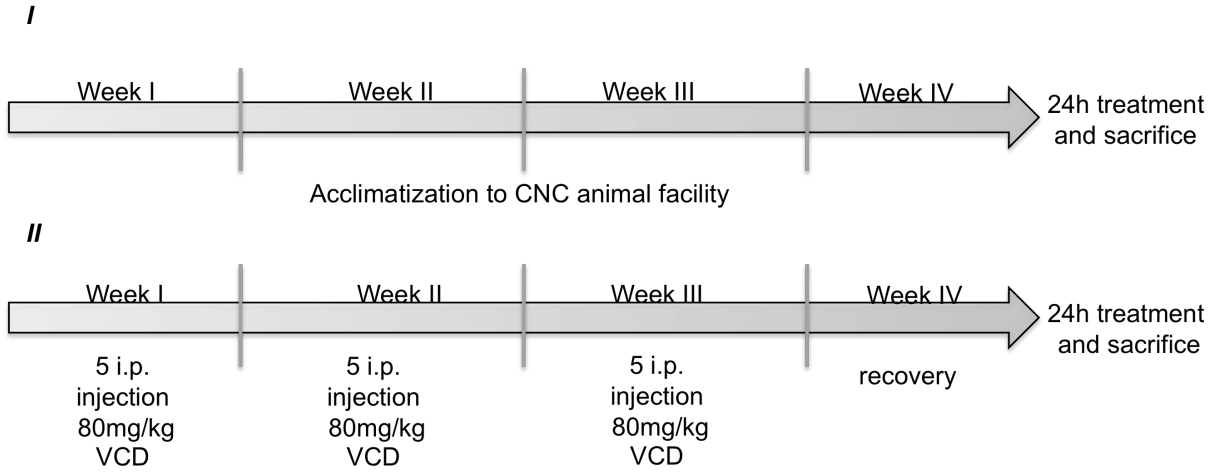

Figure 6: Experimental design of the *in vivo* studies performed.
In study I, 20 OVX rats purchased from Charles River, Laboratories were allowed to acclimate in the CNC animal facility for three weeks. Experiments were performed when animals were 16-weeks old. Animals were injected intraperitoneally with 30 µg/kg of E2, coumestrol or injected with vehicle. Twenty-four hours after the treatment animals were sacrificed. For the second study, animals received daily injections, during 5 days, for 3 weeks with 80 mg/kg of VCD. Animals were allowed to recover for one week, treated with 30 µg/kg of E2, coumestrol or vehicle and sacrificed 24h later.

In our animal facility at the CNC, University of Coimbra, Portugal, animals for each study were housed in type III-H cages (Tecniplast, Italy) with irradiated corn cob grit bedding (Scobis Due, Mucedola, Italy), following environmental requirements, with *ad libitum* access to food (2014, Harlan, Barcelona, Spain) and water (acidified at pH 2.6 with HCl) and maintained at constant temperature (22 ºC) and humidity with a 12h light/dark cycle. In study I, one week prior the experiments, a wireless temperature transponder (IPTT-200; 14 mm in length, 2 mm in diameter; BMD, Einsteinberg, The Netherlands, gently supplied by Doctor Felix Carvalho, University of Porto) was implanted in isoflurane-anesthetized animals. During the experiments animal temperature was obtained at different time points. Animal handling and sacrifice followed the procedures from the Federation of European Laboratory Animal Science Associations (FELASA).

3.5.3 Blood analysis

Blood was collected in sterile tubes. After blood clot formation, serum was obtained through centrifugation at 1,600 x *g* at 4 ºC, for 10 min. The obtained supernatant was transferred to microtubes and centrifuged again at 16,000 x *g* at 4 ºC, for 5 min (in a Eppendorf 5415 R centrifuge, Hamburg Germany). Serum was then analyzed by a certified laboratory (Faculty of Pharmacy, University of Coimbra, Laboratory of Clinical Analysis). The operators were blinded to each sample. Plasma was obtained after blood collection in proper EDTA-containing tubes (Aquisel, Spain) followed by 3,500 x *g* centrifugation during 10 min at 4 ºC. The supernatant was collected and frozen at -80 ºC for later measurement of E2 content in each sample with Estradiol EIA kit from Cayman (Item No 582251, Ann Harbor, MC, USA).

3.5.4 Electron microscopy

After collecting and washing, a small slice (~3mm) of brain and liver tissue were cut with a scalpel and fixed in 3% glutaraldeyde in phosphate buffer (100 mM NaH_2PO_4, pH 7.3). Samples were then post-fixed with 1% osmium tetroxide, dehydrated in alcohol-containing solutions and embedded in Spurr's resin. Ultrathin sections were obtained on a LKB ultramicrotome Utrotome III (GE, Healthcare, Buckinghamshire, UK), stained with methanolic solution of uranyl acetate plus lead citrate. Electron micrographs were obtained usinga JEOL Jem_100SX electron microscope (JEOL, Tokyo, Japan), operated at 80 kV. The operator was blinded to each treatment group.

3.5.5 Mitochondria isolation

Brain and liver mitochondria were isolated as described in section 3.2.2.

3.5.6 Mitochondrial respiration, ΔΨ and complex I activity

were measured as described in sections 3.2.4, 3.2.5 and 3.2.11 respectively.

3.5.7 Evaluation of oxidative stress

Aconitase, a Krebs cycle enzyme which contains ROS-susceptible Fe-S clusters, is often used as an indirect measurement of oxidative stress [266]. Two hundred micrograms of mitochondrial protein was diluted in 600 µl of buffer containing 50 mM Tris (pH 7.4) and 0.6 mM of $MnCl_2$, sonicated for 10 s and centrifuged at 16,000 x*g* for 5 min at 4 ºC (in a Eppendorf 5415 R centrifuge, Hamburg Germany). After the acquisition of a 30 s baseline, the assay began with the addition of 20 mM isocitrate to 200 µL of obtained supernatant plus 800 µL 50 mM Tris pH 7.4, 0.6mM $MnCl_2$. Absorbance was read in a Jasco V-560 spectophotometer (Jasco Inc., Easton, MD, USA). The temperature was set at 30ºC during the experiment. The enzyme activity was calculated through the mean of the slopes from both duplicates, using the extinction coefficient of ε_{240}=3.6 $mM^{-1}cm^{-1}$, values were normalized to the protein amount and expressed as U/mg protein/min. One unit (U) is defined as the amount of enzyme necessary to produce 1 µM cis-aconitate per minute.

Other parameters measured as end-points for oxidative stress included hydrogen peroxide generation and TBARS, which were measured as described in the sections 3.2.7 and 3.2.6, respectively. Mitochondrial preparations (1mg/mg) were collected in PBS and MDA and Vit E were also quantified by HPLC using a Gilson device with modular components: Pump 306, Manometric module 805 and Autoinjector 234, Lewis Center, OH, USA, and with an appropriate fluorescence detector (FP-2020/2025, Jasco, Tokyo, Japan).

3.5.8 Tissue harvesting

Once the animals were decapitated, liver and brain were quickly washed in PBS in order to exclude the blood excess, weighted and frozen in liquid nitrogen and stored at -80 ºC prior to tissue sample analysis.

3.5.9 Tissue extraction for protein content evaluation

Frozen tissue was thawed and homogenized in a glass pestle hand-held homogenizer in 20% (w/v) Ripa buffer (Sigma, St Louis, MO), supplemented with 5 µg/100 mg (tissue) of protease inhibitors cocktail. The suspension was kept in ice for 20 minutes and then centrifuged at 14,000 x *g* for 5min at 4º in order to remove cellular debris. The protein concentration of the supernatant was measured by Bradford assay [267] using BSA as standard. This method is based on the shift in maximum absorption of Coomassie Brilliant Blue dye from 465 to 595 nm upon binding to protein.

3.5.10 Protein analysis by Western Blotting

This protocol was performed as described in section 3.3.4, using the antibody cocktail shown in table 6.

Table 6: List of primary antibodies used in this part of the work

Primary Antibody	Dilution	Host specie	Company	Company code
Total OXPHOS	1:1,000	Rabbit	MitoSciences	MS604

The cocktail contained antibodies against Complex I subunit NDUFB8, 20kD, Complex II subunit 30kDa, Complex III subunit Core 2, ATP synthase subunit alpha. The antibody cocktail was prepared in 1 % milk in TBST.

3.6 Statistical analysis (Chapter 4)

Data obtained for this thesis was analyzed using the software Graph Pad Prism version 5.0c for Macintosh. All data were accessed for normality with Kolmogorov-Smirnov and Shapiro-Wilk tests. Data are expressed as mean ± SEM for the number of experiments/animals indicated in the legends of the figures. Multiple comparisons were performed using one-way analysis of variance (ANOVA) followed by Bonferroni multiple comparison posthoc test. T-test was used when only two conditions were compared. Significance was accepted when p value < 0.05 was obtained.

4. Results

4.1 *In vitro* effects of selected PE in comparison with E2 in isolated rat brain and liver mitochondria and in cell lines

4.1.1 Background and objective

The use of mitochondrial preparations of different organs to access the toxicity associated with different xenobiotics is widely recognized [191]. We restricted this work to four phytoestrogens to be studied in comparison with E2. Since one of the objectives of this thesis is to overcome hot flashes based in the hypothesis of the impaired glucose delivery, we excluded the widely studied PEs: genistein and daidzein, because those compounds inhibit the glucose transport [268, 269]. In addition, these compounds have been largely study in terms of mitochondrial function either in isolated fractions or in cell culture [199, 270-272]. From a larger list of available PE, resveratrol, coumestrol, enterodiol and enterolactone were selected.

This section is divided in 3 main subsections: in the first one, all the PEs were compared in terms of mitochondrial effects and protection against lipid peroxidation. For this objective, brain and liver mitochondrial fractions were isolated from male rats to exclude variability resulting from the estrus cycle in females. From this set of a data, a second section involved the use of the cell line HepG2 as a more complex model to investigate antioxidant protection by a selected PE vs. E2. Finally, in the third section, the same selected PE was compared with E2 in terms of proliferation of breast cancer cell lines.

4.1.2 Effects of PE on mitochondrial bioenergetics and lipid peroxidation

Several reports demonstrated that estrogens regulate mitochondrial function [273-275]. Mitochondria can be relevant targets of estrogens and PE not only due to the high lipophilicity of these compounds, but also due to the presence of ER in these organelles [276, 277].

Two parameters were used to access the quality of the mitochondrial fraction in the presence of PEs: the RCR and ADP/O. The RCR is a measure of coupling between substrate oxidation and phosphorylation. The ADP/O is a measure of the efficiency of the mitochondrial phosphorylative apparatus. The ADP/O is obtained through the ratio of nmol of ADP added to the mitochondrial suspension and the natoms of oxygen consumed during state 3 [278]. In terms of RCR, no difference was observed. However, coumestrol improved the phosphorylation efficiency of brain mitochondria shown by an increase in the ADP/O parameter from 3.6 ± 0.5 to 4.8 ± 0.6 nmol ADP/natm O (Table 7). The ADP-induced depolarization in liver mitochondria was also increased by coumestrol (Table 8).

Table 7: Phytoestrogens on mitochondrial respiratory parameters

	Brain				Liver			
	State 3	State 4	RCR	ADP/O	State 3	State 4	RCR	ADP/O
Control	58.4 ± 6.1	17.7 ± 1.4	3.5 ±0.3	3.6 ± 0.3	73.5 ± 8.7	16.6 ± 3.5	4.9 ± 0.8	3.6 ± 0.5
Coumestrol	46.4 ± 7.6	16.2 ± 2.0	3.1 ±0.3	4.8 ± 0.7 *	60.5 ± 6.7	12.2 ± 1.5	5.0 ± 0.2	4.4 ± 0.5
Enterolactone	48.5 ± 11.0	16.0 ± 2.2	3.7 ± 0.5	3.7 ±0.5	56.5 ± 8.1	13.1 ± 2.2	4.4 ± 0.2	4.7 ± 0.5
Enterodiol	53.1 ± 10.9	16.3 ± 1.2	3.6 ± 0.7	4.4 ± 0.9	62.3 ± 6.7	11.2 ± 1.6	5.7 ± 0.4	4.2 ± 0.5

Mitochondrial fractions were incubated with PE and several respiratory parameters were evaluated. State 3 and 4 values are in nmol O_2/min/mg protein. Data represent mean ± SEM of 5 to 6 different experiments. * $p<0.05$ with control values.

Table 8: Phytoestrogens on mitochondrial transmembrane potential

	Brain			Liver		
	Max ΔΨ (-mV)	Depol. (-mV)	lag phase (min)	Max ΔΨ (-mV)	Depol. (-mV)	lag phase (min)
Control	177.1 ± 2.6	12.6 ± 1.2	1.1 ± 0.1	210.0 ± 1.4	20.2 ± 1.7	1.1 ± 0.1
Coumestrol	174.5 ± 1.9	9.9 ± 0.9	1.3 ± 0.2	209.1 ± 2.3	24.5 ± 1.4 *	1.1 ± 0.1
Enterolactone	173.3 ± 4.2	11.9 ±1.9	1.3 ± 0.2	208.3 ± 2.1	27.0 ± 0.4 *	1.3 ± 0.1
Enterodiol	176.7 ± 3.9	10.4 ± 1.0	1.2 ± 0.1	205.5 ± 1.5	22.5 ± 0.8	1.2 ± 0.1

Mitochondrial fractions were incubated with PEs and mitochondrial transmembrane electric potential was evaluated. Data represent mean± SEM of 5 to 6 different experiments. *$p<0.05$ with control values.

The PE in test did not cause any significant mitochondrial toxicity, in opposition to estradiol which induced in isolated liver mitochondria a decrease in state 3, RCR and ADP/O for the same concentration (25 μM) [248].

On the other hand, the antioxidant effects of PEs on lipid peroxidation were also tested. Although being an important source of ROS, mitochondria are protected from oxidative stress by several mitochondrial antioxidant systems such as superoxide dismutase (MnSOD) or glutathione peroxidase [279, 280]. In order to evaluate the role of the tested compounds as potential antioxidants, the mitochondrial fractions were incubated with each PE in study prior to the addition of a pro-oxidant pair (ADP/Fe^{2+}), which caused mitochondrial membrane lipid peroxidation and TBARS production.

The effects of PEs were compared with those of E2, known to have antioxidant proprieties [281]. At this point, we also introduced another polyphenol with estrogenic activity: resveratrol. Considering resveratrol as a phytoestrogen is still controversial, but its characteristics such as being a natural compound, with a molecular mass close to E2 and possessing estrogenic activity in different tissues, provided support to this inclusion [80, 282, 283]. Several reports indicate resveratrol as a support to a healthier aging [284-286], justifying its use in this work as well.

As observed (Fig. 7), the pro-oxidant pair ADP/Fe^{2+} induced an increase in TBARS generation. Mitochondria pre-incubation with coumestrol and resveratrol and E2 (only for liver preparations) reduced the formation of these lipid peroxidation byproducts. Coumestrol

and resveratrol reduced TBARS content in brain from 6.2 ± 0.9 to 3.2 ± 0.6 and 2.6 ± 0.2 nmol/mg protein/10min, respectively. In liver, the decrease in TBARS was from 6.9 ± 0.9 to 1.2 ± 0.7 and 0.6 ± 0.4, nmol/mg protein/10min for coumestrol and resveratrol, respectively.

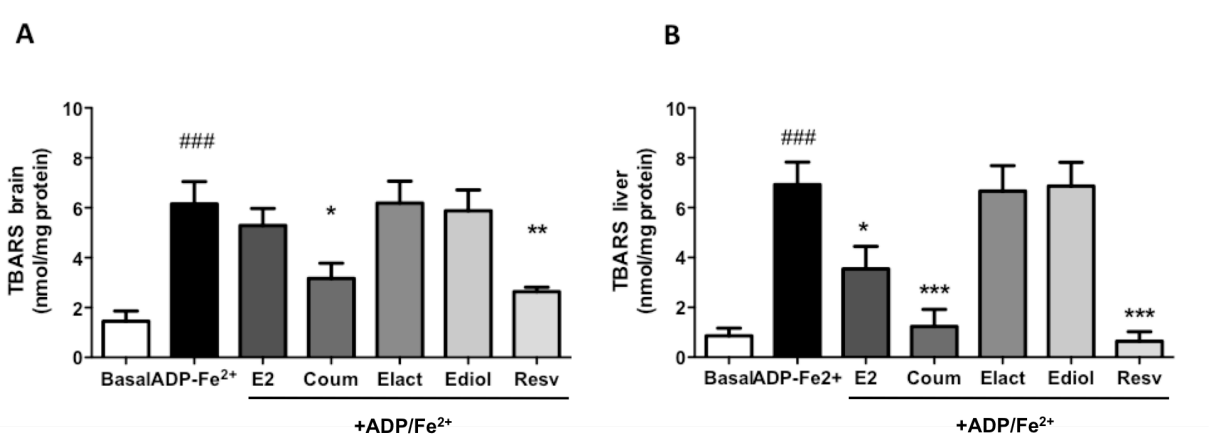

Figure 7: Effects of 25 µM PE and E2 on TBARS formation induced by the pro-oxidant pair ADP/Fe^{2+} in brain and liver mitochondria.
Lipid peroxidation and TBARS formation were induced by the pro-oxidant pair ADP/Fe^{2+}, as described in the material and methods section. The data represent the mean ± SEM of four to six experiments. Statistical significance: ### p<0.001 compared with the respective basal levels, * p<0.05, **p<0.01, ***p<0.001 compared with mitochondrial preparations in the presence of the ADP/Fe^{2+}. Legend: E2 - estradiol, Coum - coumestrol, Elact - enterolactone, Ediol - enterodiol and Resv - resveratrol.

Based on the higher antioxidant activity, we focused our study on coumestrol and resveratrol for the next tasks. Coumestrol choice is also justified by the low mitochondrial toxicity.

4.1.3 Resveratrol effects on mitochondrial bioenergetics and on oxidative stress: Investigation of the role of gender

In the first part of this task, we aimed to evaluate the effects of resveratrol on liver and brain mitochondria of male and female rats in order to study the role of gender in its potential toxicity.

The redox active polyphenol compound resveratrol (3,5,4'–trihydroxy-trans stilbene) was firstly identified in roots from white hellebore (*Veratrum album*) and later in roots from japanese knotweed (*Polygonum cuspidatum*) [287]. Resveratrol is also found in grapes (*Vitis vinifera*), grape juice, wine berries (*Vaccinium macropon*) and peanuts (*Archis hypogaea*) [288, 289]. Resveratrol has been shown to trigger several physiological effects in animal models of disease, resulting in cancer prevention, microvascular and neuroprotection, as well as in antidiabetic effects [290]. Resveratrol is one of the main components of red wine, the consumption of which is associated with a lower incidence of heart failure in France [291]. The protective effects are associated with antioxidant proprieties that were confirmed in the heart in different models [292], including lipopolysaccharide (LPS)-induced oxidative stress [293] and doxorubicin (DOX)-induced cardiotoxicity [294].

Resveratrol crosses the blood brain barrier (BBB) [295], demonstrating neuroprotective effects in several disorders such as cerebral ischemia and Alzheimer's disease [290]. Resveratrol also increases spatial memory performances in the circular platform tasks in primates [296], thus demonstrating cognitive and neuroprotective effects [297, 298]. Fukiu *et al.* showed that resveratrol induces the expression of mitochondrial superoxide dismutase (SOD2) consequently reducing mitochondrial oxidative stress and damage in neurons [299]. Specifically in the liver, resveratrol up-regulates the expression of glucogenic genes by attenuating insulin signalling and by deacetylating FOXO1 [300]. Resveratrol also decreases fibrosis and promotes hepatocyte regeneration, which increased the survival of mice during cholestatic liver injury [301].

Although the protective effects of resveratrol on heart mitochondria have been described [302], mitochondrial-specific studies are lacking in liver and brain mitochondria. To support the evidence that resveratrol presents direct effects on mitochondria, we have isolated fractions from rat liver and brain and investigated whether resveratrol alters mitochondrial bioenergetics and prevents induced oxidative damage. A second important question was whether resveratrol-induced mitochondrial effects were gender-dependent. To answer this latter question, mitochondrial fractions were isolated from female and male rats. Although isolated mitochondrial fractions are a recognized model to measure compound toxicity [191], the large majority of experiments is performed with mitochondrial fractions from male animals. Differences between mitochondrial fractions from male and female animal models may influence the final outcome of chemical-biological interactions at the mitochondrial level, which is the rationale for using mitochondria from both genders in this study. The concentrations of resveratrol used are within the concentration range used by others [303-306]. We finally compared resveratrol and E2 regarding the inhibition of mitochondrial complexes I and V.

4.1.3.1 Resveratrol decreases lipid peroxidation in brain and liver mitochondria

The effects of resveratrol on oxidative damage were assessed by mitochondrial membrane peroxidation induced by the pro-oxidant pair ADP/Fe^{2+} (Fig. 8). This effect was evaluated by following oxygen consumption (Fig. 8A) and TBARS formation (Fig. 8B). In the absence of resveratrol and after the addition of ADP/Fe^{2+}, a two-phase kinetic in oxygen consumption was observed: an initial phase with a slower oxygen consumption that was followed by a rapid oxygen consumption phase [256]. The initial phase was likely due to the time needed to generate the perferryl ion complex that has been suggested to be the responsible for the initiation of lipid peroxidation. The faster oxygen consumption probably resulted from the oxidation of polyunsaturated fatty acid acyl chains in the membrane phospholipids by ROS, leading to the propagation of lipid peroxidation [256].

As observed in figure 8A, in both genders and for both organs, the pro-oxidant pair ADP/Fe^{2+} induced an increase in oxygen consumption that is decreased in the presence of resveratrol to nearly basal levels. The data are in accordance with the results obtained by measuring TBARS formation.

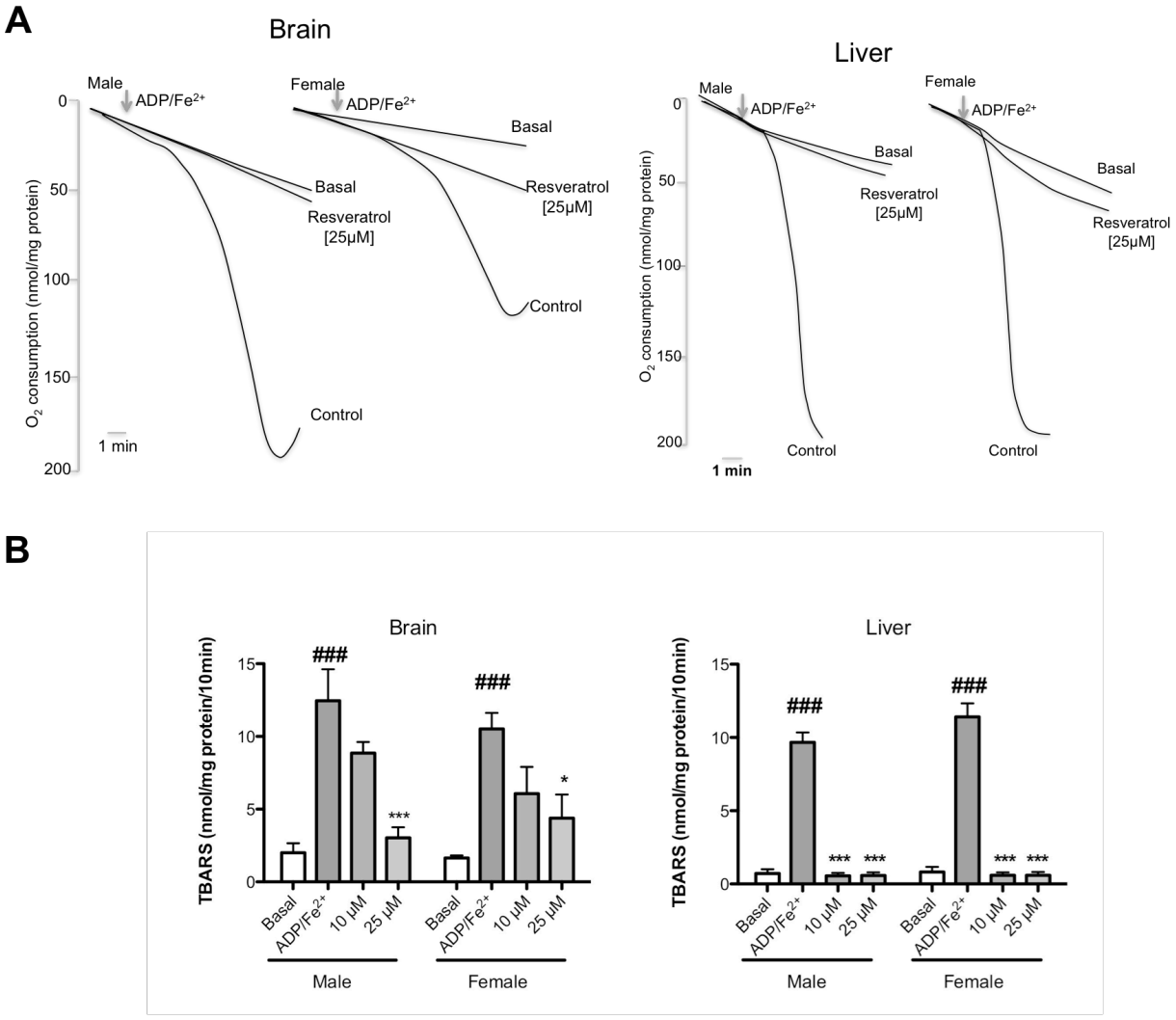

Figure 8: Effects of resveratrol on membrane lipid peroxidation of brain and liver mitochondria induced by the pro-oxidant pair ADP/Fe^{2+}.
ADP/Fe^{2+}-induced lipid peroxidation was evaluated following oxygen consumption resulting from membrane lipid peroxidation (A) and TBARS colorimetric assay (B). Panel (A) represents a typical recording of mitochondrial preparations from brain and liver of male and female rats. The data in (B) represent the mean ± SEM of four to six independent experiments. Statistical significance: ### $p<0.001$ compared with the respective basal levels, * $p<0.05$, *** $p<0.001$ compared with mitochondria in the presence of the pair ADP/Fe^{2+}.

Pre-incubation with 25 µM resveratrol led to a decrease in TBARS formation in both organs and genders (brain mitochondria, males: 12.5 ± 2.5 vs. 3.0 ± 0.7, brain mitochondria from female rats: 10.5 ± 1.1 vs. 4.4 ± 1.6; liver mitochondria from male rats: 9.7 ± 0.7 vs. 0.6 ± 0.2, liver mitochondria from females: 11.4 ± 0.9 to 0.6 ± 0.2 nmol TBARS /mg protein, absence vs. presence of resveratrol, Fig. 9B). For the lowest concentration used (10µM), resveratrol had no effect on brain mitochondrial fractions, as opposed to liver mitochondria, where

protection against lipid peroxidation-induced TBARS generation was observed for both genders.

4.1.3.2 Resveratrol increases mitochondrial H_2O_2 production in liver

Liver and brain mitochondria from male and female rats were incubated with resveratrol in order to investigate its effects on hydrogen peroxide generation by the respiratory chain. In both genders, treatment of mitochondria with rotenone (a complex I inhibitor) or antimycin A (a complex III inhibitor) maximally induced H_2O_2 generation, as expected [307, 308] (Fig. 9). When analyzing H_2O_2 production in basal conditions (Fig. 9), liver mitochondria from female rats have generally a lower basal H_2O_2 generation when compared with preparations from male rats. The same effect was not observed in brain mitochondrial fractions.

When resveratrol was added to the different experimental groups, some interesting effects were observed. Once added to liver mitochondria, resveratrol increased H_2O_2 generation when glutamate-malate was used alone (Fig. 9B) in preparations from both male and female rats. In brain mitochondrial fractions (males only), resveratrol amplified the effect of antimycin A, increasing H_2O_2 generation (Fig. 9A). We also compared directly liver and brain mitochondrial fractions from both genders in terms of basal activity of glutathione peroxidase (GPx) and glutathione content. In general, liver mitochondria have increased GPx activity, with fractions from females having the highest activity (345.80 ± 46.01 vs 216.40 ± 17.71 U/mg protein in mitochondrial fractions from males, Fig. 10).

No differences were observed in terms of GSH, GSSG or GSH/GSSG ratio (Table 9). The total glutathione content was also similar in liver mitochondria from males (0.88 ± 0.04 nmol/mg protein) vs. females (0.83 ± 0.03 nmol/ mg protein).

4.1.3.3 Resveratrol decreases state 3 respiration in brain mitochondria

We next investigated direct effects of resveratrol on liver and brain mitochondrial respiration in fractions isolated for both genders. In the absence of resveratrol, no differences between genders were observed.

The addition of resveratrol [10 or 25μM] to freshly isolated brain mitochondria induced a decrease in state 3 respiration from 44.0 ± 1.8 to 33.5 ± 3.5 nmol O_2/min/mg protein (preparation from males) and from 44.1 ± 3.0 to 32.8 ± 3.7 nmol O_2/min/mg protein (preparations from female animals, Fig. 11A). The alterations in respiration state 3 in brain mitochondria were not reflected in the RCR (Fig. 12C), which may be due to the fact that the oxygen consumption during state 4 shows a trend for a decrease induced by resveratrol ($p=0.059$, Fig. 11B). No alterations were observed for liver mitochondria (Fig. 11). The ADP/O was not altered by resveratrol in any of the groups studied (Fig. 11D).

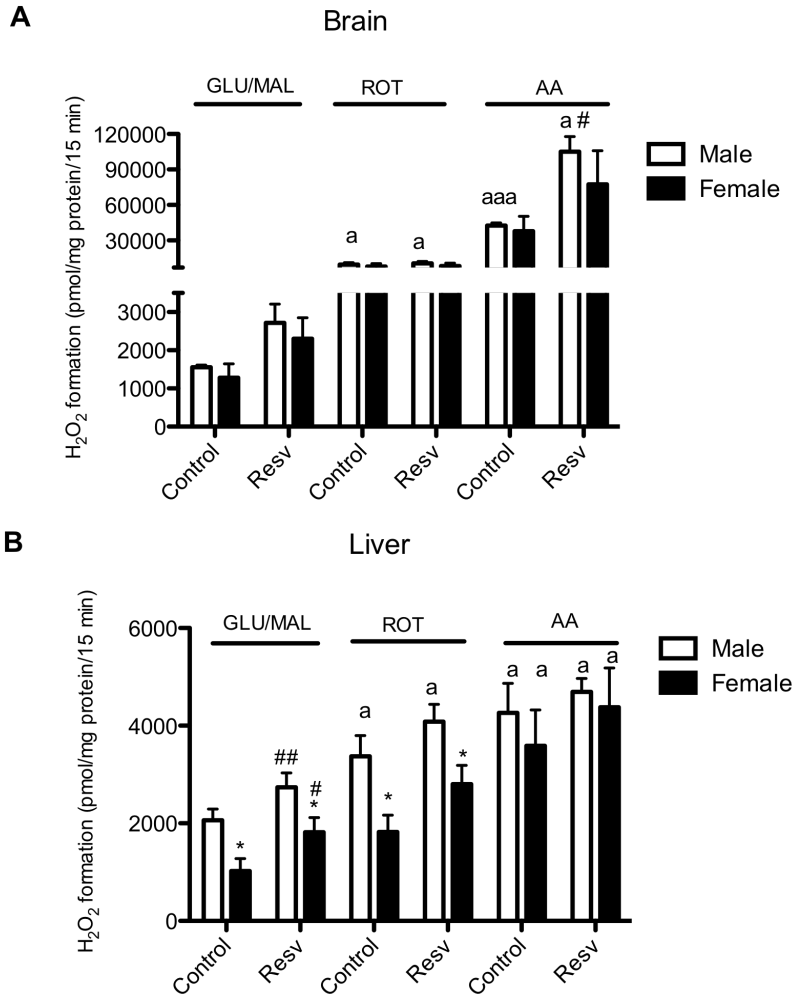

Figure 9: Effect of resveratrol on mitochondrial hydrogen peroxide (H_2O_2) production.
The production of hydrogen peroxide by the mitochondrial respiratory chain was evaluated as described in the materials and methods section. Mitochondrial fractions from brain (0.5 mg) and liver (1 mg) of male and female Wistar-Han rats were incubated with standard respiratory medium in the presence or absence of resveratrol. Basal levels of H_2O_2 production were determined in the absence of mitochondrial substrates. Glutamate/malate (5 mM/2.5 mM) was used as substrate. Rotenone (1.0 µM) and antimycin A (0.5 µM) were used to increase H_2O_2 production. Data represent mean ± SEM from five independent experiments. Statistical significance: * $p< 0.05$, when compared with the other gender counterpart, # $p<0.05$ or ## $p< 0.01$ when compared with respective control, a $p<0.05$ or aaa <0.001 when compared with the absence of inhibitors. Legend: AA – antimycin A, Glu/Mal – glutamate/malate, Resv- resveratrol, ROT- rotenone.

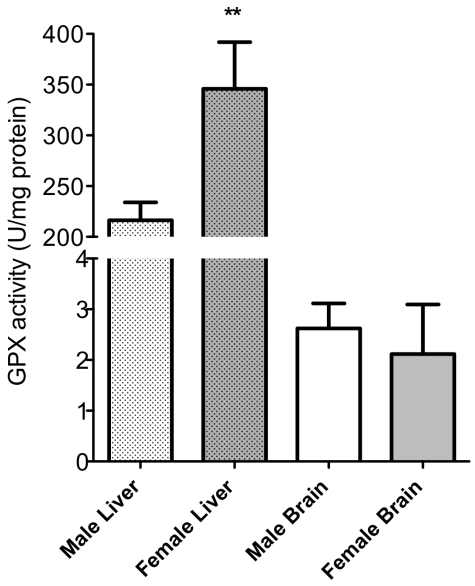

Figure 10: Gender-related differences on glutathione peroxidase (GPx) activity in brain and liver mitochondria.
Glutathione peroxidase activity was evaluated as described in the materials and methods section. Data represent mean ± SEM of 3 to 6 different experiments. Statistical significance: ** $p<0.01$ when compared with GPx activity in liver mitochondria from male rats.

Table 9: Gender-related differences in glutathione content in liver mitochondria.

	Male Liver	Female Liver
GSH (nmol/mg protein)	0.833 ± 0.057	0.779 ± 0.043
GSSG (nmol/mg protein)	0.049 ± 0.013	0.054 ± 0.010
GSH/GSSG ratio	17.00 ± 4.38	14.43 ± 4.30

The values represent mean ± SEM of 6 different experiments. GSG and GSSG levels were obtained as described in the material and methods section. Legend: GSH – reduced glutathione, GSSG – oxidized glutathione.

4.1.3.4 Mitochondrial membrane potential during ADP phosphorylation is affected by resveratrol

Gender did not influence the different end-points regarding mitochondrial transmembrane electric potential, ΔΨ (Fig. 12). Likewise, resveratrol did not affect the maximum transmembrane electric potential developed by mitochondria for both genders and organs (Fig. 12A). However, the depolarization induced by ADP was decreased by 25 μM resveratrol in brain and liver mitochondria (Fig. 12B). In brain mitochondria, the decrease observed was from 15.3 ± 1.0 to 10.3 ± 2.7 (preparations from males) and 14.2 ± 1.0 to 9.3 ± 1.5 (preparations from females), values in (-mV). When using liver mitochondria, the decrease was from 20.4 ± 2.1 to 15.7 ± 0.8 (preparations from male) and from 19.5 ± 0.4 to 16.2 ± 0.4 (preparations from females), with values in (-mV). Although there is not a statistical difference, the lag phase showed a tendency to be increased in brain mitochondria from male rats when incubated with 25 μM resveratrol ($p=0.059$).

4.1.3.5 Resveratrol has a direct effect on mitochondrial complex I

By using disrupted mitochondrial membranes and in the presence of specific substrates, we can evaluate distinct sites of drug-induced toxicity. Resveratrol decreases oxygen consumption in frozen/thawed mitochondrial preparations from liver and brain when using NADH as substrate (Fig. 13 A and E).

Preparations from brains of male rats showed a resveratrol-induced decrease in oxygen consumption from 56.3 ± 4.4 to 48.81 ± 3.6 nmol O_2/min/mg protein; while a decrease from 44.8 ± 5.2 to 36.2 ± 3.4 nmol O_2/min/mg protein was observed in brain preparations from female rats. When investigating liver mitochondrial preparations, resveratrol also inhibited NADH-sustained respiration in male (24.7 ± 1.7 to 21.0 ± 1.4 nmol O_2 consumed/min/mg) and female rats (19.9 ± 0.9 to 16.4 ± 0.9 nmol O_2 consumed/min/mg). Interestingly, NADH-sustained oxygen consumption in both tissues was higher in preparations from males when compared with preparations from female animals.

The same experiments were performed by using the complex II substrate succinate (in the presence of complex I inhibitor rotenone). In this case, resveratrol had no effect on succinate-induced mitochondrial respiration.

4.1.3.6 Differences on the effects of resveratrol and estradiol on mitochondrial bioenergetics

Based on the data obtained for resveratrol on mitochondrial respiration (Fig.11) and previous published data from our lab on E2 effects on isolated mitochondria [248], the two molecules were compared in terms of effects on mitochondrial complex I and V. It was previously described that E2 decreases ADP-induced depolarization in liver mitochondria [309], suggesting that E2 may interact with the phosphorylative system. Later, it was shown that E2 decreases the phosphorylation rate of isolated liver mitochondria in an ATP-dependent mechanism, inhibiting ATP synthase [310]. Similarly, resveratrol also inhibits complex V both in liver and heart mitochondria [200, 311]. The antioxidant effects of resveratrol were already described in isolated mitochondria through increasing the manganese superoxidase dismutase activity in liver mitochondria [303] and by the reduction of TBARS both in liver and brain mitochondrial fractions as previously shown in this thesis (Fig. 8). However, a comparative study of resveratrol and estradiol on mitochondrial function was not performed so far. We then compared the effects of both molecules on complex I and ATP synthase. We initially followed respiration in disrupted mitochondria in order to obtain the maximal electron flux. NADH (complex I) and succinate (complex II) were used as substrates to determine whether resveratrol inhibits any of the two segments of the respiratory chain. The results (Fig. 13) show that, regardless of the gender, resveratrol inhibited NADH- but not succinate - sustained maximal respiration.

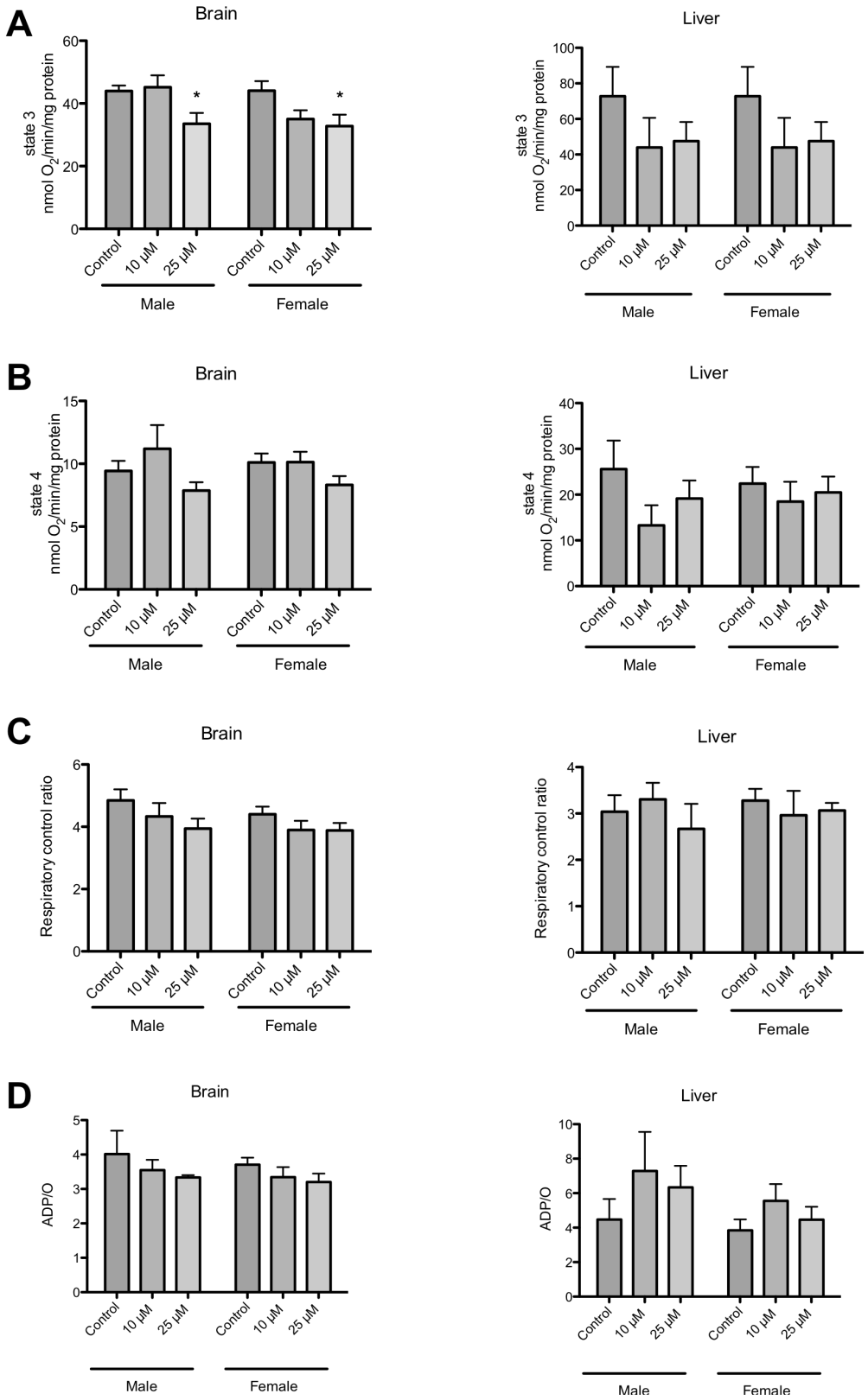

Figure 11: Resveratrol effects on mitochondrial respiration.
(A) Mitochondrial state 3 respiration; (B) Mitochondrial state 4 respiration; (C) Respiratory control ratio (RCR); (D) ADP/O. Brain (0.5 mg) and liver (1 mg) mitochondria were incubated with 10 or 25 μM of resveratrol for 3 min in 1 mL of respiration media supplemented with 5 mM glutamate and 2.5 ml malate. ADP (75 nmol for brain mitochondria and 125 nmol for liver mitochondria) was added to induce state 3 respiration. The RCR was calculated as the ratio between state 3 and state 4 respiration. The ADP/O was calculated as the number of nmol ADP phosphorylated per natom oxygen consumed during state 3. Data represent mean ± SEM from four to six independent experiments. Statistical significance: * $p<0.05$, when compared with the respective control.

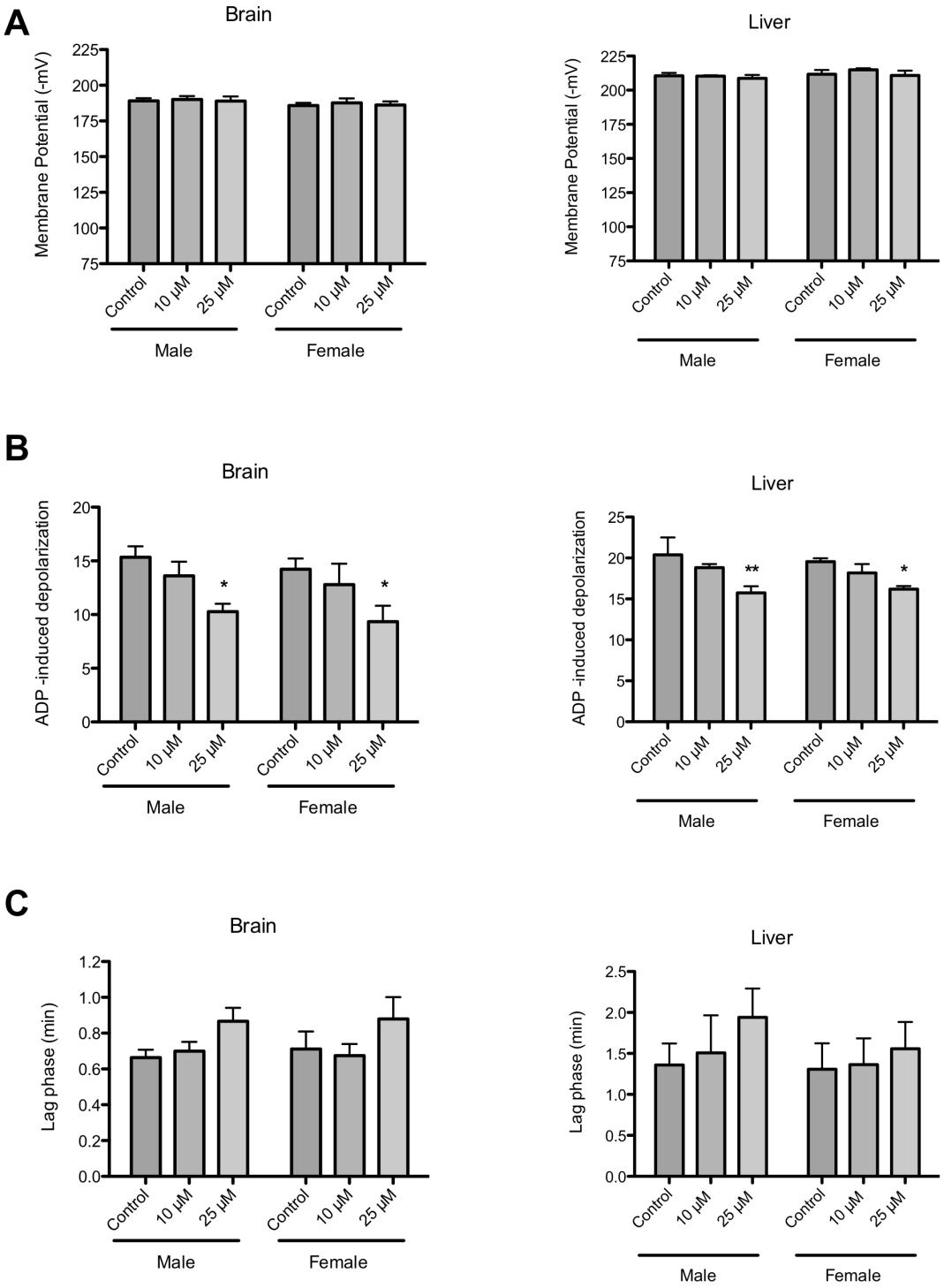

Figure 12: Resveratrol effects on mitochondrial ΔΨ fluctuations.
(A) Maximum mitochondrial membrane potential developed (ΔΨ) after mitochondrial energization; (B) Depolarization induced by ADP addition (C) Time elapsed during complete ADP phosphorylation (lag phase). Brain (0.5 mg) and liver (1 mg) mitochondria were incubated with 10 or 25 µM of resveratrol for 3 min in 1 ml of standard respiratory medium. Mitochondria were energized with 5 mM glutamate and 2.5 mM malate and the phosphorylation cycle was initiated with ADP (75 nmol for brain mitochondria and 125 nmol for liver mitochondria). Data represent mean ± SEM from four to six independent experiments. Statistical significance * $p<0.05$ and ** $p<0.01$ when compared with the respective control.

In parallel, the maximum activity of complex I was investigated using a colorimetric method. For both organs and genders, resveratrol decreased complex I specific activity. In brain

mitochondria, a decrease of 22% and 11% was observed in preparations from male and female preparations, respectively. No effects were observed when succinate was used, thus excluding downstream effects from complex I (Fig.13 C, G, D, H).

A higher magnitude effect was observed in liver mitochondria, where the activity in the presence of resveratrol decreased 73% for male preparations and practically 100% for preparations from female rats. The maximal activity of complex I did not differ between genders (Table 10).

4.1.3.6.1 Complex I inhibition is higher for estradiol than for resveratrol

In order to compare the magnitude of complex I inhibition by resveratrol and E2, both compounds were incubated with disrupted mitochondrial membranes and oxygen consumption was measured by using NADH or succinate (+rotenone) substrate, similarly to Fig.13. No effects were observed for succinate (+rotenone)–stimulated respiration, although both compounds decreased respiration when NADH was used as substrate (Fig.15). Moreover the inhibition of complex I by E2 was observed at an earlier time point comparing with the effect of resveratrol (Fig. 14). Oxygen consumption in the presence of E2 was much lower than in the presence of resveratrol, when the respiration was stimulated by NADH. A concentration-response curve was made for both compounds and again the results were confirmed: a) E2 is a more potent inhibitor of complex I than resveratrol and b) the effects occurs on complex I, since succinate-dependent respiration was not affected. To further investigate the type of complex I inhibition of each compound, Michaelis Menten constant (K_M) was calculated following Lineweaver–Burk plots based in the rate oxygen consumption versus the concentration of NADH (Fig. 16). From our analysis of the curve crossing points, E2 is suggested to behave as a non-competitive inhibitor with a K_M of 30.2 ± 3.0 μM in comparison with a K_M 31.5 ± 7.3 μM in the absence of inhibitor. Resveratrol behaves as a competitive inhibitor with a K_M of 46.1 ± 10.8, corresponding to the lower affinity binding of resveratrol to the active center of the complex, which may explain the lower effects of resveratrol on complex I function.

4.1.3.6.3 Resveratrol, but not E2, decrease ATP synthase activity

Data from literature showed that resveratrol inhibits ATP synthase in cardiac mitochondria [200, 312]. Thus, we measured ATP synthase activity and the phosphorylative lag phase, in order to determine the magnitude of effects of both compounds on the mitochondrial phosphorylative system. We observed a decrease in ATP synthase activity and an increase in lag phase when mitochondrial respiration is supported by complex I substrate (71.0 ± 8.6 and 62.6 ± 9.6 for E2 and resveratrol, respectively, in percentage to the control). When respiration was sustained by succinate, the effect was only observed for resveratrol (98.3 ± 1.1 and 73.3 ± 9.1 in percentage of control for E2 and resveratrol, respectively).

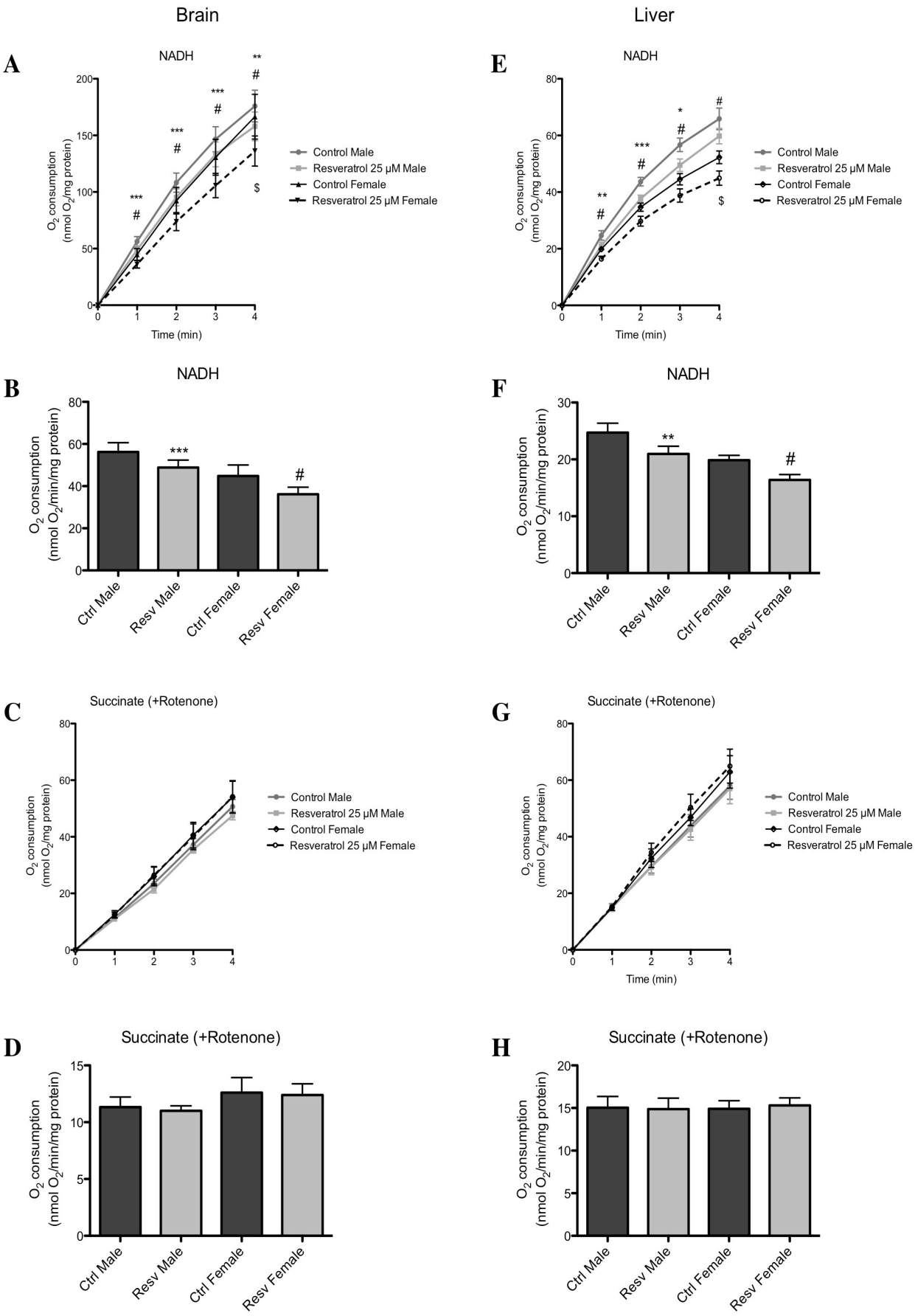

(legend next page)

Figure 13: Resveratrol inhibition of mitochondrial Complex I.
Resveratrol (25 μM) effects on mitochondrial oxygen consumption in disrupted mitochondrial membranes was measured in a Clark-type electrode during 4 min after NADH (Complex I, A, B, E, F) or succinate plus rotenone addition (Complex II, C, D, G, H) in preparations from male and female Wistar rats. Data represent mean ± SEM from five to eight independent experiments. Statistical significance: for male populations * p<0.05, ** p<0.01, *** p<0.001 when compared with the respective control and for female preparations #<0.05 when compared with respective control, $ p<0.05, compared with male preparations. Legend: Ctrl - control, Resv - resveratrol

Table 10: Effect of Resveratrol on brain and liver mitochondrial respiratory complex I maximal activity

	Male		Female	
	Ctrl	**Resv**	**Ctrl**	**Resv**
Brain	135.70 ± 16.82	106.6 ± 13.05 *	112.4 ± 4.72	99.61 ± 4.3 *
Liver	49.74 ± 12.14	13.65 ± 13.27 *	52.12 ± 4.97	0.00 ± 12.47 *

Activity expressed as nmol DCPIP/min/mg protein. Data are the mean ± SEM of 4 independent experiments. Statistical significance: *p<0.05 when compared with the respective control. Ctrl- control, Resv-resveratrol

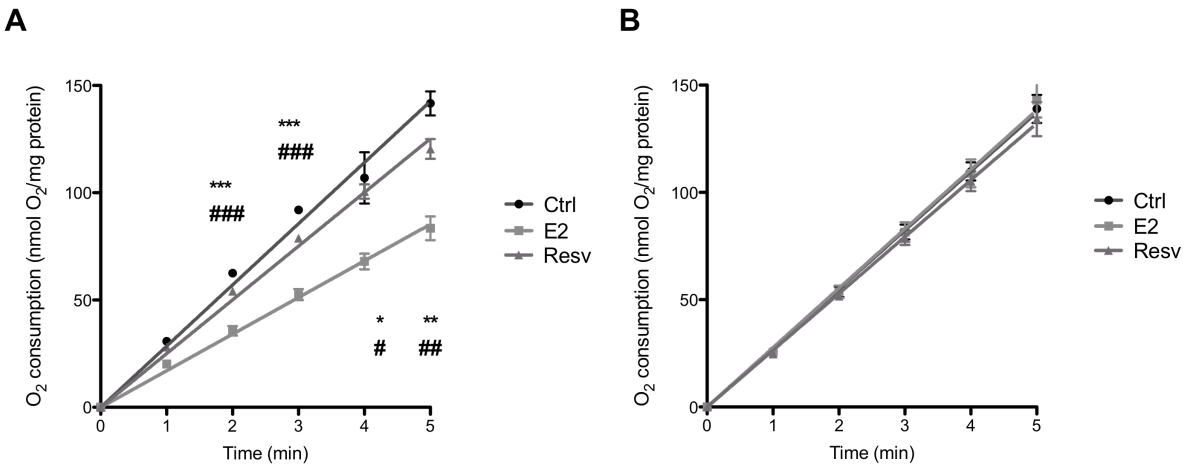

Figure 14: Resveratrol and E2 inhibit mitochondrial Complex I.
The effects of both compounds at 25 μM on mitochondrial oxygen consumption in disrupted mitochondrial membranes was measured in a Clark-type electrode during 5 min after NADH (Complex I, A) or succinate plus rotenone addition (Complex II, B) in liver preparations from male rats. Data represent mean ± SEM from four independent experiments. Statistical significance: resv * p<0.05, ** p<0.01, *** p<0.001 when compared to control, # p<0.05, ## p<0.01, Resv ### p<0.001 when compared with control. Legend: Ctrl - control, E2 – estradiol, Resv - resveratrol.

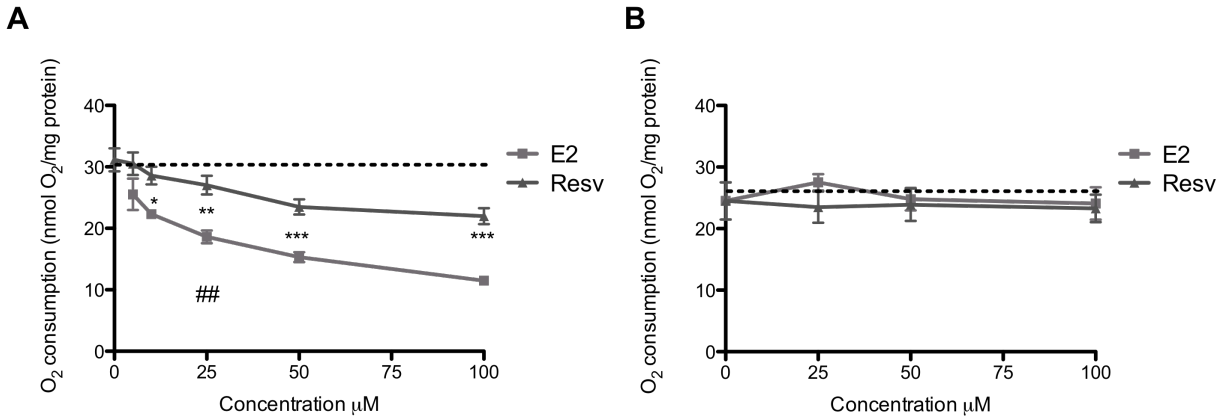

Figure 15: Resveratrol and E2 inhibit mitochondrial Complex I at different concentrations. Dose-dependent effects on mitochondrial oxygen consumption in disrupted mitochondrial membrane were measured with a Clark-type electrode during 5 min after NADH (Complex I, A) or succinate plus rotenone addition (Complex II, B) in liver preparations from male rats. Data represent mean ± SEM from four to seven independent experiments. Statistical significance: E2 * p<0.05, ** p<0.01, *** p<0.001 when compared to resveratrol. Legend: E2 – estradiol, Resv- resveratrol.

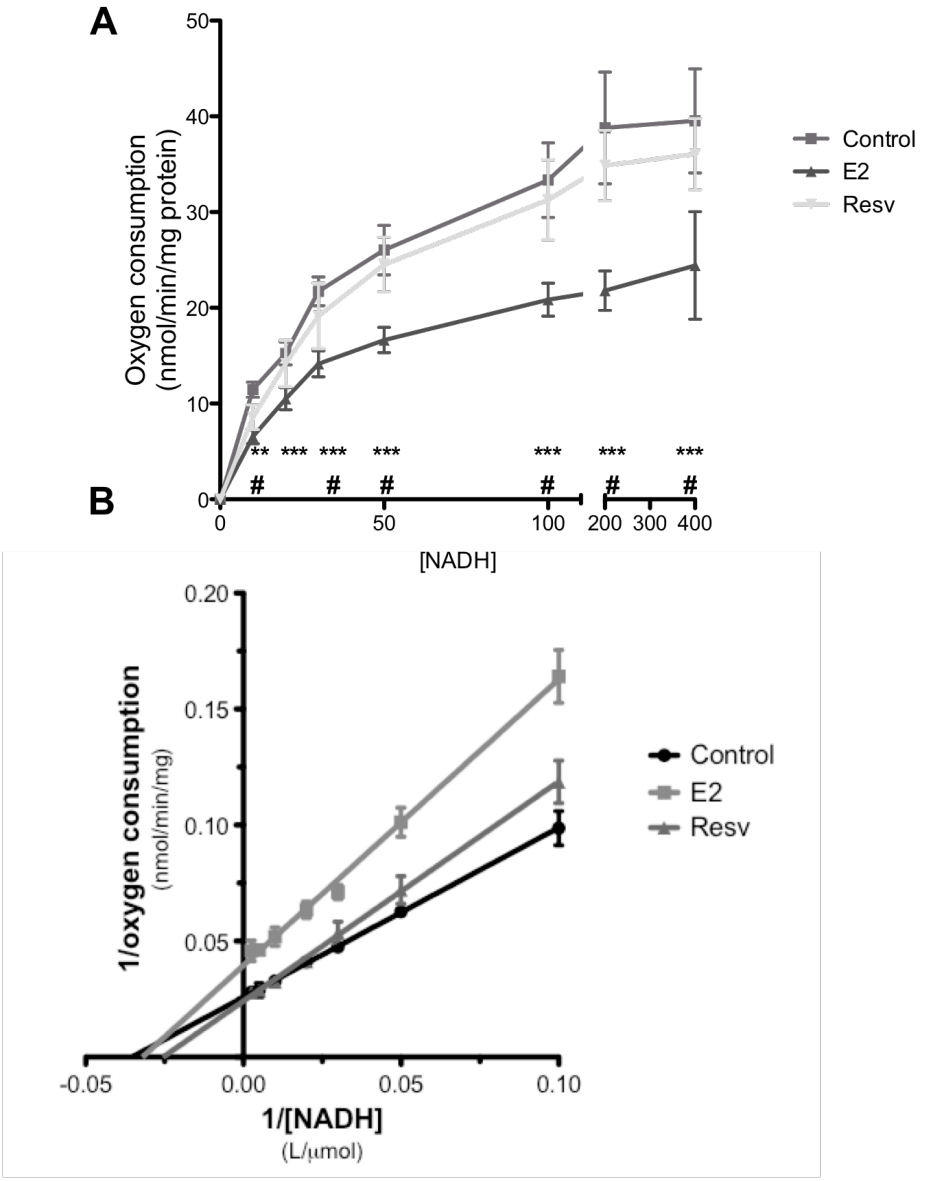

Figure 16: Resveratrol and E2 differently inhibit complex I.
The type of inhibition of complex I was calculated based on the Lineawer-Burk plots. (A) Vmax of oxygen consumption dependent of [NADH] (μM). (B) K_M of E2 does not differ from control. Control K_M = 31.5 ± 7.3 μM; E2 K_M = 30.2 ± 3.0 μM; Resveratrol K_M = 46.1 ± 10.8μM. Data are mean ± SEM of 4 independent experiments. ** p<0.01, *** p<0.001 E2 compared with control, # p<0.05 E2 compared with resveratrol. Legend: E2 – estradiol, Resv - resveratrol

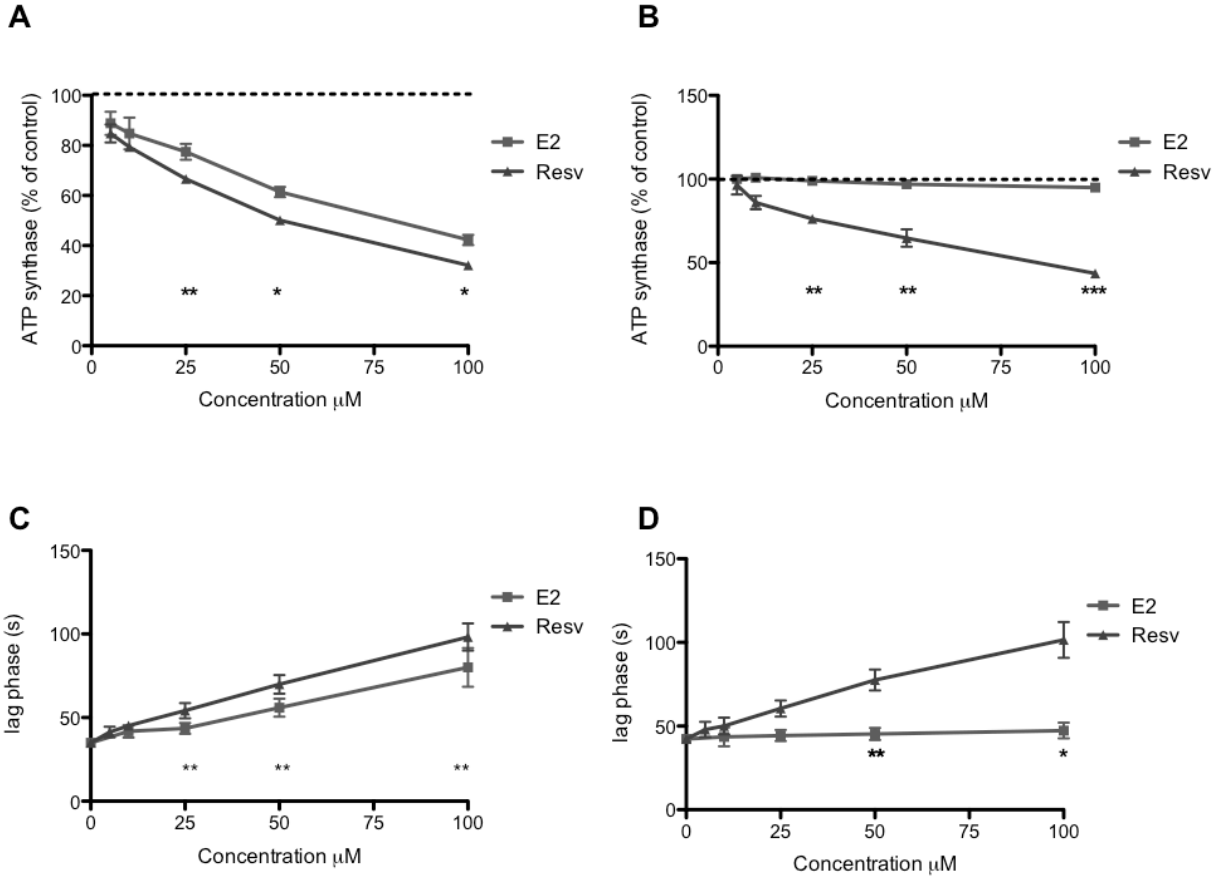

Figure 17: Resveratrol inhibits ATP synthase.
Dose-dependent effects of E2 and resveratrol on ATP synthase activity sustained by glutamate/malate (A) or succinate (B) in freshly isolated mitochondrial liver preparations and the respective phosphorylative lag phases (C, D, respectively) from liver preparations of male rats. Activity of ATP synthase was obtained by measuring external pH variation during oxidative phosphorylation. Mitochondria (1.0 mg) were suspended in 1 ml of the medium composed of 125 mM sucrose, 65 mM KCl, 2.5 mM MgCl2, 2 mM KH_2PO_4, 0.5 mM Hepes, pH 7.2, 5 mM glutamate, 2.5 mM malate. The phosphorylation was initiated by adding ADP 375 nmol to the mitochondrial suspension containing glutamate plus malate. The system was calibrated by adding known amounts of HCl at the end of the experiments. Data represent mean ± SEM from three to six independent experiments. Statistical significance: * p<0.05, ** p<0.01, *** p<0.001 when E2 is compared to Resveratrol. Legend: E2 – estradiol, Resv - resveratrol

Although both compounds inhibited complex I activity, the differences on oxygen consumption may have reflected resveratrol inhibition of ATP synthase in a process independent of the presence of ATP. While the antioxidant proprieties of resveratrol were demonstrated by the decrease in TBARS generation (Fig. 8), this compound presented some toxicity, in isolated mitochondria, inhibiting complex I and ATP synthase. For this reason, it was excluded from further *in vivo* testing.

4.1.4 *In vitro* coumestrol activity on HepG2 cells

Besides resveratrol, coumestrol also decreased mitochondrial lipid peroxidation through a decrease in the generation of TBARS in the presence of a peroxidizing agent (Fig. 7). As opposed to resveratrol, coumestrol did not present mitochondrial toxicity.

The coumestan coumestrol was firstly identified in alfafa in 1957 [313], but it can also be found in spinach or soy based products. Since this PE is not very explored, we investigated antioxidant/toxicologic proprieties of this compound in a more complex system. With this purpose, we used the cell line HepG2, which has been widely used to study the cytotoxicity of different compounds [242, 243]. This cell line exhibits many of the features of normal liver cells [239] and is highly differentiated, therefore it can be used to screen the toxicity of new chemicals [241]. These cells are highly polarized, based on cell asymmetry resulting from the presence of basolateral and apical poles, similarly to human hepatocytes. They can activate and detoxify xenobiotics, reflecting the metabolism of xenobiotics in the human body better than other metabolically incompetent cells used in conventional *in vitro* assays [242, 243]. The objective of this section was to investigate coumestrol in comparison with E2 in the antioxidant protection of HepG2 cells.

4.1.4.1 Coumestrol, similarly to E2 and NAC, prevents the cytotoxicity induced by H_2O_2 and rotenone.

Initially, coumestrol was compared with E2 and N-acetylcystein (NAC), a glutathione precursor [314], in terms of antioxidant potential in HepG2 cells. Cells were pre-incubated with these three compounds 2 h prior to treatment with H_2O_2 and rotenone, two well know oxidizers, with the latter acting through increasing $O_2^{\bullet -}$ release from complex I [315, 316]. In fact, the higher mitochondrial ROS production by rotenone results from increased ubisemiquinone at complex I, one of the sites of ROS production by mitochondria [317]. N-acetylcysteine (NAC), the acetylated variant of the amino acid L-cysteine, is a source of sulfhydryl (SH) groups, and serves as a precursor of GSH synthesis, promoting detoxification and antioxidant effects [318]. Our data indicate that coumestrol prevents the reduction of cell mass after H_2O_2 and rotenone treatment (Fig. 18). The measure of cell mass is possible since SRB binds to the basic amino acids of proteins. This means that the total amount of cells is indirectly given by the dye bound to proteins. On the other hand, NAC and E2 were also effective in preventing toxicity resulting from H_2O_2. The compounds *per se* did no show noticeable toxicity.

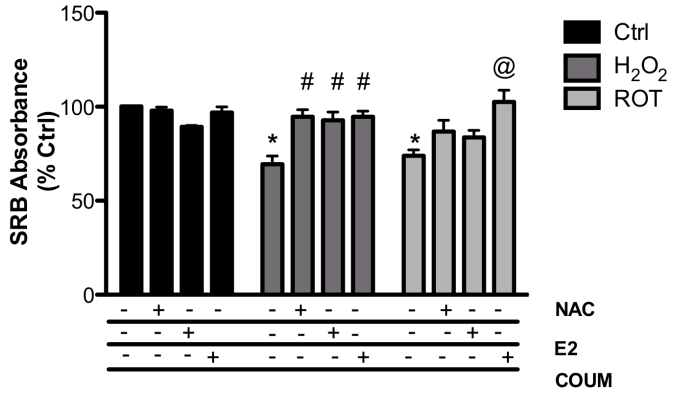

Figure 18: Coumestrol, E2 and NAC avoid the cellular death induced by H_2O_2 and Rotenone.
Twelve hours after seeding (40,000 cells/ml – 20,000 cells/cm^2) HepG2 cells were pre-incubated with E2 or Coum, or 100 µM of NAC for 2 h before treatment with 100 µM H_2O_2 or 2 µM rotenone for 24 h. Data were obtained through SRB assay as described in the methods section. Data represent mean ± SEM from 4 experiments. * p<0.05 compared with control HepG2 cells, # p<0.05 compared with cells only treated with H_2O_2, @ p<0.05 compared with cells only treated with rotenone. Legend: Ctrl - control, Coum - coumestrol, E2 - estradiol, H_2O_2 - hydrogen peroxide, NAC - N-acetylcysteine, Rot – rotenone.

In order to confirm the antioxidant protection from ROS generation in HepG2, these cells were labeled with MitoSox Red or 2', 7'-dichlorodihydrofluorescein diacetate (H_2DCFDA) to measure mitochondria superoxide anion and global oxidative stress, respectively.

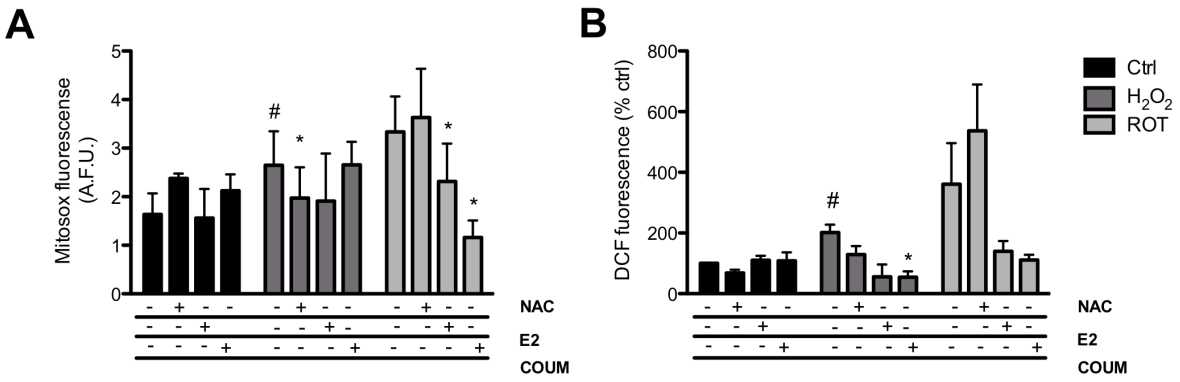

Figure 19: Coumestrol decreases superoxide anion after incubation with rotenone and global oxidative stress caused by H_2O_2.
Twelve hours after seeding (20,000 cells/cm^2) HepG2 cells were pre-incubated with E2 or Coum, or 100 µM of NAC for 2 h before treatment with 100 µM H_2O_2 or 2 µM rotenone for 24 h. For plates incubated with MitoSox red (A), 15 min prior the end of the treatment cells were incubated with the probe and fluorescence was read in a multiplate reader. In another experimental set-up, cells were incubated with H_2DCFDA (B) and the kinetics of fluorescence was read in a multiplate reader. Data represent mean ± SEM from 3 experiments. * p<0.05 compared with cells treated only with H_2O_2, or rotenone; # p<0.05 compared with control. Legend: Ctrl - control, Coum - coumestrol, E2 - estradiol, H_2O_2 - hydrogen peroxide, NAC - N-acetylcysteine, Rot – rotenone.

MitoSox (Fig. 19A) or H_2DCFDA (Fig. 19B) fluorescence was not altered by the protective compounds, showing that these did not increase oxidative stress *per se* at tested concentrations. Hydrogen peroxide treatment resulted in an increased fluorescence of both probes, which was inhibited by NAC (MitoSox) and coumestrol (H_2DCFDA). Although rotenone also led to an increased fluorescence of both probes, the increase was not

statistically significant due to the large variability observed. Nevertheless, both E2 and coumestrol decreased MitoSox fluorescence after rotenone treatment (Fig. 19A). Although not statistically significant, both compounds also reduced H_2DCFDA fluorescence after rotenone treatment (Fig. 19B).

4.1.4.2 Coumestrol increases SOD2 and HSP90 levels after treatment with pro-oxidant agents

We next investigated the protein content regarding the antioxidant enzymes mitochondrial superoxide dismutase (SOD2) and glutathione peroxidase (GPx). In addition, we also analyzed the expression of the heat-shock protein 90 (Hsp90). This latter protein assists in protein folding and stabilizes proteins required for cell growth [319, 320]. Although its role in oxidative stress is not fully understood, it has been suggested that under oxidative stress conditions [321, 322], Hsp90 is cleaved, leading to loss of functions.

Hydrogen peroxide and rotenone decreased Hsp90 content, which is prevented by incubation with coumestrol for 2 h prior to the stress inducer. No differences regarding GPx content were observed. However, coumestrol increased the expression of mitochondrial SOD, after rotenone treatment (Fig. 20B) and E2 mimicked the same effect, which may help to explain the lower levels of mitochondrial superoxide anion in cells treated with rotenone (Fig. 19A). The results from this and from the previous sections consolidate the idea that coumestrol presents a cytoprotective function based on antioxidant activity.

4.1.5 The proliferation rate of breast cancer and normal cells in the presence of coumestrol is lower than in the presence of estradiol

As the main side effect of HRT is the widely recognized increased risk of breast cancer [63], we intended, in a pilot study, to test whether the selected PE, coumestrol, alters the proliferation of breast cancer cells and compare the results with those with E2.

To perform this small study, two endothelial breast cancer (MDA-MB-231 and MCF-7) and one immortalized breast-derived normal (MCF-12A) breast cells lines were used. MCF-7 and MDA-MB-231 are, respectively, estrogen-dependent and estrogen-independent human breast carcinoma cells while the human immortalized MCF-12A is routinely used for normal breast cells [323, 324].

Charcoal-stripped FBS has been used in studies regarding estrogen effects on cell behavior. Cells were grown in regular and charcoal FBS medium and difference in the cellular growth was evaluated by using SRB dye-binding assay. As expected, all the three cell lines showed lower proliferation rates in the presence of charcoal stripped FBS than in the presence of regular FBS (Fig. 21). In addition to charcoal-stripped FBS that has little estrogen content, we used phenol red free media since phenol red has estrogenic activity [262, 263].

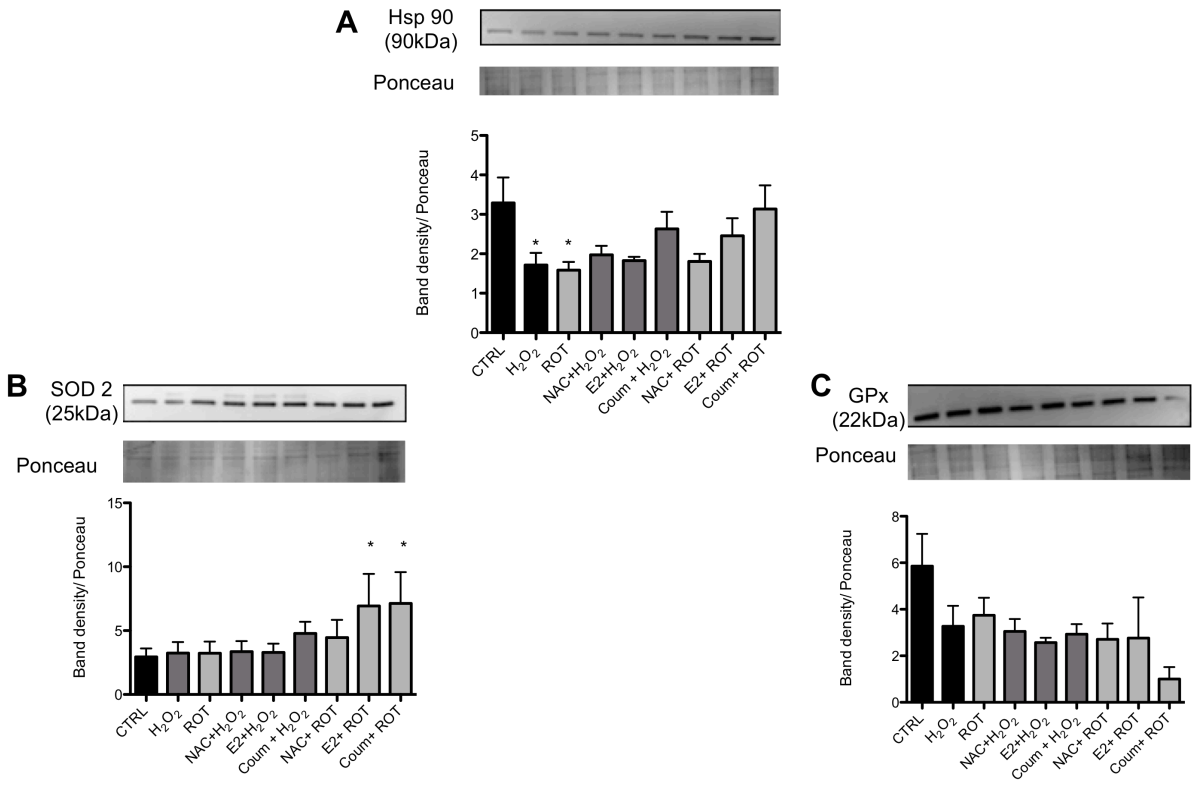

Figure 20: Coumestrol avoids the loss in Hsp 90 expression and promotes an increase in SOD2 expression in cells exposed to oxidizers.
Cells were treated as previously described in the material and methods section and harvested for protein expression analysis through Western blotting for Hsp 90 (A), SOD2 (B) and GPx (C). Data represent mean ± SEM of three to five independent experiments. *p<0.05 compared with the respective control (no protective agent).

The differences in the MDA-MB-231 cell line were only observed after 6 days in culture (Fig. 21B), which may be explained by the reduced content of estrogen receptors in this cell line (Fig. 21D), making it less responsive to estrogenic fluctuations in the medium (Fig. 21).

The presence of estrogen receptors in cells is a helpful indication of their potential regulation by estrogenic stimuli. ERs are expressed in the epithelial cells of the mammary gland as in other tissues, a classic target tissue in which estrogens play a key role during development and growth [325].

We evaluated the morphology of these three cell lines cultured in a regular vs. low estrogen medium. Those cells were observed by phase contrast as well as by epifluorescence, following cell incubation with the mitochondrial probe TMRM, which labels polarized mitochondria. It is apparent from the images obtained that cells in low estrogen medium present a more apoptotic phenotype, with a decrease in volume (shrinkage) and loss of mitochondrial TMRM accumulation (Fig. 22).

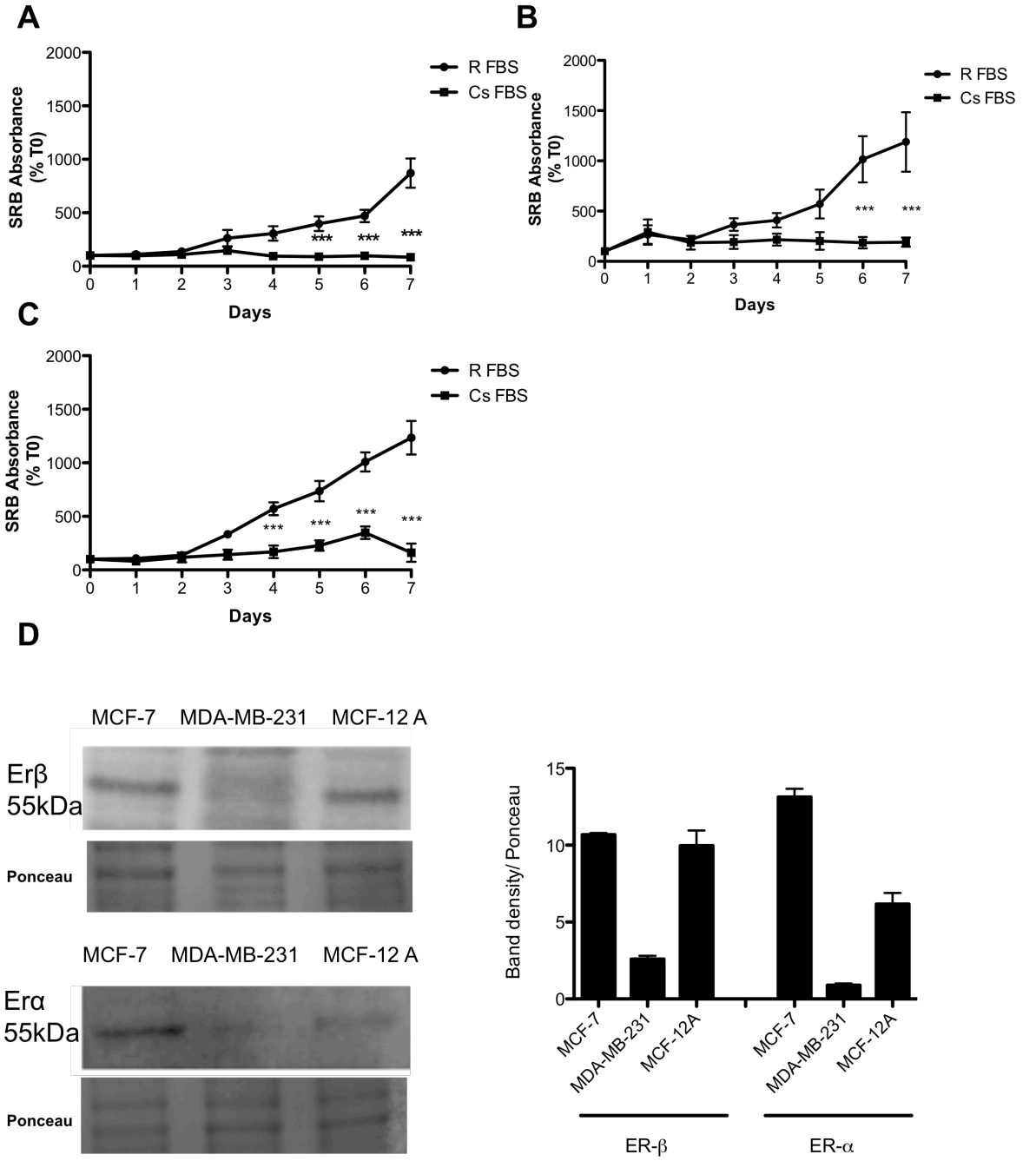

Figure 21: Alterations in breast normal (MCF-12A) and cancer (MDA-MB-231 and MCF-7) cell lines proliferation in charcoal stripped FBS and phenol red free medium vs regular medium. Charcoal removes hormones from the medium, decreasing estrogen content in (A) MCF-7 cell line, (B) MDA-MB-231 cell line, (C) MCF-12A cell line. Cells were seeded at 5,000 cells/ml in a 48-well plate. (D) Estrogen receptor in the three cell lines MCF-7, MDA-MB231 and MCF-12A cell lines. Data represent mean ± SEM of three to four independent experiments. *** $p<0.001$ cells grown in charcoal stripped FBS compared with regular FBS.

In parallel and based on the previous results shown in this thesis (chapter 4.1.1 and 4.1.4), we compared the proliferation of these cell lines in the presence of coumestrol and E2, in order to evaluate the risk of coumestrol in increasing the proliferation of breast cancer cells which would limit its use in HRT (Fig. 23). Of note, the following experiments were done in regular medium, because charchoal-stripped FBS also removes aminoacids and vitamins

that are required for cell regular cell growth [326]. The effects of E2 and coumestrol at different concentrations (10 nM, 100 nM) on cell proliferation in regular media were evaluated by the SRB technique. The proliferation is lower in the presence of coumestrol than in the presence of known doses of E2.

Since one of the main risks of the HRT, already described in this thesis, is the development of breast cancer [63], these data might have some relevance in the context of finding alternatives to E2 for HRT. We observed cell lower proliferation rates in coumestrol vs. E2-treated cells.

4.1.6 Discussion

There are a growing number of studies focusing on natural compounds and their possible benefits in terms of human health. Although the antioxidant, anti-inflammatory and anti-tumoral effects of PEs [327, 328] have been widely described, the cellular toxicity was not yet completely evaluated, especially regarding mitochondrial bioenergetics, which is of critical importance, since alterations in mitochondrial function are indicative of toxicity of compounds.

The first objective of this chapter was to identify PE with low mitochondrial toxicity and elevated potential as antioxidants.

From our data, coumestrol and resveratrol showed a good antioxidant potential (Figs. 7, 8). After selecting resveratrol and coumestrol, we next investigated their mitochondrial effects in more detail.

Following previous works showing protective effects of resveratrol on brain and liver [300, 328, 329], its toxicity on isolated mitochondria was studied at concentrations that decrease oxidative stress. The use of brain and liver mitochondria in this specific aim is due to the fact that PE are able to cross the BBB [295] and are highly metabolized in the liver [330], respectively, being important targets for the effects of the PE. The present work also highlights the relevance of using mitochondrial-isolated fractions from male and female rats, which is rarely seen in the literature.

Although we did not observe basal differences in mitochondrial preparations from both genders in most of the parameters investigated, except when measuring maximal respiration in permeabilized mitochondria, it is known that estrogens have protective effects, enhancing antioxidant defenses and decreasing mitochondrial dysfunction [331-333]. For instance, H_2O_2 production by liver mitochondria is lower in females than in males (Fig. 9). This can be due to the activity of GPx, which is augmented in liver preparations from females (Fig. 9), although no differences were measured in brain GPx or in reduced and oxidized glutathione (Table 9). Female rats have better mitochondrial capacity showing less oxidative stress generation

based in estrogen levels [334, 335]. Sex hormones have neuroprotective effects, which have also been shown to increase mitochondrial efficiency [273].

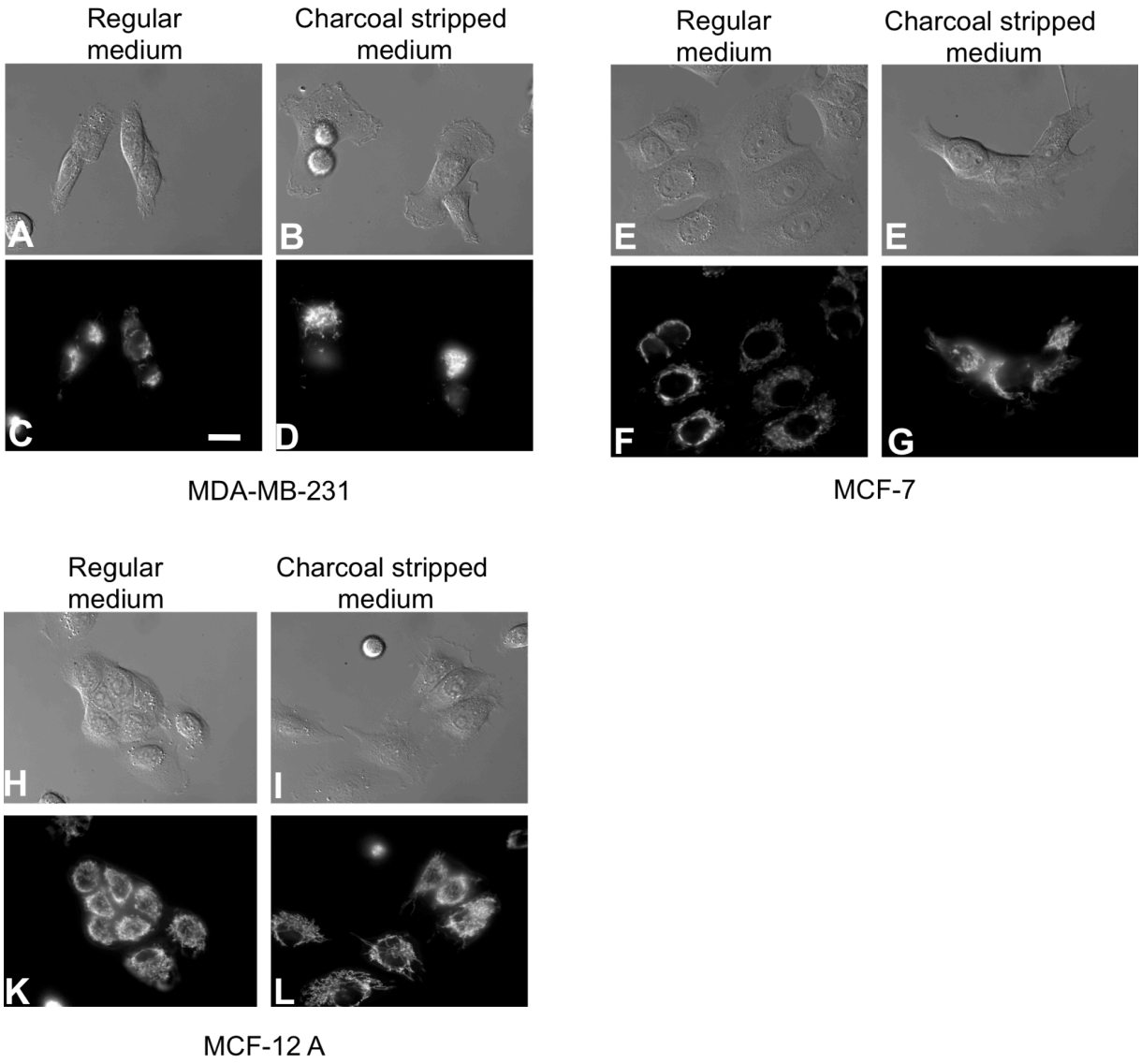

Figure 22: Effects of low estrogen medium on MDA-MB-231, MCF-7 and MCF-7 cell morphology and mitochondrial polarization.
Morphologic images by phase contrast (A, B, E, F, H, I) and mitochondrial alterations were observed by using the mitochondrial-selective fluorescent probe TMRM (C, D, F, G, K, L). The three cell lines were culture in regular or low estrogen medium. Epifluorescent microscopy images are representative of 3 different cell preparations. Scale bar corresponds to 20 μm. The images were obtained using a Nikon Eclipse TE2000U microscope.

Besides identifying gender-related effects, we aimed to investigate the nature of the interaction between resveratrol and mitochondria for concentrations known to be antioxidant. Our results confirm previous studies [336-339] regarding the antioxidant properties of resveratrol (Fig. 8). Our data show that resveratrol acts as an antioxidant, inhibiting lipid peroxidation, regardless of the gender origin of the mitochondrial preparation (Fig. 8). Interestingly, resveratrol increases H_2O_2 generation in liver mitochondria from males and females in the presence of the substrate (glutamate-malate) alone.

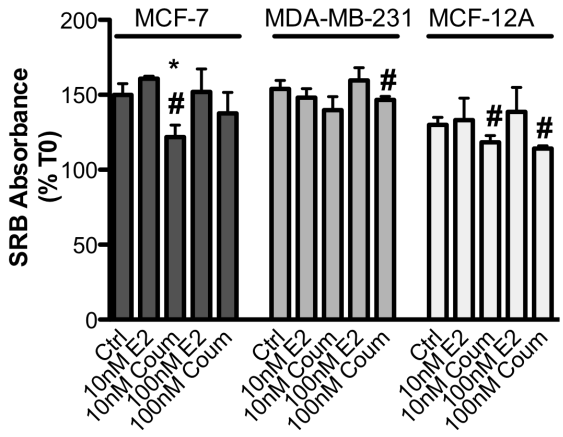

Figure 23: Breast cell proliferation in the presence of coumestrol and E2.
Cells were plated at a density of 20,000 cells/cm^2 and treated for 24 h with coumestrol and E2. Coumestrol and E2 were compared in terms of inhibition of cell proliferation by using the SRB assay. Data represent mean ± SEM of five independent experiments when compared with E2 condition. # $p<0.05$ when compared with the respective E2 condition, * $p<0.05$ when compared with control. Legend: E2-estradiol, Coum-coumestrol.

Resveratrol effects on liver mitochondria in terms of H_2O_2 generation can be explained by a direct action on Complex III, or instead, as previously reported, by the modulation of mitochondrial manganese-superoxide dismutase [340], increasing the flux of hydrogen peroxide production. The effect was not observed with brain mitochondria (Fig. 9), except when mitochondria were incubated with complex III inhibitor, antimycin A (Fig. 9A).

Concerning the effects of resveratrol on mitochondrial bioenergetics, Zini *et al.*, showed that resveratrol inhibits brain mitochondrial respiratory chain at the complexes I to III span [341]. In this work, the enzymatic activity of ubiquinol cytochrome *c* reductase in the presence of resveratrol was decreased by 20% [341]. The authors suggested that resveratrol can preserve mitochondrial functions by three different mechanisms: antioxidant-mediated effect, complex III direct effect and membrane stabilizing effects [342]. A decrease of state 3 respiration in brain mitochondria of female and male rats was observed in the presence of resveratrol (Fig. 11). Since the maximal $\Delta\Psi$ developed was not affected by resveratrol (Fig. 12), this suggests that the respiratory chain was not greatly inhibited. Although we cannot exclude that increased H_2O_2 generation results from inhibition of complex I and/or III. Instead, the results from both respiration (Fig. 11) and $\Delta\Psi$ (Fig. 12) suggest an effect on the phosphorylative system, namely in the adenine nucleotide transporter, the phosphate transporter or even in ATP synthase [311].

We further described that resveratrol inhibits mitochondrial respiration induced by NADH, but not succinate, in freeze/thawed preparations, which allows to study maximal respiration rate (Fig. 13). In accordance, resveratrol also reduced complex I specific activity as followed by the reduction of DCPIP (Table 10). These data confirms that resveratrol acts as a complex I inhibitor in mitochondrial preparations from both organs and genders. Interestingly, although

resveratrol induced a larger inhibition of complex I activity in hepatic permeabilized preparations, the same type of effect was not visible when using intact mitochondria (Fig. 13). This may imply that the site of resveratrol inhibition on complex I faces the matrix side, being more accessible when mitochondrial membranes are disrupted. The data also supply evidence that resveratrol may also target complex I besides the already described complex III [341], thus contributing to increase the generation of hydrogen peroxide by the respiratory chain (Fig. 9).

The results may also suggest that increased generation of H_2O_2 by resveratrol in liver and, under some conditions, in brain mitochondria can act to stimulate several signaling pathways, including those related with the up-regulation of antioxidant enzymes. The effects of resveratrol in the metabolism of different organs and gender-mediated effects should be explored in further detail to determine potential toxic effects and mechanisms by which resveratrol is described to cell fitness.

We further compared the effects of E2 and resveratrol on liver mitochondrial complex I. Our data suggest that both compounds act in complex I, decreasing its activity, with a consequent decrease in oxygen consumption sustained by substrates for this complex. From a Lineweaver-Burk plot analysis, resveratrol acts as competitive inhibitor of complex I whether E2 acts as noncompetitive inhibitor, reducing the Vmax of complex I (Fig. 16). Inhibition of ATP synthase activity by resveratrol was also observed, as described previously [311]. A decrease of ATP synthase activity was observed with resveratrol whereas we did not observe effects promoted by E2 in the absence of ATP in the medium at the beginning of the experiment (Fig.19). Previously, it was shown that E2 inhibits ATP synthase but only when ATP was present in the medium in the beginning of the experiment [248].

Initial results of this thesis (section 4.1.2), showed that coumestrol reduced lipid peroxidation induced by the pro-oxidant pair ADP/Fe^{2+}. We increased the complexity of the system by investigating its effects in the human HepG2 cell line, regularly used as model for liver cells [343-345]. This cell line expresses numerous enzymes involved in liver metabolism and is used in toxicological studies [240]. Coumestrol and E2, as well as the positive control NAC, inhibited cellular death induced by H_2O_2 and rotenone (Fig. 18), showing an antioxidant effect (Fig. 19). The protection afforded by coumestrol and E2 was similar to that of NAC, a precursor of glutathione, previously shown to prevent oxidative stress in various models [346, 347]. Further work is clearly necessary to determine the mechanisms of action of both compounds in decreasing oxidative stress. We further observed that the chaperone Hsp90, a protein that assists on protein folding and responds to heat stress and protein degradation [348], is augmented in cells under the treatment with rotenone upon a treatment with E2 or coumestrol (Fig. 20).

Interestingly, E2 and coumestrol also increased SOD2 content after rotenone treatment. In this case, it may be that both compounds act by increasing the expression of that stress response as a first-responder to $O_2^{\bullet -}$ caused by rotenone-mediated complex I inhibition.

After obtaining the results regarding coumestrol, we next confirmed that coumestrol induces a lower proliferation of breast cancer cells than E2. We need more assays to determine the mechanism but at this point, we cannot exclude that in cancer cells, coumestrol may inhibit the cell cycle. Our data are in accordance with Lee *et al*., that have shown that coumestrol induces cellular senescence through p53-p21 pathway, inducing ROS generation in MCF-7 and HCT116 cell lines. As senescence is important in the context of cancer, and we observed a reduction on cell proliferation when compared with E2 incubated cells, these data are relevant to support this previous study [349].

Highlights of the present chapter:

- Coumestrol and resveratrol, similarly to E2, reduced lipid peroxidation of isolated mitochondria.
- Resveratrol inhibit complex I and complex V activities.
- Resveratrol behaved as a competitive inhibitor of complex I whereas E2 acted as a non-competitive inhibitor.
- Coumestrol, similarly to E2 and NAC, protects HepG2 cells from pro-oxidant agents.
- Coumestrol had a higher anti-proliferative effect on breast cancer cells when comparing with E2.

4.2. Modulation of GLUT-1 expression by estradiol and coumestrol at the blood brain barrier

4.2.1 Background and objectives

More than 75% of women worldwide experience hot flashes during menopause [35, 350]. Hot flashes are sudden heat sensations that are most intense over the face, neck and chest area and are accompanied by sweating [351]. Other symptoms include rapid heartbeat, nausea, dizziness, anxiety, headache, weakness, or a feeling of suffocation. The cause of hot flashes is currently unknown, but Dormire proposed the "*impaired glucose delivery hypothesis of menopausal hot flashes*" [36, 244]. This hypothesis states that glucose transport across the blood-brain barrier into the brain decreases during menopause, which is compensated by the sympathetic nervous system through the increase of blood flow to the brain, thus causing hot flashes [36]. This is supported by studies showing that ovariectomy in female rats lowers blood glucose levels and leads to temperature variation in those animals [352, 353]. Overall, these studies suggest that inadequate glucose transport into the brain is one cause of hot flashes in women [353, 354].

The mammalian brain requires 20-25% of total body glucose and since the brain has limited capacity to store energy, a continuous glucose supply is critical for normal brain function. This high glucose demand is met by glucose transporter 1 (GLUT-1; *SLC2A1*), which the brain almost exclusively depends on, providing GLUT-1 with a critical role in proper brain function [355]. This transporter is a highly specific uniporter facilitating glucose transport across the blood-brain barrier from the blood into the brain [356, 357]. Within the brain, GLUT-1 is predominantly expressed in the brain capillaries of the blood-brain barrier, where it is located in the abluminal and luminal capillary membranes [358].

One hypothesis postulates that hot flashes in menopausal women are associated with transient deficiencies in brain glucose levels as a consequence of decreased blood-brain barrier GLUT-1 levels due to ovarian E2 decline [359]. This is supported by several studies. Shi and Simpkins suggest that GLUT-1 expression is modulated by E2 [353]. Reports also showed that decreased E2 levels in female rats correlate with reduced GLUT-1 mRNA levels in the cerebral cortex and that E2 deficiency in ovariectomized rats decreases GLUT-1 protein expression and diminishes glucose availability in brain endothelial cells [353, 354]. Thus, E2 has the potential to increase GLUT-1 expression and function at the blood-brain barrier, which is able to restore full GLUT-1 activity, ensuring proper glucose supply, and reducing menopausal hot flashes. Therefore, insights into the mechanism through which E2 regulates GLUT-1 could provide new strategies for the therapy of hot flashes in menopausal women.

Here, the focus was on the regulation of blood-brain barrier GLUT-1 by 17β-estradiol and selected PEs. In this study, we determined the effect of E2 on blood-brain barrier GLUT-1

protein expression levels and assessed several PEs for their potential to mimic the E2 effect.

4.2.2 GLUT-1 expression at the blood-brain barrier

To determine GLUT-1 protein expression levels at the blood-brain barrier, we performed immunofluorescence and western blotting of isolated rat brain capillaries. The western blot in figure 24 shows a weak band for GLUT-1 in brain capillary membranes when 0.1 or 0.5 µg of protein was loaded, but a strong GLUT-1 band with 1 µg protein. Consistent with GLUT-1 being a membrane protein, the signal in capillary membranes is substantially stronger compared to that in brain capillaries and brain capillary lysate, where the GLUT-1 protein signal is weak even with 10 µg protein loading. Digital molecular weight analysis revealed that the GLUT-1 signal is at 55 kDa, which is consistent with literature values [353, 360]. Immunofluorecence experiments of isolated rat brain capillaries localized GLUT-1 at both luminal and abluminal membranes (Fig. 24).

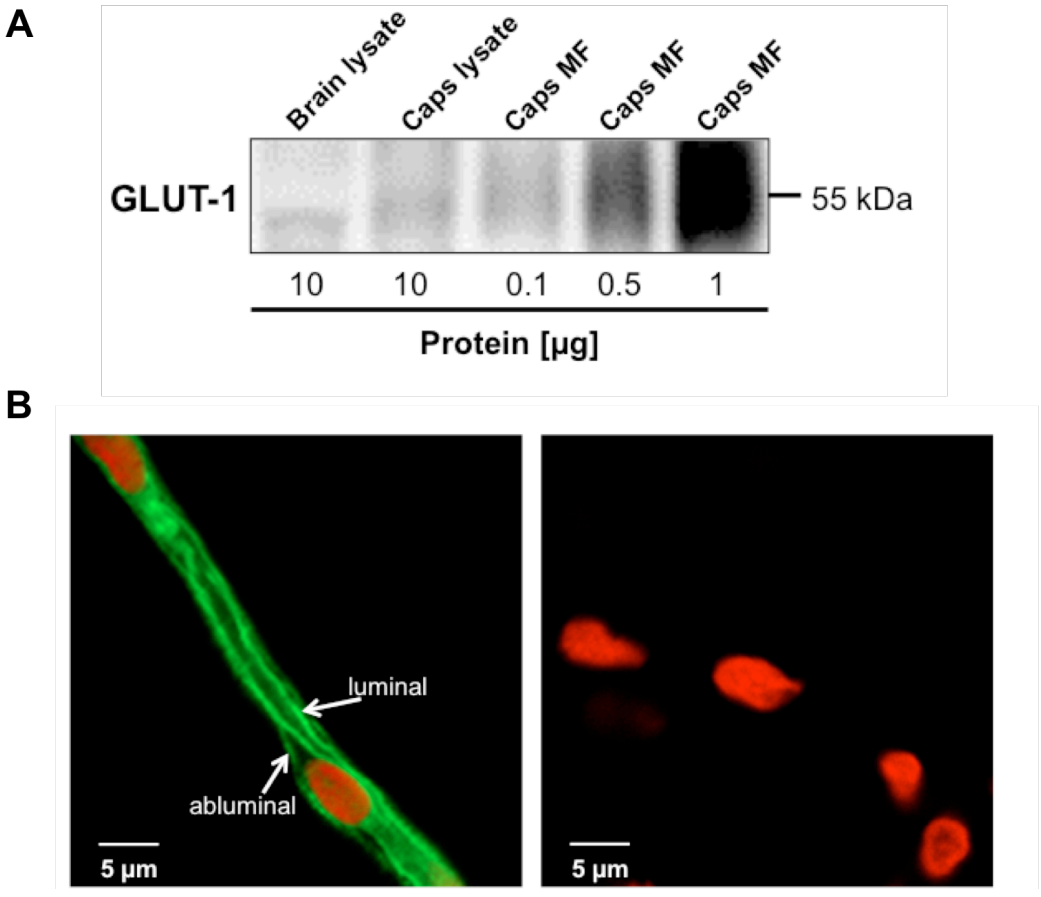

Figure 24: GLUT-1 expression in isolated brain capillaries.
(A) Western blot of total brain lysate, brain capillary lysate and brain capillary membranes showing GLUT-1 expression. GLUT-1 protein is enriched in brain capillary membranes. (B) Representative image of an isolated brain capillary immunostained for GLUT-1 (green) and counterstained with propidium iodide for nuclei (red). Consistent with the Western blot, GLUT-1 is localized in the luminal and abluminal membranes (arrows). Legend: Caps- capillaries, MF – membrane fraction.

Together, these data demonstrating high GLUT-1 expression levels in isolated rat brain capillaries are consistent with previously published studies [357, 361].

4.2.3 Estradiol increases GLUT-1 expression levels at the blood-brain barrier

To test our hypothesis that E2 regulates GLUT-1 expression at the blood-brain barrier, we exposed freshly isolated brain capillaries to 10 nM E2 for 1, 3 and 6 hours. Capillary membranes were isolated and analyzed by Western blotting. GLUT-1 expression increased in a time-dependent manner and was maximal after 6 hours of exposure to 10 nM E2 (Fig. 25). We observed a similar increase with 100 nM E2, which increased GLUT-1 expression levels by 22 ± 4% compared to control GLUT-1 expression levels (Fig. 25).

To determine the effect of E2 on GLUT-1 expression at the blood-brain barrier *in vivo*, we dosed mice with 0.1 mg/kg E2 by i.p. injection and isolated brain capillaries 1, 6, and 24 hours after E2 dosing. The Western blots of brain capillary membranes showed a change in GLUT-1 expression levels 1 hour after E2 dosing (Fig. 25), but a substantial increase in GLUT-1 levels was observed 6 hours after E2 administration. 24 hours after E2 dosing, GLUT-1 expression was back to control levels (note that the difference in control GLUT-1 levels at time points 1 and 24 hours vs. 6 hours is not due to actual differences in GLUT-1 expression levels, but due to different exposure times of the Western blots).

This GLUT-1 expression pattern follows E2 plasma concentrations after administration of 0.1 mg/kg E2 by ip injection, where E2 levels increase rapidly within one hour after dosing and then fall over the course of 24 hours [265]. Together, these data demonstrate that E2 increases GLUT-1 protein expression levels in isolated rat brain capillaries and at the rat blood-brain barrier *in vivo*.

4.2.4 Estradiol increases GLUT-1 expression levels in brain capillaries through estrogen receptor-α

To determine the mechanism through which E2 modulates GLUT-1 at the blood-brain barrier, we exposed freshly isolated brain capillaries to 10 nM propylpyrazoletriol (PPT), an estrogen receptor α (ERα) specific agonist, or to 10 nM diarylpropionitrile (DPN), an estrogen receptor β (ERβ) specific agonist [362]. Figure 26 shows that specific activation of ERα with PPT mimicked the E2 effect and increased GLUT-1 expression, whereas specific activation of ERβ with DPN (Fig. 26) had no effect. Note that we refrained from using ER inhibitors since commercially available inhibitors are receptor-unspecific.

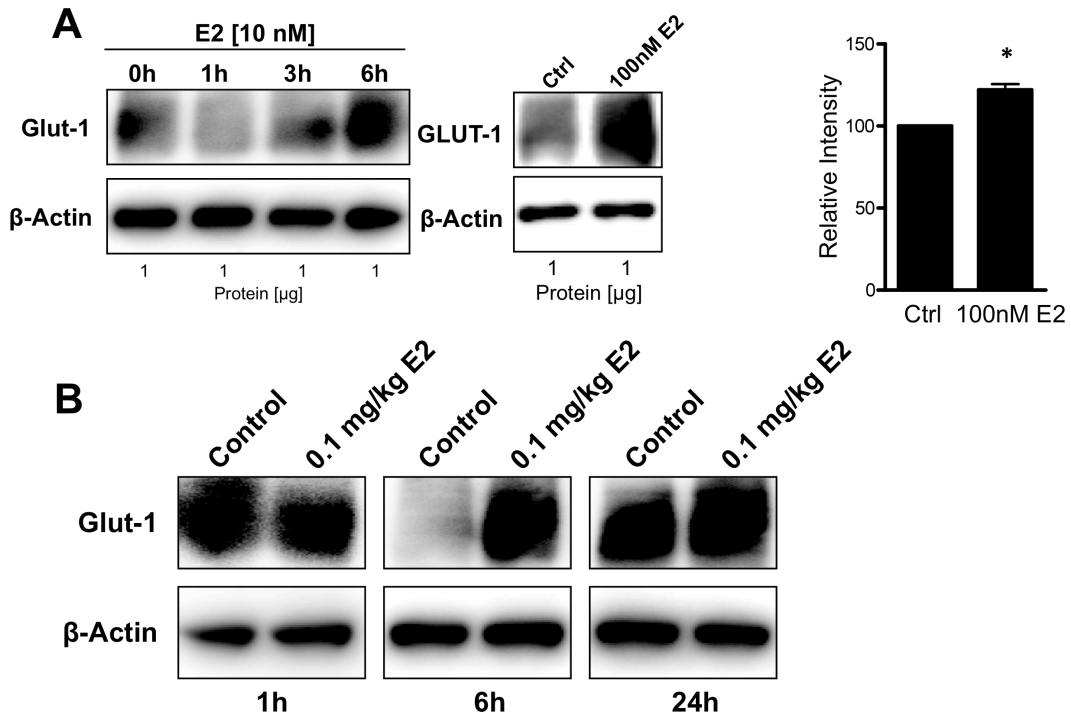

Figure 25: E2 increases GLUT-1 protein levels in brain capillaries.
(A) Western blot showing the time-dependent effect of 10 nM E2 on GLUT-1 protein expression levels in isolated brain capillaries *ex vivo*. The GLUT-1 signal is stronger when brain capillaries were exposed to E2 for 6 hours. Western blot showing the effect of 6 hours exposure of 100 nM E2 on GLUT-1 protein levels in isolated brain capillaries *ex vivo*. Data are mean ± SEM of three independent experiments. * $p<0.05$ when compared with control. (B) Western blot showing the *in vivo* effect of 0.1 mg/kg E2 on GLUT-1 protein levels in brain capillaries from mice 1, 6, and 24 hours after treatment. β-Actin was used as loading control. Images are representative of three different experiments of a pool of 10 animals.

To confirm involvement of ERα, rather than ERβ, in E2 signaling to induce GLUT-1 expression, we exposed isolated brain capillaries from ERα and ERβ knock out (KO) male and female mice to 10 nM E2. Figure 28 shows that in brain capillaries from both male and female wild type (WT) mice, 10nM E2 increased GLUT-1 expression levels, which is consistent with our data in rat (Fig. 26). We observed the same E2-effect on GLUT-1 in brain capillaries from ERβ KO mice, but not in brain capillaries from ERα KO mice. Thus, these data indicate that E2 induces increase of GLUT-1 expression at the blood-brain barrier through ERα.

4.2.5 Coumestrol increases GLUT-1 expression levels in brain capillaries

Given the side effects of E2 administration in post-menopausal women [63], we tested the effect of four PEs (resveratrol, enterolactone, enterodiol, coumestrol) on GLUT-1 expression levels in isolated rat brain capillaries as an alternative strategy to hormone replacement therapy. At the concentrations tested (100 and 1000 nM), resveratrol, enterolactone and enterodiol had no effect. However, we observed an increase in GLUT-1 protein levels in isolated rat brain capillaries that were exposed to 10 and 100 nM coumestrol, the same

concentrations we used for E2 (Fig. 27). Thus, these findings imply that the phytoestrogen coumestrol has the potential to modulate GLUT-1 at the blood-brain barrier.

4.2.5 Discussion

Based on the impaired glucose delivery hypothesis by Dormire [36, 363], hot flashes are an exaggerated response of the neurovascular coupling system to decreased glucose delivery into the brain via GLUT-1 in menopausal women. That is, when estrogen levels decrease in menopause, blood-brain barrier GLUT-1 levels are impaired and do not meet the brain's demand for glucose. Hot flashes are considered a compensatory neurovascular response initiating sympathetic nervous system-mediated vasodilation, which leads to increased blood flow to the head, and thus, resulting in increased delivery of glucose and oxygen to meet the needs of the brain.

In our study, we addressed this clinically important topic and investigated the effect of E2 and PE on blood-brain barrier GLUT-1. We show here that GLUT-1 is highly expressed in plasma membranes of isolated brain capillaries and located on both the luminal and the abluminal membranes of capillary endothelial cells (Fig. 24). These findings are consistent with previously published literature [354, 360]. Our study also provides new insights into the regulation of GLUT-1 by estrogens. We show that exposing isolated brain capillaries to nanomolar concentrations of E2 increases GLUT-1 protein expression within 6 hours (Fig. 25). Consistent with this, we found increased GLUT-1 levels 6 hours after treating mice with 0.1 mg/kg E2 (Fig. 25). Experiments with capillaries from ERα and ERβ agonists and with ERα KO and ERβ KO mice revealed that E2 signals through ERα to increase GLUT-1 expression in brain capillaries (Fig. 26). We further assessed the effect of PE on GLUT-1 expression in isolated brain capillaries. Resveratrol, enterolactone, and enterodiol had no effect on GLUT-1 levels (Fig. 27) whereas coumestrol increased GLUT-1 expression to a similar extent as E2 did. Thus, coumestrol can potentially be one option in estrogen replacement therapy to improve hot flashes in menopausal women with less side effects than E2 [364, 365].

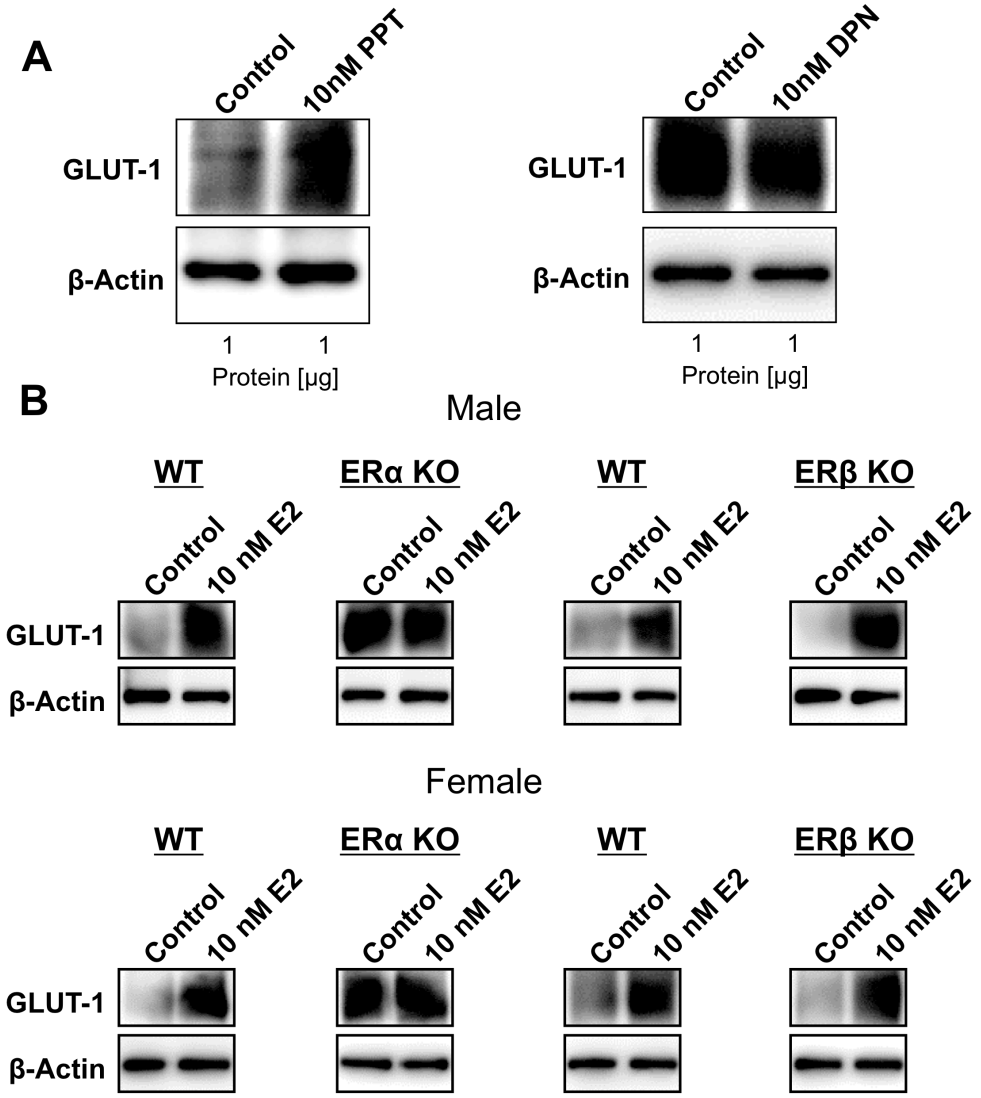

Figure 26: E2 signals GLUT-1 induction in brain capillaries through ERα.
Western blots showing the effect on GLUT-1 expression after 6 hours exposure of isolated brain capillaries to the ERα agonist propylpyrazoletriol (PPT) and the ERβ agonist diarylpropionitrile (DPN). Only PPT exerted an effect on GLUT-1 protein levels indicating that E2 signals GLUT-1 induction via ERα in isolated brain capillaries. Western blots showing the effect of 6 hour exposure of brain capillaries from female and male wild type mice, ERα knockout mice, and ERβ knockout mice to 10 nM E2. E2 had no effect on GLUT-1 protein levels in brain capillaries from ERα knockout mice, confirming that E2 signals GLUT-1 induction via ERα. β-Actin was used as loading control. These images are representative of 3 different experiments, each one of a pool of capillaries from 10 animals.

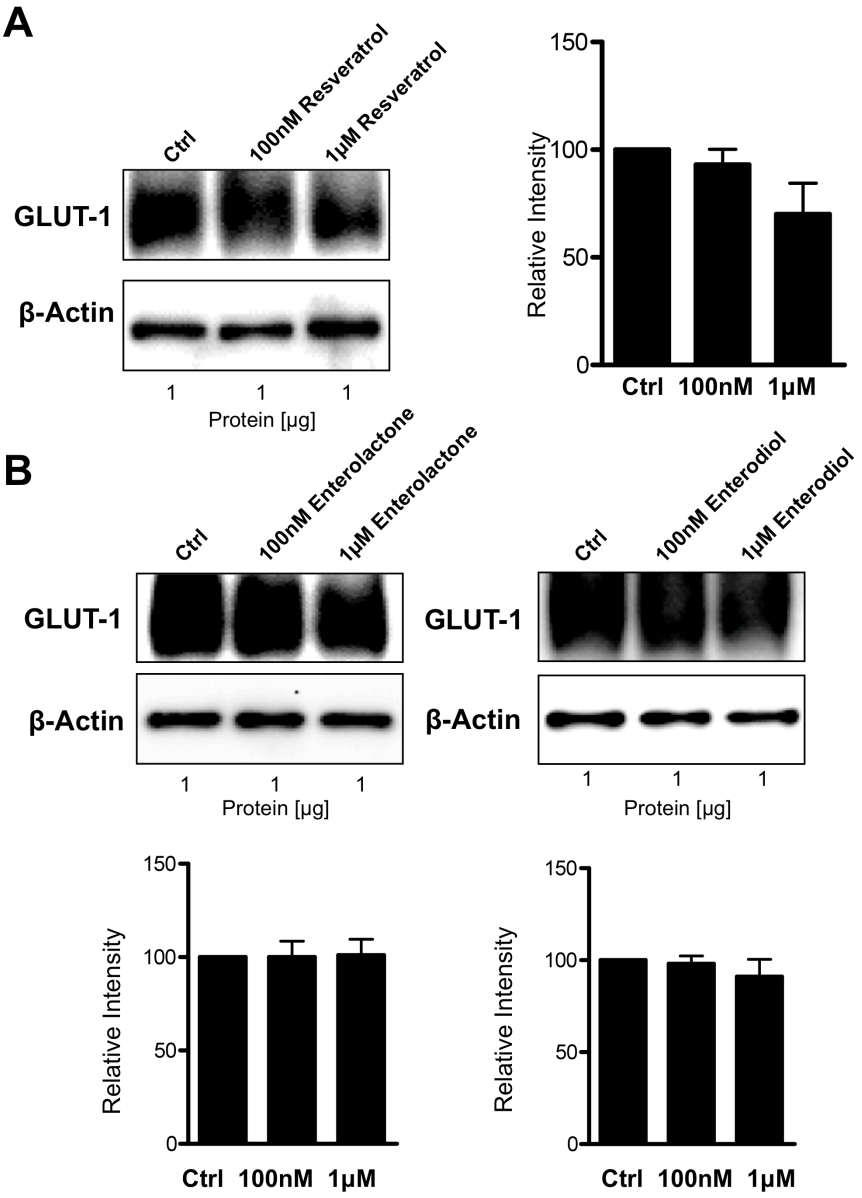

(figure continues next page)

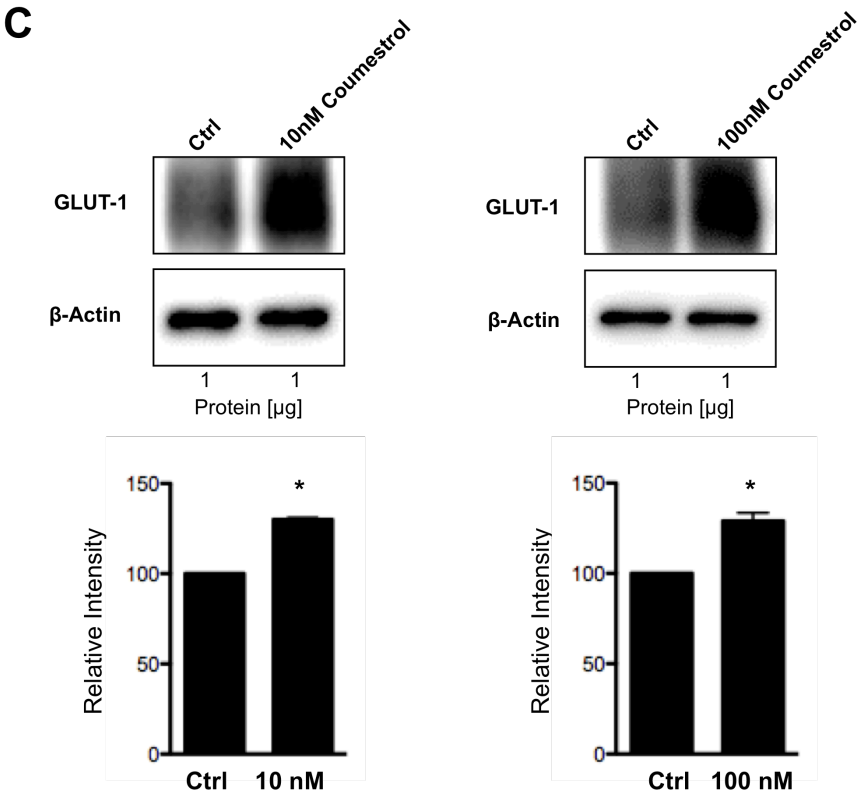

Figure 27: Effect of phytoestrogens on GLUT-1 protein levels in brain capillaries.
(A, B) Western blots showing that resveratrol, enterolactone, or enterodiol had an effect on GLUT-1 expression levels in isolated brain capillaries. (C) Western blots showing the effect of 6 hours exposure of isolated brain capillaries to 10 and 100 nM coumestrol on GLUT-1 protein expression levels. β-Actin was used as loading control. These images are representative of 3 different experiments, each one of a pool of capillaries from 10 animals. Data shows mean ± SEM of three independent experiments. * $p<0.05$ when compared with control

With regard to E2 effects on blood-brain barrier GLUT-1, the only available study on this topic is the one by Shi and Simpkins [354]. These authors reported that treating ovariectomized rats with E2 increased GLUT-1 protein expression and 2-deoxy-[^{14}C] glucose uptake in isolated brain capillaries in a dose- and time-dependent manner [354]. Four hours after administration of 10 µg/kg E2, a 30% increase of GLUT-1 expression was observed. E2 also transiently increased GLUT-1 mRNA with a peak (55% increase) at 15 min after dosing that normalized to basal levels within 2 hours after E2 administration [353]. Similar to the data by Shi and Simpkins [353], our data demonstrate that E2 effect on GLUT-1 expression was small (~22%), confirming the previously published findings. These results suggest that estrogens play a role in modulating the brain glucose transport, which is different from peripheral tissue, where glucose transport is regulated by insulin and can be increased by up to 20-fold [366, 367].

Second, previous work showed that both ERα and ERβ are expressed in rat brain capillaries [265, 368]. The present study demonstrates that E2 signals through ERα to increase GLUT-1 protein expression at the blood-brain barrier. Although estrogen receptors activate transcription of their target genes by binding to the corresponding estrogen response

element (ERE), previous studies found no consensus about the ERE sequence in the gene for rat GLUT-1 [369, 370]. One possibility of how ERα could signal GLUT-1 transcription is by binding to a variation of the consensus ERE or to ERE half-sites to increase GLUT-1 transcription. While this mechanism has been verified for the progesterone receptor, more studies are needed to confirm this for E2 modulation of GLUT-1 [370]. The present experiments with ER agonists and KO mice for ERα and ERβ, clearly show for the first time that E2 signalling through ERα increased GLUT-1 protein levels at the blood-brain barrier.

Third, PEs are plant-derived compounds with estrogenic activity that could potentially be used as alternatives to E2 [237, 371]. In a set of experiments we tested the effect of several PE on GLUT-1 expression in isolated rat brain capillaries, specifically resveratrol, enterolactone, enterodiol and coumestrol (Fig. 27). Although the isoflavones genistein and daidzein are well-known PE, they are also inhibitors of glucose transport, and therefore, were not tested [268, 269]. Our experiments showed that resveratrol had no effect on GLUT-1 expression. Although resveratrol binds to ERα and ERβ with comparable affinities, they are about 7,000 - fold lower than those of E2 [92]. This might explain why no effect of resveratrol on GLUT-1 expression was detected. The lignans enterolactone and enterodiol, for which the binding affinities to ERα and ERβ are unknown, also had no effect on GLUT-1 expression. In contrast, 10 - 100 nM coumestrol increased GLUT-1 expression in isolated rat brain capillaries. Coumestrol is derived from sprouting plants such as alfalfa and is present in clover and soy beans as well. It is the most potent coumestan with binding affinities to human ERα (20%) and ERβ (140%) and the transactivation activity is about 102% for ERα and 98% for ERβ which is comparable to that of E2 [90]. Thus, compared to other PE, higher coumestrol binding affinities to ERα and ERβ likely explain its effect on GLUT-1 expression and why other phytoestrogens we tested lacked this effect.

Lastly, during menopause, E2 production is reduced, decreasing circulating E2 levels which is thought to cause hot flashes. It is thought that absence of E2 decreases GLUT1-expression leading to neuroglycopenia (low glucose brain levels). Neuroglycopenia is considered to initiate a reactive, sympathetic nervous system-driven increase in blood flow to counteract glucose shortage in the brain, thus causing hot flashes [36]. Our study shows that E2 and coumestrol upregulate GLUT-1 expression in brain capillaries, which suggests that coumestrol could be used as a potential alternative to E2 in hormonal replacement therapy for menopausal women regarding hot flashes symptoms. Nonetheless, investigations about the role of coumestrol and E2 on the GLUT-1 function must be performed to see if the positive modulation on its expression results in increased glucose delivery to the brain.

Highlights of the present chapter:

- GLUT-1 was highly expressed in the membranes of brain microvessels
- E2 increased the expression of GLUT-1 in the BBB at physiological concentrations, in both *ex vivo* and *in vivo models*
- GLUT-1 expression was modulated by ERα, as found in *ex vivo* and *in vivo studies*
- From the several PEs in study, coumestrol was the only one able to increase GLUT-1 expression in a similar fashion as E2

4.3. Coumestrol effects in two different menopause *in vivo* models

4.3.1 Background and objectives

As described elsewhere in this thesis, the control of mitochondrial functionality coupled with cytosolic signaling and energy demand is essential for cell survival. Some of the mitochondrial components are regulated by ovarian hormones and suggest sex differences in mitochondrial fitness [335]. The role of estradiol replacement on ovariectomized animals was associated to bioenergetic changes in brain mitochondrial proteome, shifted to an increase in oxidative phosphorylation and ATP synthase corroborated by an increased brain mitochondrial efficiency [372].

From data obtained in the previous chapters of this thesis, the compound with best results was coumestrol, showing low mitochondrial toxicity and high antioxidant proprieties, reducing proliferation of breast cancer cells and positively modulating GLUT-1 expression at the BBB. Others published that it also increases the expression of SOD and reduces the proliferative growth, showing its cytoprotective effects [373]. Coumestrol is one of the PE with highest estrogenic activity when compared to E2, which argues for its use as a potential alternative to HRT during menopause [90].

However, we are far from understanding if coumestrol has the same mitochondrial effects *in vivo*. Thus, a comparison of the effects of coumestrol and E2 in mitochondrial bioenergetics and oxidative stress in brain and liver fractions of two distinct menopausal models was performed.

For the present experimental aim, young adult Wistar rats were previously ovariectomized at Charles River's laboratories (L'Arbresle, France) in order to eliminate the main endogenous source of estradiol. The animals were allowed to recover from surgery during one week prior to be shipped into our animal facility, where they were allowed to acclimate three weeks prior the treatment with the tested compounds. Sixteen-weeks old ovariectomized (OVX) animals were then intraperitoneally injected with 30 µg/kg of E2 or coumestrol or equivalent volume of vehicle oil (stripped corn oil). The same experimental design was also used in VCD-treated animals, a second menopause in vivo model.

4.3.2 Models used

Although the pathophysiology of menopause has been widely studied, there is still a controversy regarding the best model to investigate menopause in rats. The use of OVX animals has positively contributed for the understanding of menopausal hormone effects. Nevertheless, this model has clear limitations as the lack of the initial phase of menopausal transition, the perimenopause; the process results in the absence of any ovarian tissue instead of a selective loss of follicular estrogens as in regular menopause and it does not allow the manipulation of the hypothalamic-pituitary-ovarian axis [218]. Thus a new model

based on the injection of VCD to animals has been used recently. This model involves an apoptotic mechanism of follicular atresia similar to what occurs in women [374].

4.3.3 Ovariectomy model of menopause

4.3.3.1 Animal mass and serum biochemistry

Twenty-four hours after E2 or coumestrol administration, animals were sacrificed and blood samples collected for analysis: no substantial alterations were observed in blood biochemical analysis (Table 11), indicating that the treatment with E2 or coumestrol did not increase markers of hepatic and renal damage. However, we observed a slightly but significant, increase in the E2 values in the blood from 0.30 ± 0.06 (OVX) to 0.40 ± 0.08 pg/ml (OVX + E2), ($p=0.038$, $n = 4$).

Table 11: Estradiol and coumestrol do not alter serum markers

	OVX	OVX+E2	OVX+Coum
Urea	41.3±1.9	38.00±2.31	39.8±1.85
GOT	132.4±9.4	139.8±12.0	159.0±10.8
GPT	47.1±4.0	44.8±3.5	49.6±1.7
Creatinine	0.59±0.0	0.56±0.02	0.52±0.01
Cholesterol	112.1±5.4	95.8±14.4	108.8±3.9
Protein	6.5±0.2	6.43±0.1	6.5±0.03
Triglycerides	118.9±7.0	105.0±23.4	119.4±18.4
CK	3830±914.8	4845±1260	4807±585.3

Blood biochemical analysis from OVX rats treated with vehicle, E2 and coumestrol. Legend and units: Urea (mg/dl), GOT- glutamic oxaloacetic transaminase (U/l), GPT - glutamic-pyruvic transaminase (U/l), Creatinine (mg/dl), Cholesterol (mg/dl), Protein (U/l), Triglycerides (mg/dl), CK- creatine kinase (U/l) Data represent mean ± SEM of 6 to 8 animals.

4.3.3.2 Coumestrol increases the respiratory control ratio in glutamate-malate energized brain mitochondria

We first measured mitochondrial respiration of freshly isolated brain and liver mitochondria using either glutamate/malate or succinate as substrates. *In vivo* treatment of OVX rats with E2 and coumestrol causes increased the respiratory control ratio in brain mitochondria, although only coumestrol reached a statistical difference (Table 12). No differences were observed when using succinate as substrate, however in liver the lag phase has a tendency to decrease ($p=0.058$), (Table 12).

4.3.3.3 Coumestrol increased mitochondrial complex I maximal activity in liver

So far, the effects of E2 or coumestrol (especially the latter) on mitochondrial bioenergetics were only observed in glutamate/malate - linked respiration. Hence, we next aimed to

investigate if both compounds would act directly by increasing complex I maximal activity. Therefore, after the isolation of these mitochondrial fractions, a small tissue sample was frozen for further experiments.

Table 12: Coumestrol increases the RCR of brain mitochondrial fraction in ovariectomized rats

		Brain			Liver		
		OVX	**OVX+E2**	**OVX+Coum**	**OVX**	**OVX+E2**	**OVX+Coum**
Glu/Mal	**state 3**	37.7±4.6	62.0±11.6	60.1±3.4	52.5±3.6	52.9±5.1	63.3±2.5
	state 4	15.8±2.5	13.0±1.7	13.2±1.2	12.9±1.2	13.0±1.1	14.2±1.6
	RCR	3.5±0.4	4.6±0.7	4.7±0.3 **	4.3±0.4	4.5±0.5	4.8±0.4
	ADP/O	2.0±0.1	1.9±0.1	1.7±0.4	1.8±0.1	1.9±0.1	1.7±0.1
	FCCP	44.9±4.6	43.9±7.5	44.7±2.5	75.2±9.9	90.4±14.5	92.4±15.0
	Olygomycin	11.0±1.4	9.2±1.2	11.0±1.0	9.1±0.8	8.9±0.9	10.92±1.0
	FCCP/O	4.2±0.2	4.8±0.4	4.2±0.3	8.4±0.9	10.2±1.3	8.3±0.7
Succinate	**state 3**	68.4±5.2	60.5±0.2	63.8±3.2	80.6±5.8	85.3±9.5	91.3±4.4
	state 4	24.1±2.6	23.3±2.6	36.0±1.6	25.8±2.1	26.0±2.6	30.9±3.4
	RCR	3.0±0.3	2.6±0.2	2.6±0.2	3.2±0.2	3.4±0.4	3.1±0.3
	ADP/O	1.14±0.0	1.2±0.1	1.1±0.0	1.1±0.0	1.0±0.0	1.1±0.1
	FCCP	70.7±14.80	62.0±10.7	76.5±16.9	140.6±12.0	160.3±12.3	167.9±9.6
	Olygomycin	19.3±3.3	18.5±2.8	18.6±1.0	18.7±0.9	20.5±1.5	23.2±3.9
	FCCP/O	4.0±0.8	3.3±0.2	4.2±1.1	7.6±0.7	7.8±0.2	7.7±0.8

Mitochondria function was evaluated as previous described in the material and methods section. Data represent mean ± SEM of 6 to 8 animals. **p<0.01 when compared with OVX non-treated rats. FCCP/O ratio indicated the elasticity of mitochondrial respiratory chain. Units: state 3, 4, FCCP and oligomycin – nmol O_2/min/mg protein.

Table 13: Absence of treatment-related effects on mitochondrial transmembrane electric potential (ΔΨ)

		Brain			Liver		
		OVX	**OVX+E2**	**OVX+Coum**	**OVX**	**OVX+E2**	**OVX+Coum**
Glu/Mal	**Max ΔΨ**	169.9±4.1	171.3±2.9	166.4±2.05	211.3±1.9	211.8±2.3	214.3±1.2
	Depolarization	16.2±0.9	16.7±1.3	15.3±0.9	26.7±2.0	25.9±1.7	22.9±1.7
	lag phase	61.3±6.6	56.6±6.6	57.8±3.3	63.0±7.9	57.0±5.8	54.0±9.2
Succinate	**Max ΔΨ**	173.3±1.8	175.0±2.3	172.8±1.2	217.3±2.8	219.2±4.2	213.7±6.8
	Depolarization	16.9±1.5	19.6±2.4	17.7±2.3	25.7±2.2	24.5±1.6	23.7±4.1
	lag phase	84.9±16.3	76.5±9.9	66.0±8.8	79.7±12.4	84.6±18.0	56.0±3.8

Data represent mean ± SEM of 6 to 8 animals. Legend and units: Max ΔΨ – maximal developed ΔΨ, Depolarizarion - ADP-induced depolarization – (-) mV, lag phase - seconds

The maximal activity of complex I was accessed in disrupted mitochondrial membranes through the reduction of 2,6-dichlorophenolindophenol (DCPIP), as a substitute. Our data suggest that the maximal activity of complex I is augmented through the treatment with coumestrol in liver and brain preparations of about 20% (Fig. 28).

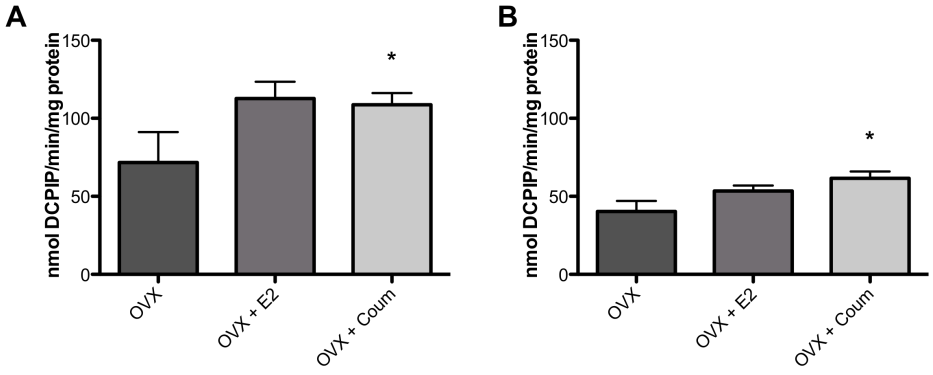

Figure 28: Coumestrol increases complex I maximal activity in liver mitochondrial fraction.
Mitochondrial membranes were disrupted and the maximal activity of complex I was indirectly obtained by the reduction of DCPIP. A) data from brain mitochondria, B) data from liver mitochondria. Activity expressed as nmol DCPIP/min/mg protein Data are the mean ± SEM of 4 to 6 animals. Statistical significance: *p<0.05 when compared with the respective control. Legend: OVX - ovariectomized animals, E2 – estradiol, Coum – coumestrol.

4.3.3.4 Coumestrol and estradiol do not alter the mitochondrial ultrastructure or the content of mitochondrial complex

After observing the differences in terms of mitochondrial bioenergetics, we next explored the brain and liver tissue ultra-structure, especially looking at mitochondrial morphology. We were interested in evaluating whether E2 or coumestrol would alter mitochondrial ultrastructure and morphology. We did not observe any tissue-related difference regarding mitochondrial morphology for each tissue (Fig. 29).

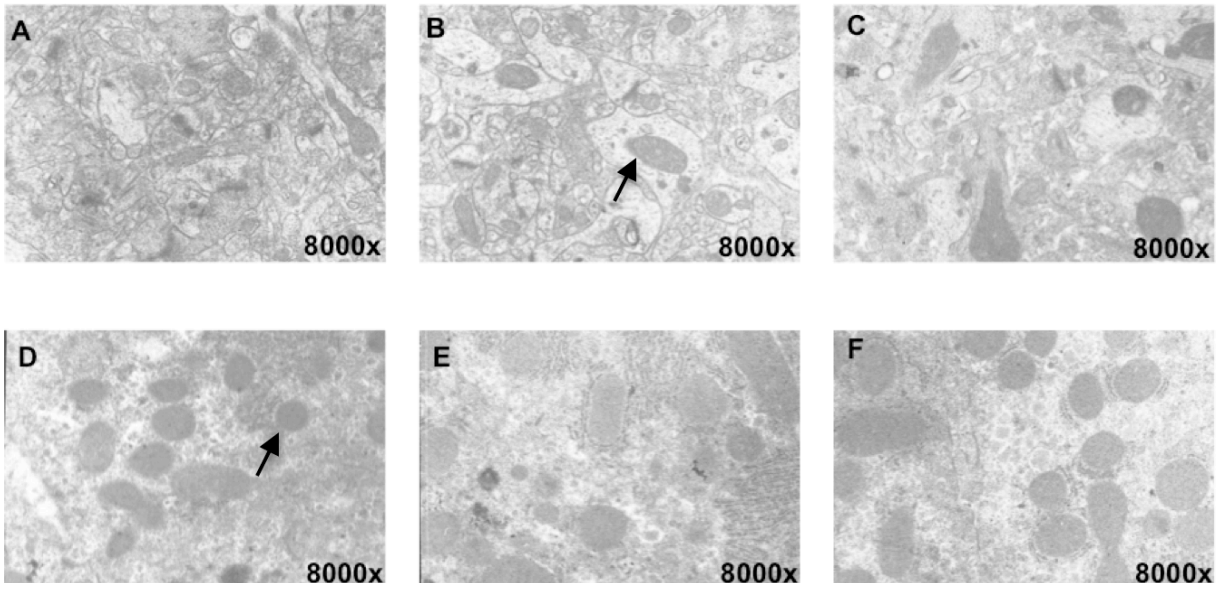

Figure 29: Cellular ultrastructure remains intact after E2 or coumestrol treatment. No differences were observed in terms of mitochondrial structure (arrow) in both tissues after each treatment.
Electronic microscopy of brain and liver tissue was performed as described in the material and methods section. Panel A, B, C, brain mitochondria of OVX, OVX + E2, OVX + Coum, respectively. D, E, F, liver mitochondria of OVX, OVX +E2, OVX + Coum, respectively.

In order to determine the effects of E2 and coumestrol in the content of protein subunits of oxidative phosphorylation apparatus, we extracted protein from the brain and liver tissue and used a cocktail of antibodies target to selected subunits of the respiratory mitochondrial chain. These results show that complex I NFUDB8 in brain has a tendency (p = 0.057) to increase in coumestrol-treated OVX rats (Fig. 30).

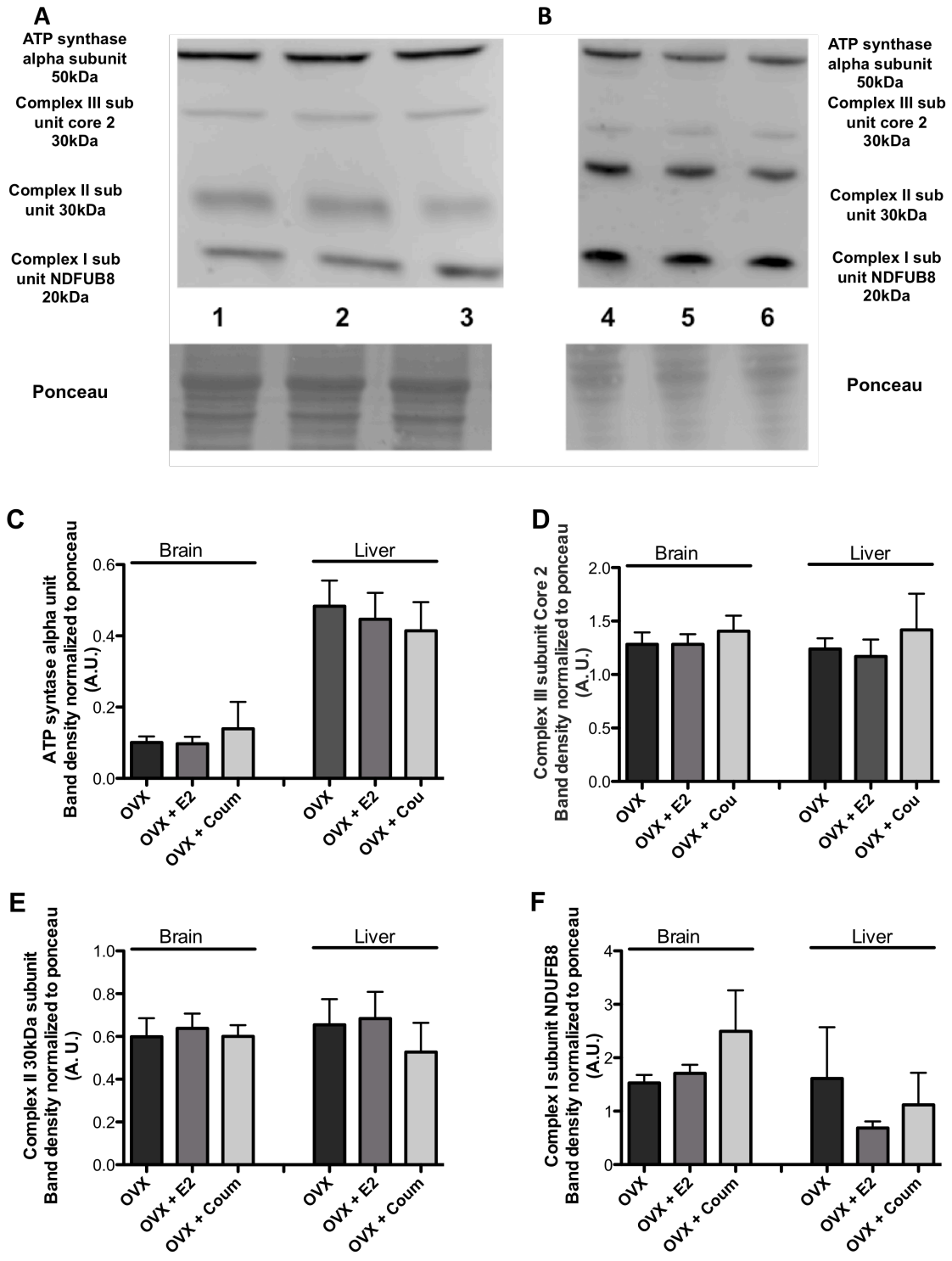

Figure 30: Evaluation of respiratory chain complexes subunits by western blotting after E2 and coumestrol treatment.
Mitochondrial oxidative phosphorylation content was identified by western blotting in brain (A) and liver (B) tissues after E2 and coumestrol administration. Ponceau staining was used as gel loading control, with C, D, E, F graphs showing the densitometry analysis of bands of each protein normalized to the

ponceau intensity. The results are representative of 4 to 8 separated samples. 1) OVX, 2) OVX + E2, 3) OVX + Coum, 4) OVX + Coum, 5) OVX + E2, 6) OVX. Legend: OVX - ovariectomized animals, E2 – estradiol, Coum - coumestrol

4.3.3.5 Coumestrol antioxidant proprieties in brain and liver mitochondria

Although we did not observe differences on hydrogen peroxide generation (Fig. 31) in the mitochondrial respiratory chain with glutamate/malate or succinate as substrates, we evaluated lipid peroxidation in the same sample. Brain mitochondria from E2 or coumestrol treated animals have a lower content of malondialdehyde (MDA), a marker of lipid peroxidation, decreasing from 0.94 ± 0.12 in OVX animals, to 0.7 ± 0.04 (OVX + E2) or 0.61 ± 0.05 µM (OVX + coumestrol). An increase in vitamin E levels from 1.6 ± 0.2 to 2.4 ± 0.3 µM was found in coumestrol-treated OVX animals (Fig. 32).

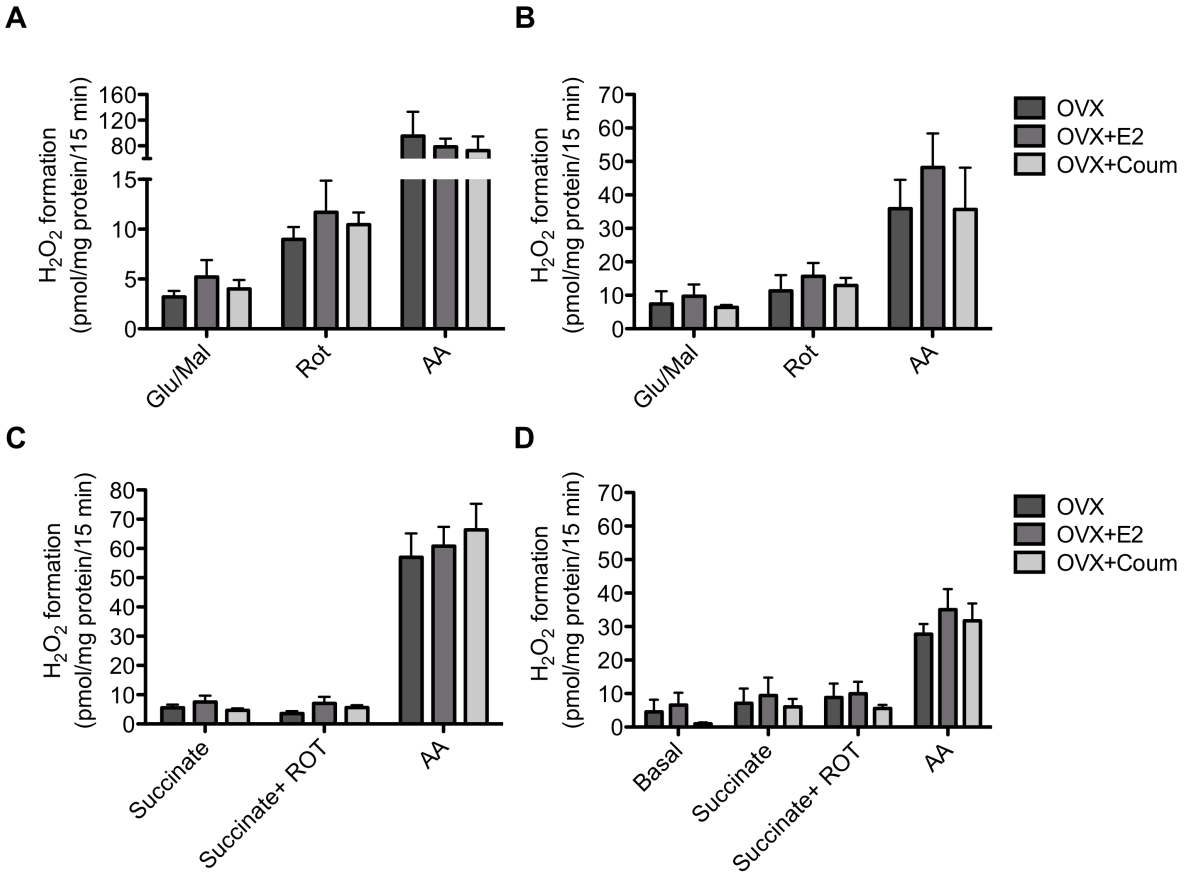

Figure 31: Effect of E2 or coumestrol administration on mitochondrial hydrogen peroxide (H_2O_2) production.
The production of hydrogen peroxide by the mitochondrial respiratory chain was evaluated as described in the materials and methods section. Mitochondrial fractions from brain and liver of female ovariectomized Wistar-Han rats were incubated with standard respiratory medium. Glutamate/malate (5 mM/2.5 mM) or succinate (5 mM) were used as substrates. Rotenone (1.0 µM) and antimycin A (0.5 µM) were used to increase H_2O_2 production. Mitochondrial hydrogen peroxide generated in (A) brain and (B) liver in the presence of glutamate/malate; (C) brain and (D) liver in the presence of succinate. Data represent mean ± SEM from three to four independent experiments. Legend: OVX - ovariectomized animals, E2 – estradiol, Coum - coumestrol

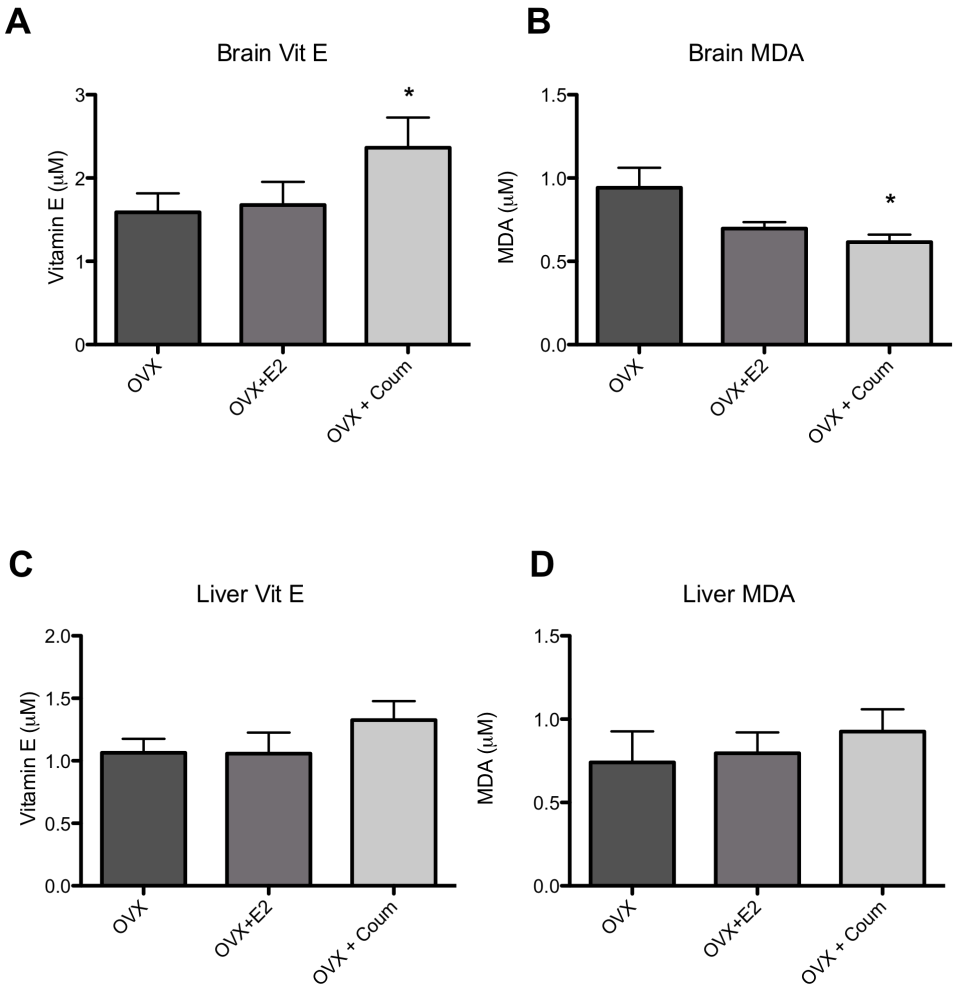

Figure 32: Coumestrol treatment decreases the lipid peroxidation marker MDA and increases vitamin E content in brain mitochondria.
Oxidative markers were measured as described in the material and methods section. A, C) Vit E content in brain and liver mitochondria, respectively, B, D) MDA content in brain and liver mitochondria respectively. Data represent mean ± SEM of 6 to eight independent preparations. *$p<0.05$ compared to OVX animals. Legend: OVX - ovariectomized animals, E2 – estradiol, Coum - coumestrol

4.3.3.6 Coumestrol and E2 decrease temperature variations in OVX rats

Under constant ambient temperatures, the measurement of rat temperature is considered to be proportional to blood flow [375]. Although the difficulty to obtain a reproducible model for hot flashes in rats similar to what women experience, cutaneous vasodilation of the rat tail can be an indirect telltale of temperature changes [376]. During the estrous cycle, the vasomotor state of the rat tail varies [376], depending on the levels of estrogens. In accordance, tail skin vasodilatation is increased by ovariectomy [90] and decreased by treatment with estrogens [375-379]. In our model, the temperature variation in OVX rats was decreased in the presence of E2 or coumestrol (Fig. 33).

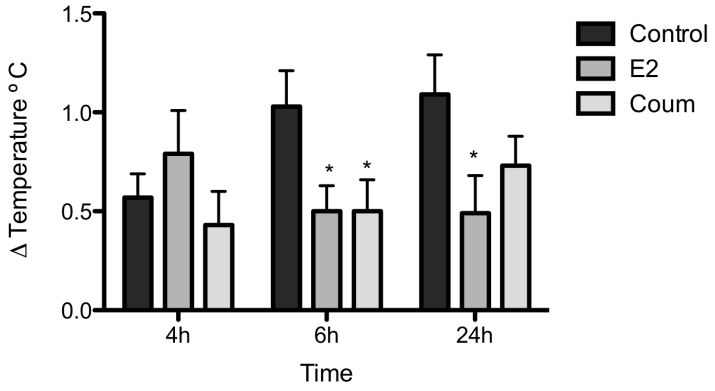

Figure 33: Coumestrol and estradiol decrease temperature variation in ovariectomized rats. Temperature transponder was implanted in OVX rats one week prior the experiments. Temperature was recorded at different time points after coumestrol (Coum) or E2 administration and compared with the core temperature before injection. Coumestrol and E2 decrease the temperature at 6 h, and the effects of coumestrol lasts for 24h. Data represent mean ± SEM of 4 animals *p<0.05 when compared with respective control. Legend: E2 – estradiol, Coum – coumestrol.

4.3.3.7 Discussion

Finding alternatives to HRT is critical to overcome menopausal symptoms, minimizing at the same time potencial negative side effects in a susceptible population. The effects of coumestrol and E2 were compared in OVX rats, regarding temperature changes, mitochondrial bioenergetics and oxidative stress markers. Estradiol regulates mitochondrial function, regulating ATP, calcium homeostasis and cell redox status [142]. The role of E2 on mitochondrial function is especially important to menopausal women that do not have ovarian E2 production.

It was previously shown that E2 treatment in OVX rats induces an increase in mitochondrial respiratory function [380], by increasing complex I activity or by decreasing oxidative stress. Our results were not as obvious as previously shown [362, 380], which might be explained by the different rat strain used in each study. In the present work, coumestrol, which has also been shown to cross the BBB, similarly to E2, was studied [78, 126]. In terms of mitochondrial oxidative stress prevention, coumestrol mimics E2 by preventing lipid peroxidation, explaining in part the lower levels of MDA (Fig. 32) when compared to OVX untreated rats. Also, the higher content of Vit E in brain mitochondria from coumestrol-treated rats, and the increased activity of superoxide dismutase similarly to what occurs with E2, [381] may indicate that coumestrol can be as effective as E2 regarding antioxidant protection of mitochondrial function. The strength of coumestrol effects in comparison to E2 regarding mitochondrial function may be justified by the estrogenic affinity to each estrogen receptor (ER). It is suggested that coumestrol has a higher affinity to ERβ than to ERα [90] Not only both receptors are present in mitochondria [277, 382], but also most of estrogen-mediated

effects on mitochondrial function occur through both receptors but depending in a larger extension on ERβ [362].

Although, few studies reported the alterations of mitochondrial function during menopause, although an increase in the expression of the voltage-dependent anion channel 1 (VDAC), adenine nucleotide transporter (ANT) and cytochome *c*, were previously shown, suggesting alterations in mitochondrial signaling [228]. Previously, a link between brain mitochondrial dysfunction, menopause and Alzheimer's disease was suggested, focusing the role of decreased estrogen content. In fact, surgically induced early menopause may increase cognitive vulnerability and estrogen re-introduction may promote a better outcome. However, there is still a missing link between age at menopause and Alzheimer risk [236]. Kemper and colleagues [235] have shown that ovariectomy decreases mitochondrial biogenesis and alter mitochondrial function in cerebral endothelium, reducing mtDNA/nuDNA ratio and ATPase 1α subunit. Although we did not measure ATP synthase activity, we were able to verify that coumestrol improves mitochondrial function, by increasing complex I maximal activity and RCR. However, we did not observe changes in state 3 respiration.

Mitochondrial function decline plays a role in the aging process and menopause is a critical period among women [201]. Several lines of study suggest that certain molecular and cellular changes are involved in the development of alterations that lead to impaired mitochondrial energy metabolism [202]. The free radical theory of aging postulates that oxidative stress is a determinant factor that limits longevity [203, 204]. The increased oxidative stress promoted by elevated production of reactive oxygen species is considered a determinant factor in mitochondrial dysfunction associated with aging. Here we show that coumestrol administration increases brain mitochondrial function in ovariectomized rats, which may be important in the context of neuroprotective effects of coumestrol.

Our data suggests that coumestrol, similarly to E2, has a protective vasomotor effect, by reducing temperature variations in OVX rats. Although the increase in the average changes in temperature after ovariectomy does not reflect an episodic event such as a flash, the changes on temperature by a pharmacological agent has been widely used to evaluate its efficacy in reducing flashes in women [383]. This important finding is another positive sign regarding the use of that compound on hormone replacement therapy. We also showed with the present study that coumestrol administration *in vivo* does not affect brain and liver mitochondria, mimicking what occurred *in vitro* (section 4.1). Nevertheless, it remains to be determined if animal age would impact the observed data since the present study was performed with young female rats.

4.3.4 Venylcyclohexene diepoxide (VCD) model of menopause

4.3.4.1 Animal mass and serum biochemistry

In order to measure morphometric and blood data, animals were individually analysed and the intrinsic weight variation of each animal was calculated for each week. Only in the third week of treatment a reduction on weight gain was observed. The weekly weight gain represents the variation between the weight in a certain day and the weight measured in the previous week. However, during the injection-free week the animals recovered the weight gain similarly to the control group (Fig. 34A). When we compared the initial and final weights of the two groups, no differences were observed (Fig. 34 B).

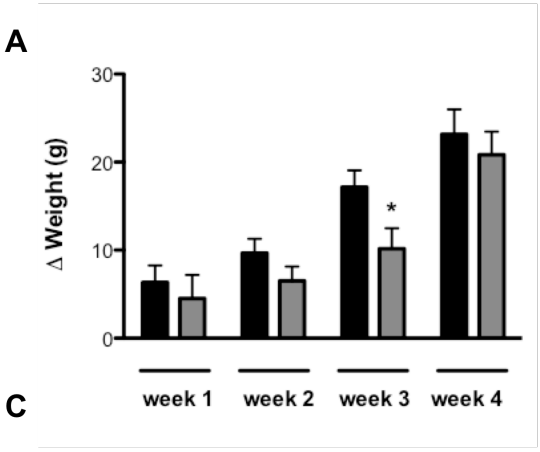

B

Treatment	Initial body mass (g)	Final body mass (g)	brain mass (g)	bM:BM
Ctrl	219.3 ± 3.3	242.5 ± 5.8	1.85 ± 0.02	0.76 ± 0.02
VCD	220.3 ± 4.2	241.2 ± 5.0	1.85 ± 0.02	0.77 ± 0.02

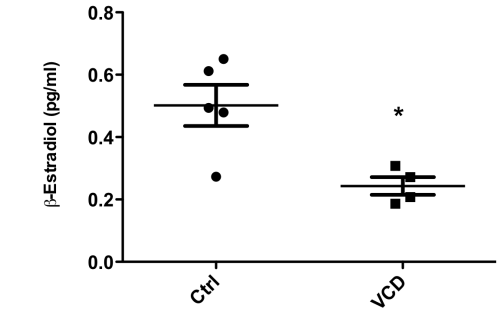

D

	CTRL	VCD
Urea (mg/dL)	55.60 ± 2.68	56.67 ± 4.92
Crea (mg/dL)	0.52 ± 0.01	0.56 ± 0.02
UA (mg/dL)	25.98 ± 1.24	26.47 ± 2.31
Prot (g/L)	6.60 ± 0.18	6.90 ± 0.07
GOT (U/L)	185.40 ± 45.56	394.30 ± 112.60
GPT (U/L)	54.60 ± 11.23	79.83 ± 14.53
Choles (mg/dL)	59.40 ± 7.51	71.63 ± 4.49
Trig (mg/dL)	104.60 ± 24.04	112.30 ± 9.07
CK (U/L)	1292.00 ± 232.40	1566.00 ± 129.10

Figure 34: VCD-animal model characterization.
Twelve-weeks female Wistar rats were injected i.p. for 15 days with 80mg/kg of VCD in sesame oil or vehicle. Animals were weighted before each injection and blood was collected after sacrifice with several parameters being measured. (A) animal weight variation during the treatment; (B) animal body mass gain during the treatment, bM-brain mass, BM-body mass; (C) Estradiol levels variation with the treatment. Data represent mean ± SEM of 5 independent samples, * $p<0.05$ when compared to control. (D) Blood marker analysis, Urea (mg/dl), GOT- glutamic oxaloacetic transaminase (U/l), GPT-glutamic-pyruvic transaminase (U/l), Creatinine (mg/dl), Cholesterol (mg/dl), Protein (U/l), Triglycerides (mg/dl), CK- creatine kinase (U/l) Data represent mean ± SEM of 4 to 6 different samples. Legend Ctrl- control animals, VCD-VCD injected animals

Moreover, VCD treatment did not result in decreased brain mass/body mass (Fig. 34B). In terms of blood analysis, we did not observe any significant difference between control and VCD-treated rats (Fig. 34D). In order to validate the model, circulating E2 levels were

measured. A decrease in E2 plasma was observed in VCD-treated animals (Fig. 34C), suggesting the eventual atresia in the follicles and a lower production of E2 by the ovaries.

4.4.4.2 Mitochondrial bioenergetics is not altered by VCD

The role of extra-ovarian mitochondria in this model was never evaluated so far. The literature only reported two studies of follicle atresia and the involvement of mitochondria in this process. VCD-induced atresia is mediated by the activation of caspase-3 in ovarian follicles, suggesting that the loss of ovarian follicles occurs through caspase-mediated apoptosis [217]. In accordance, the same group showed an increased expression of the pro apoptotic protein Bad, translocation of Bcl-x_L, augmented Bax: Bcl-x_L ratio in mitochondria and increased cytochrome *c* translocation from mitochondria to cytosol [215], confirming activation of the mitochondrial pathway for apoptosis.

The administration of VCD did not result in any alteration of mitochondrial respiration or ΔΨ parameters in glutamate-malate energized mitochondria, as well as in complex I maximal activity (Table 14, 15 and 16), which indicates that for the time-point studied no extra-ovarian mitochondrial damage was found.

Table 14: Mitochondrial oxygen consumption and maximal complex I activity in control and VCD-treated animals

Complex I		Brain	Liver
State 2 (nmol O_2/min/mg protein)	**Ctrl**	17.7 ± 2.5	16.7 ± 0.9
	VCD	15.8 ± 2.6	15.92 ± 1.3
State 3 (nmol O_2/min/mg protein)	**Ctrl**	51. 1 ± 11.3	40.9 ± 11.6
	VCD	52.2 ± 12.1	40.4 ± 10.7
State 4 (nmol O_2/min/mg protein)	**Ctrl**	37.2 ± 18.7	42. 3 ± 12.6
	VCD	38.2 ± 17.9	39.6 ± 10.7
RCR	**Ctrl**	6.2 ± 0.4	4.1 ± 0.3
	VCD	6.0 ± 0.4	3.8 ± 0.2
ADP/O	**Ctrl**	2.6 ± 0.2	2.5 ± 0.2
	VCD	2.6 ± 0.1	2.6 ± 0.1
State Oligomycin (nmol O_2/min/mg protein)	**Ctrl**	8.9 ± 1.6	11.8 ± 1.2
	VCD	10.7 ± 1.9	11.2 ± 1.2
State FCCP (nmol O_2/min/mg protein)	**Ctrl**	46.4 ± 7.1	120.2 ± 5.9
	VCD	61.7 ± 12.0	108. 0 ± 5.7
FCCP/O	**Ctrl**	5.8 ± 0.4	10.06 ± 1.0
	VCD	4.8 ± 0.2	10.3 ± 11.0

Brain (0.5 mg) and liver (1 mg) mitochondrial oxygen consumption was measured in the presence of 5 mM glutamate and 2.5 mM malate. ADP (75 nmol for brain mitochondria and 125 nmol for liver mitochondria) was added to induce state 3 respiration. The RCR was calculated as the ratio between

state 3 and state 4 respiration. The ADP/O was calculated as the number of nmol ADP phosphorylated per natom oxygen consumed during state 3. FCCP/O was calculated as the ratio between state FCCP and oligomycin respiration. Data are the mean ± SEM of 6 independent experiments. Legend: Ctrl - control animals, VCD - VCD injected animals

Table 15: Complex I maximal activity in isolated mitochondria from control and VCD-treated animals

	Ctrl	VCD
Brain	96.44±11.71	100.7±14.38
Liver	71.51± 5.9	58.76±8.3

The activity of complex I was obtained in disrupted mitochondria through the reduction of DCPIP. Activity is expressed as nmol DCPIP/min/mg protein. Data are the mean ± SEM of 6 independent experiments.

Table 16: ΔΨ measurements in control and VCD-treated animals

Complex I		Brain	Liver
Maximum Δψ	**Ctrl**	180.5 ± 2.8	231.4 ± 1.6
	VCD	176.2 ± 3.7	228.4 ± 1.3
Depolarization (-mV)	**Ctrl**	14.9 ± 2.8	25.7 ± 1.9
	VCD	15.0 ± 2.3	22.4 ± 1.1
Lag Phase (s)	**Ctrl**	64.1 ± 4.1	46.0 ± 5.1
	VCD	72.8 ± 4.3	50.8 ± 4.4

Brain (0.8mg) and liver (1mg) mitochondria were energized with 5 mM glutamate and 2.5 mM malate and the phosphorylation cycle was initiated with ADP (75 nmol for brain mitochondria and 100 nmol for liver mitochondria). Data represent mean ± SEM from six independent experiments.

4.4.4.3 An increase in brain mitochondrial hydrogen peroxide generation is observed after VCD administration

We next examined hydrogen peroxide generation by the mitochondrial respiratory chain as well as the susceptibility of brain and liver mitochondria from vehicle and VCD-treated animals to lipid peroxidation induced by ADP/Fe^{2+}. Finally, we evaluated the activity of aconitase, since its activity is decreased by the oxidative stress [266]. In this latter case, no differences within groups were observed (Fig. 35 A). Regarding ADP/Fe^{2+}-induced lipid peroxidation, no differences were found between the two groups when measuring TBARS (Fig. 35D). However hydrogen peroxide generated in brain mitochondria were significantly higher in VCD-treated animals than in control animals (from 812.7 ± 164.1 to 1,394.0 ± 209.0 in glutamate/malate-sustained respiration, from 4,668.0 ± 447.4 to 5,730.0 ± 624.2 in the presence of rotenone and from 1,4610.0 ± 2 038.0 to 2,1025.0 ± 1,900.0 pmol H_2O_2/mg protein/15min, Fig 35 B and C).

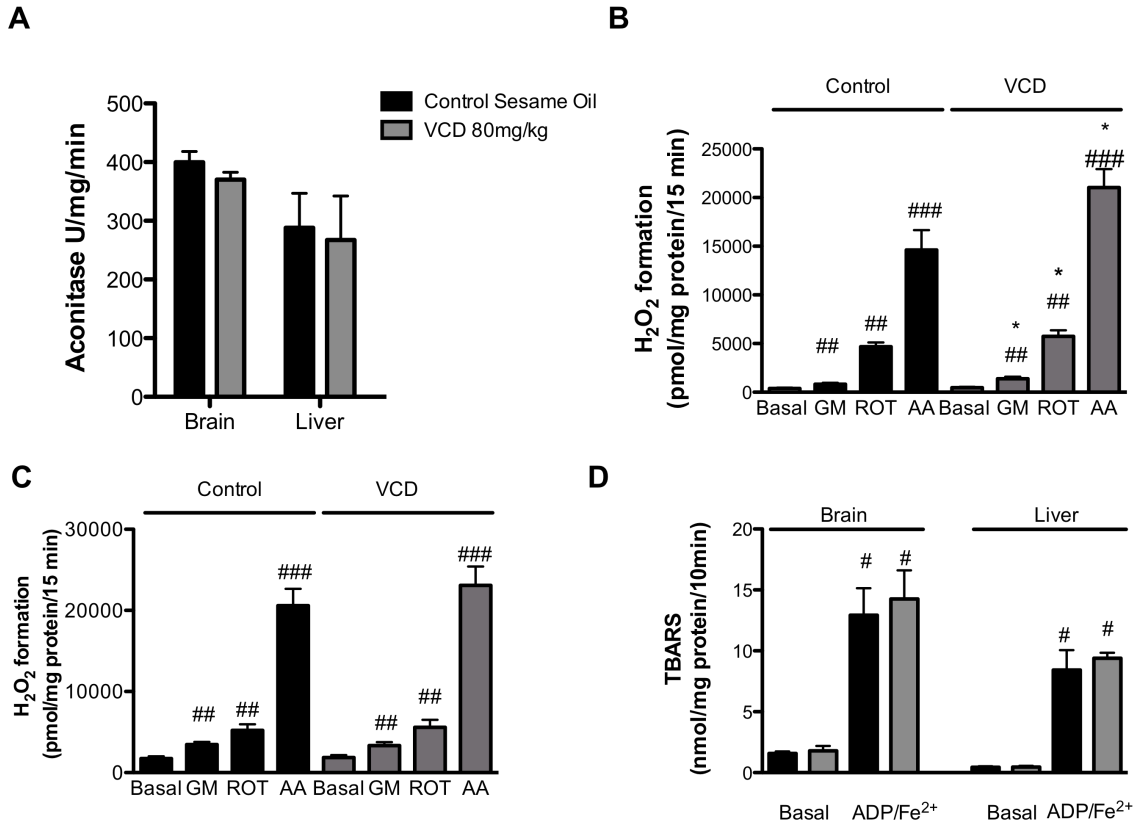

Figure 35: Effect of VCD administrations on oxidative stress.
(A) Aconitase activity was evaluated by the conversion of citrate to isocitrate through cis-aconitate. (B, C) The production of hydrogen peroxide by the mitochondrial respiratory chain was evaluated as described in the materials and methods section, (B)-brain mitochondrial preparation, (C)-liver mitochondrial fraction. (D) ADP/Fe^{2+}-induced lipid peroxidation was evaluated by TBARS colorimetric assay, as described in the material and methods section. Data represent the mean ± SEM of four to six independent experiments. Statistical significance: # $p<0.05$, ## $p<0.01$, ### $p<0.001$ compared with the respective basal levels, * $p<0.05$ compared with control animals. Legend: AA - antimycin; GM – glutamate/malate, ROT – rotenone.

After testing the toxicity of the VCD treatment in Wistar rats, a comparison of coumestrol and E2 administration on mitochondrial bioenergetics was our next experimental aim. Animals were treated with VCD as in the previous section and one week of recovery, animals were treated with vehicle or 30 µg/kg E2 or coumestrol for 24h and mitochondrial parameters were analyzed. We hypothesized that the treatment with E2 or coumestrol may increase mitochondrial bioenergetics as in the OVX model, or eventually cause some toxicity in this VCD model.

4.4.4.4 Coumestrol and E2 effects on mitochondrial bioenergetics in the VCD model

An increase in some of the mitochondrial parameters was observed. In glutamate/malate - energized mitochondria, E2 resulted in an increase in state 3 respiration in both liver and brain mitochondria. E2 also resulted in an increase in brain mitochondria state 4 respiration while an increase in the RCR from 4.9 ± 0.6 to 6.2 ± 0.7 was observed in brain mitochondria

from coumestrol-treated animals (Fig. 36). No other parameters were affected by E2 or coumestrol treatment.

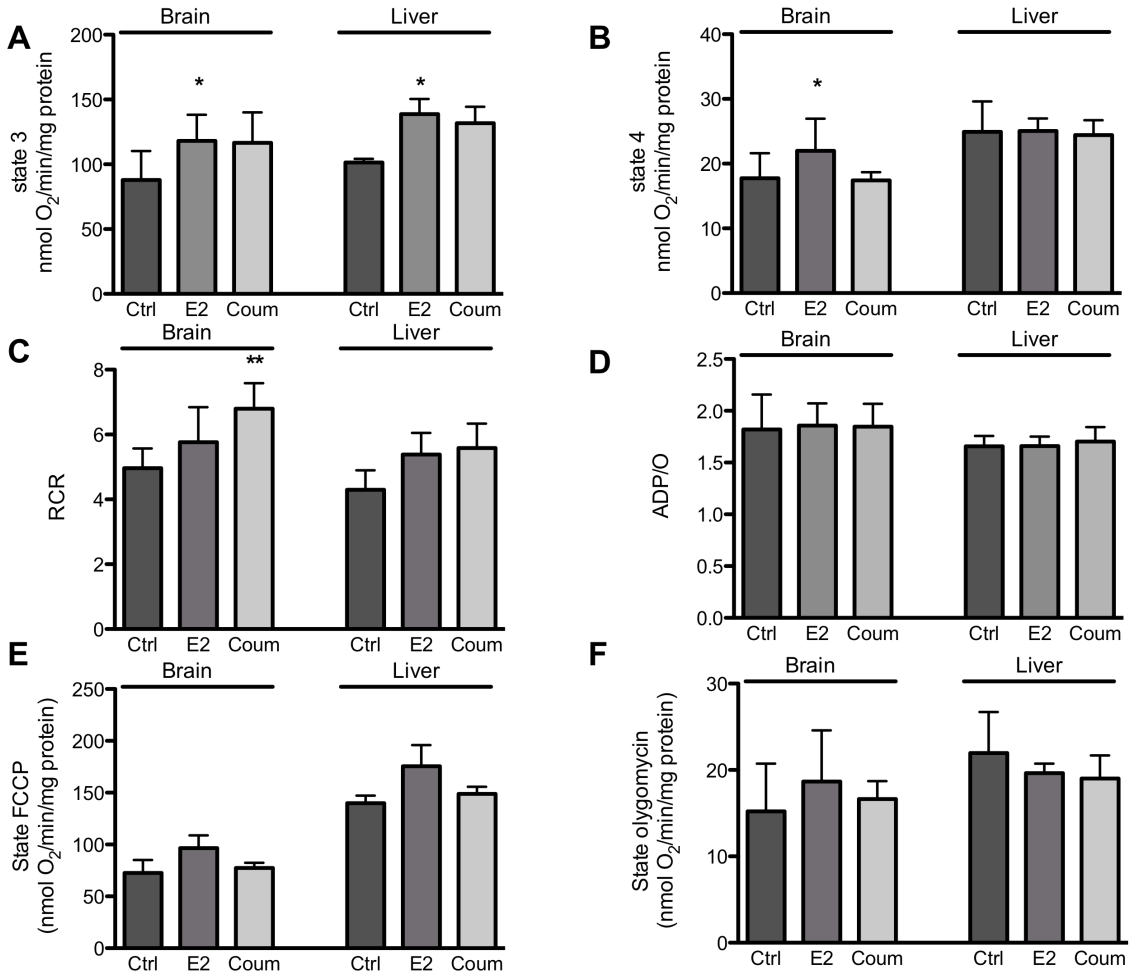

Figure 36: E2 and coumestrol effects on complex I-sustained mitochondrial oxygen consumption.
Brain (0.8 mg) and liver (1 mg) mitochondria were energized with 5mM glutamate and 2.5 mM malate and the phosphorylation cycle was initiated with ADP (75 nmol for brain mitochondria and 100 nmol for liver mitochondria). Data represent mean ± SEM from three to six independent experiments. * $p<0.05$, ** $p<0.01$ when compared with Ctrl. Legend: Ctrl - VCD-treated animals injected with vehicle only for 24h, E2 - VCD-treated animals injected with E2 for 24 h; Coum - VCD-treated animals injected with coumestrol for 24h.

These results were complemented with an observed increase caused by E2 in brain mitochondrial ΔΨ from 186.5 ± 6.3 to 198.5 ± 3.6 (-) mV (Fig. 37B). In liver mitochondria, the phosphorylative lag phase is lower in E2 animals (Fig. 37C) compared to the respective control (from 43.0 ± 3.6 to 38.3 ± 3.8 s), which is in accordance with the increase in state 3 respiration (Fig. 36C). Both of these effects were observed in complex I-sustained respiration (Fig. 36 and 37). When brain mitochondria were energized at complex II with succinate, E2 or coumestrol increased the ADP-induced depolarization from 15.4 ± 1.2 to 21.2 ± 0.7 and 19.6 ± 1.5 (-) mV, respectively. Also, the brain mitochondria RCR increased after coumestrol treatment 3.2 ± 0.2 to 3.9 ± 0.2 (Fig. 38). In liver mitochondria, the lag phase was reduced in

E2-treated animals from 23.7 ± 2.6 to 27.8 ± 2.0 seconds (Fig. 39). The results suggest that coumestrol and E2 promoted an improvement in mitochondrial function of brain and liver mitochondria from VCD-treated animals, as observed in OVX animals.

Regarding oxidative stress markers, no alterations on hydrogen peroxide generation by the respiratory chain were observed, except when generated by complex I in animals treated with VCD + E2. In terms of TBARS levels, although as we expected ADP-Fe^{2+} induced lipid peroxidation in rat brain mitochondria, E2 and coumestrol showed no protective effect (Fig. 41).

4.4.4.5 Discussion

An usual model rodent for menopause involves ovariectomy. However, this is a mechanical procedure that usually does not occur in women. The transition to menopause involves a continuous fluctuation in hormones, instead of an abrupt loss of circulating estrogens. Due to this, the use of VCD as a model of chemical induction of menopause is getting a wider acceptance. Although ovariectomy is still used in the majority of studies [214].

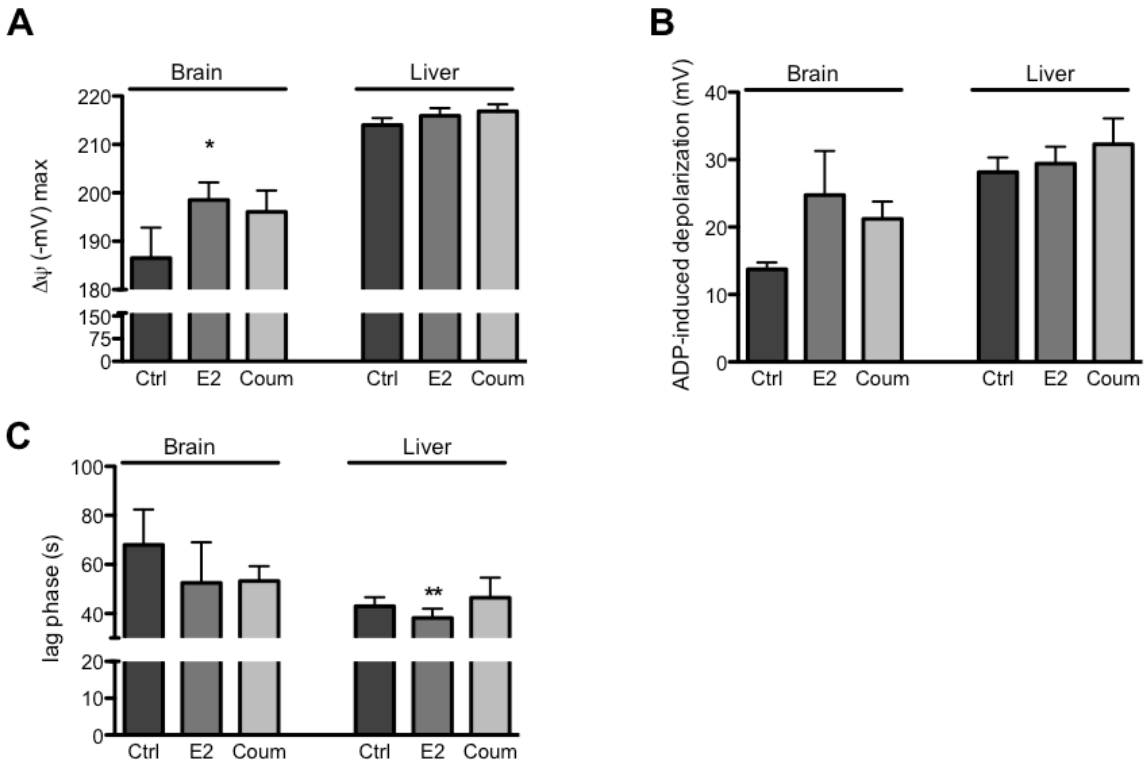

Figure 37: E2 and coumestrol effects on complex I-sustained mitochondrial ΔΨ fluctuations. (A) Maximal mitochondrial membrane potential developed (ΔΨ) after mitochondrial energization; (B) Depolarization induced by ADP addition; (C) Time elapsed during complete ADP phosphorylation (lag phase). Brain (0.8 mg) and liver (1 mg) mitochondria were energized with 5mM glutamate and 2.5ml malate and the phosphorylation cycle was initiated with ADP (75 nmol for brain mitochondria and 100 nmol for liver mitochondria). Data represent mean ± SEM from three to four independent experiments. * p<0.05, ** p<0.01 when compared with Ctrl. Legend: Ctrl- VCD-treated animals injected with vehicle for 24h, E2, VCD-treated animals injected with E2 for 24 h, Coum-VCD-treated animals injected with coumestrol for 24h.

VCD is a chemical by-product of rubber manufacturing which has been demonstrated to selectively destroy ovaries of rats and mice without producing effects in large follicles or other tissues. Unlike ovariectomy, VCD treatment preserves the period of irregular cycling and fluctuating hormone levels that precedes ovarian failure, usually diagnosed as perimenopause. Although the levels of other hormones should have been measured, we showed that E2 levels were lower in treated animals in this model (Fig. 34C).

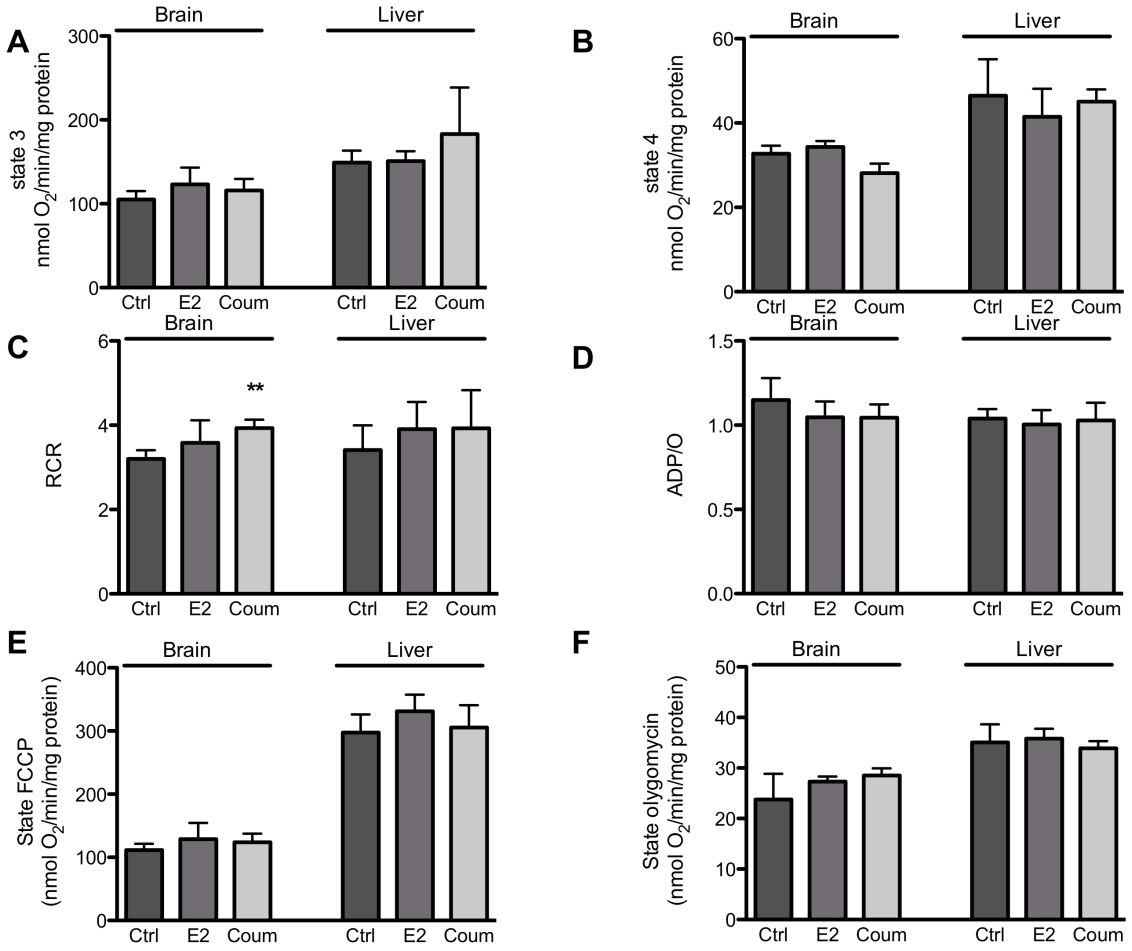

Figure 38: E2 and coumestrol effects on complex II-sustained mitochondrial oxygen consumption.
Oxygen consumption in complex II sustained mitochondrial respiration; Brain (0.8 mg) and liver (1 mg) mitochondria were energized with 5 mM succinate and the phosphorylation cycle was initiated with ADP (75 nmol for brain mitochondria and 100 nmol for liver mitochondria). Data represent mean ± SEM from three to four independent experiments. ** $p<0.01$ when compared with Ctrl. Legend: Ctrl - VCD-treated animals injected with vehicle for 24 h; E2 - VCD-treated animals injected with E2 for 24 h; Coum - VCD-treated animals injected with coumestrol for 24 h.

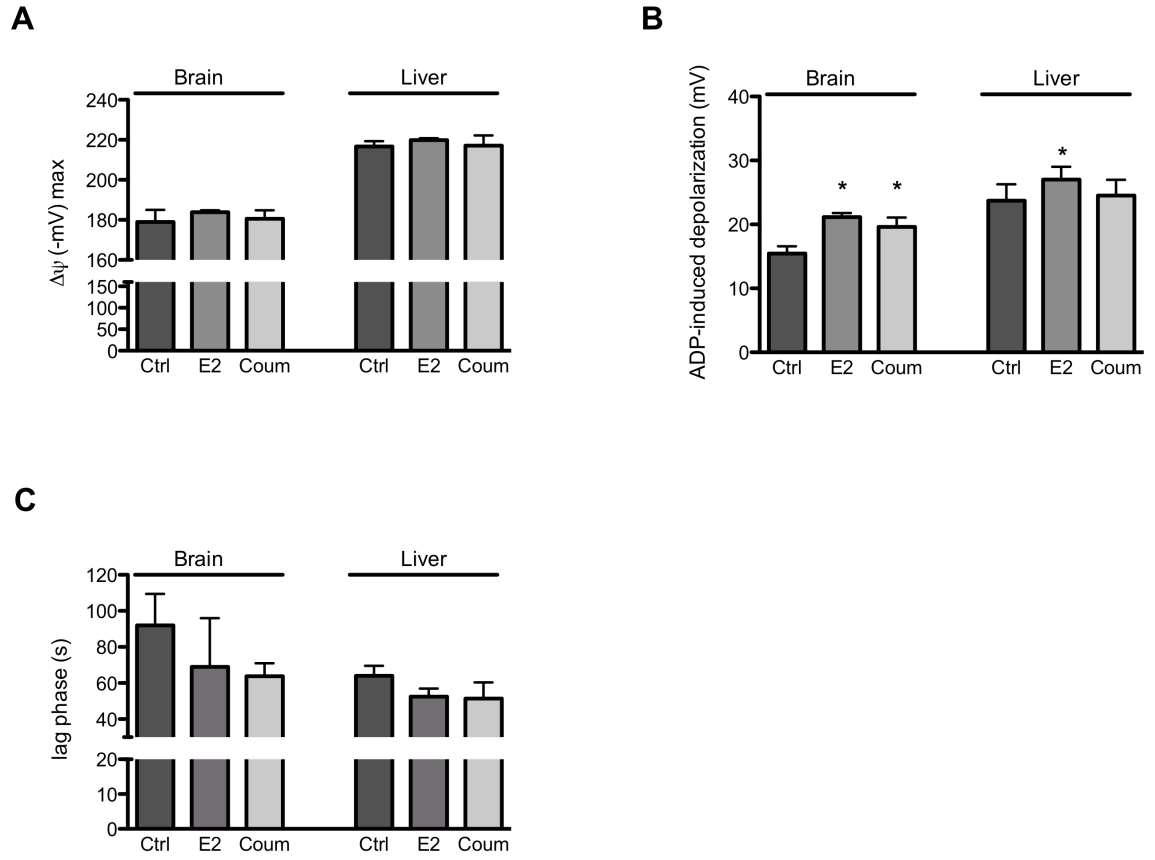

Figure 39: E2 and coumestrol effects on mitochondrial ΔΨ fluctuations.
(A) Maximal mitochondrial membrane potential developed (ΔΨ) after mitochondrial energization; (B) Depolarization induced by ADP addition, (C) Time elapsed during complete ADP phosphorylation (lag phase). Brain (0.8 mg) and liver (1 mg) mitochondria were energized with 5mM succinate and the phosphorylation cycle was initiated with ADP (75 nmol for brain mitochondria and 100 nmol for liver mitochondria). Data represent mean ± SEM from three to four independent experiments. * $p<0.05$ when compared with control. Legend: Ctrl - VCD-treated animals injected with vehicle for 24 h, E2, VCD-treated animals injected with E2 for 24 h; Coum - VCD-treated animals injected with coumestrol for 24 h.

When the experiments were performed, the kits for the measurement of FSH, LH, activins and inhibins were not available for rats. This model is particularly interesting since it is possible to choose the age of the animal for the onset of hormonal variations [218].

We initially evaluated the eventual toxicity associated with the administration of VCD in terms of blood biochemistry followed by the impact of the selected compound on hepatic and brain mitochondrial bioenergetics, something never explored before. In terms of animal mass, we did not observe any effects, except for the weight gain during the third week (Fig. 34).

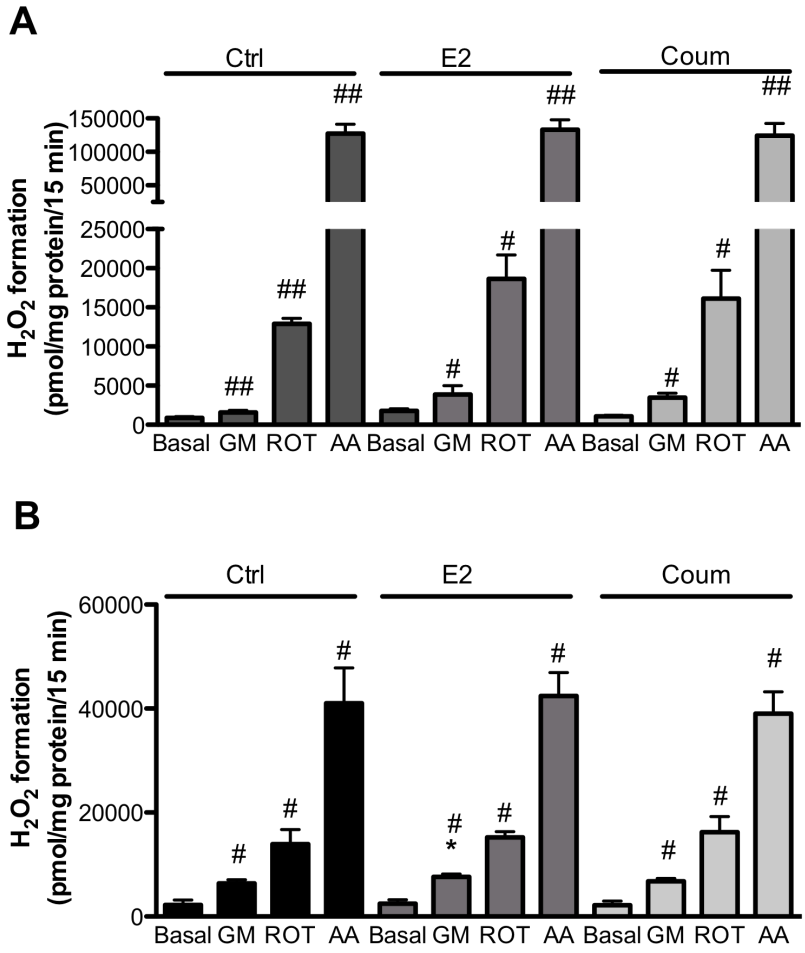

Figure 40: Effect of E2 or Coumestrol administration on mitochondrial hydrogen peroxide (H_2O_2) production.
The production of hydrogen peroxide by the mitochondrial respiratory chain was evaluated as described in the materials and methods section. Mitochondrial fractions from brain and liver of female VCD-treated rats were incubated with standard respiratory medium. Glutamate/malate (5 mM/2.5 mM) was used as substrate. Rotenone (1.0 μM) and antimycin A (0.5 μM) were used to increase H_2O_2 production. (A) Brain and (B) liver mitochondrial hydroperoxide generation in the presence of glutamate/malate, respectively. Data represent mean ± SEM from three to four independent experiments. # $p<0.05$, ## $p<0.01$ when compared with the respective basal levels, * $p<0.05$ when compared with control. Legend: Ctrl - VCD-treated animals injected with vehicle for 24h; E2 - VCD-treated animals injected with E2 for 24 h; Coum - VCD-treated animals injected with coumestrol for 24 h.

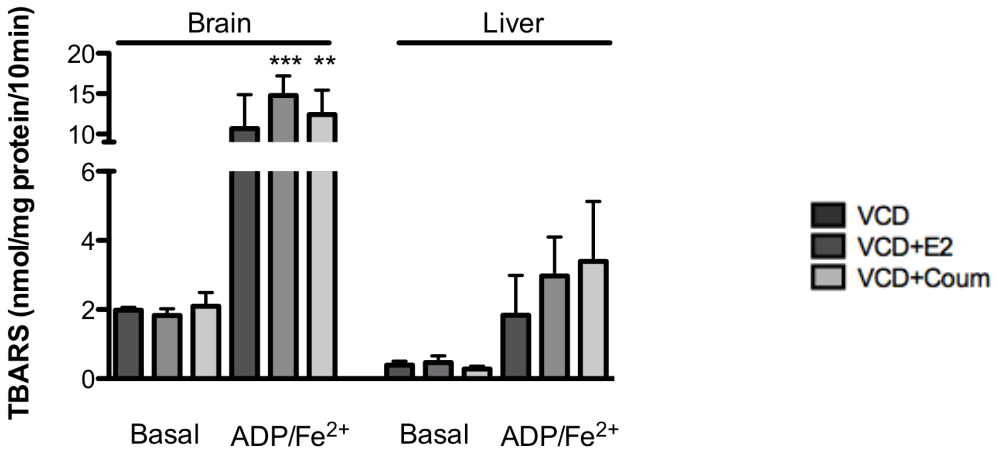

Figure 41: Effects of Coumestrol and E2 on membrane lipid peroxidation of brain and liver mitochondria induced by the pro-oxidant pair ADP/Fe^{2+}.
ADP/Fe^{2+}-induced lipid peroxidation was evaluated by the TBARS colorimetric assay as previously described in the material and methods section. The data represent the mean ± SEM of three to four independent experiments. Legend: Ctrl - VCD-treated animals injected with vehicle for 24 h; E2 - VCD-treated animals injected with E2 for 24 h; Coum - VCD-treated animals injected with coumestrol for 24 h.

Also, no VCD-induced alterations on mitochondrial bioenergetics parameters were observed. Although being a good point favouring the model, it was a suprising fact because in general, environmental pollutants as VCD, affect mitochondrial function at multiple levels [384, 385]. However, an increase in hydrogen peroxide generation by the respiratory chain was observed, which may resemble the increase in oxidative stress seen with aging and menopause [203, 204, 232]. Further experiments are needed to find the cause of this small but significant increase. Additional studies are still needed to get more insights of the VCD model. This could have been done by the measurement of other hormones that vary in perimenopause [214]. Although this was not done due to the reasons expressed before. VCD dosing can be used to modulate the magnitude of elevations in key reproductive hormones, such as FSH and dose-dependent effects of these hormones can now be investigated in animals whose hypothalamic–pituitary–ovarian axis remains essentially intact [218]. Although, we did not observe significant changes in isolated brain and liver mitochondria parameters in VCD-treated animals, it is also necessary to explore the role of aging in the moments of VCD treatment as well as the role of estrogens and how their decrease in menopause affects central and peripheral systems. One of our objectives in this section was to identify *in vivo* effects of both coumestrol and E2 that would mimic the ones found in OVX rats and previous shown by others in the ovariectomy model.

When animals were treated with coumestrol or with E2, an increase in RCR, when mitochondria respiration was supported by complex I substrate, was found. These data are in accordance with Brinton and colleagues [362], where steroid hormones were found to improve mitochondrial function, contributing to cell and tissue fitness. Steroid hormones are

molecules that control several physiological processes in the body, as different as reproductive signalling and responsive to oxidative stress [125]. Here we did not observe the antioxidant effects of E2 and coumestrol as observed by others in OVX rats for E2. For example, both E2 and P4 decreased oxidative stress generation by increasing the expression of mitochondrial antioxidant enzymes superoxide dismutase and peroxiredoxin V [380]. Moreover, in terms of respiratory chain complexes in brain mitochondria, 24 h E2 treatment resulted in increased expression of complexes I, III, and IV subunits in OVX rats [362]. In the present study, only an increase in mitochondrial RCR and state 3 were observed, which are already an indication of an improvement of mitochondrial function, a fact that was not observed *in vitro* (section 4.1.3.6).

Despite the small number of animals used in this work, we think the data obtained here have some relevance as a support to further studies using coumestrol as a safe and effective alternative to the HRT.

Concluding, the VCD model in rodents rats appears to provide an important tool, either used alone or in comparison to the well-studied OVX rat model, in order to expand our knowledge of the interaction of hormones, aging and disease risk in women across the menopausal transition.

Highlights of the present chapter:

- VCD treatment decreased E2 levels in female wistar rats.
- VCD treatment did not affect liver or brain mitochondrial bioenergetics.
- Coumestrol and E2 increased brain and liver mitochondrial bioenergetics in VCD-treated animals.

5. General Conclusions

In the context of menopause, HRT allows the delay or the prevention of several symptoms associated with this period of women's life [30, 50]. The importance of steroid hormones as modulators of mitochondrial function is well characterized. In this thesis, we aimed to select a PE which could work as a valid alternative to the conventional HRT. The ideal PE should decrease the main symptom occurring in menopausal women's, hot flashes, without further complications as an increase of breast cancer risk.

In this thesis, we aimed at selecting a PE with low toxicological effects, namely at the mitochondrial level and with good antioxidant profile.

Our initial data resulted in the selection of resveratrol and coumestrol based on their capacity to reduce mitochondrial lipid peroxidation. Resveratrol has showed later to have mitochondrial toxicity at antioxidant-relevant concentrations. Moreover, we did not observe any modulation of GLUT-1 expression at the BBB by this compound. Thus our data do not support the potential use of resveratrol as an alternative to the HRT.

The data presented in this work show that coumestrol lacks *in vitro* or *in vivo* mitochondrial toxicity. On the other hand, coumestrol increased GLUT-1 expression at the BBB, which is a potential link with the decrease of temperature variations in OVX rats. An explanation for the similarly effects in terms of GLUT-1 expression may be the resemblance of the structure of E2 and coumestrol. However, from the data obtained coumestrol appears to present several advantages over E2. Besides the lack of mitochondrial toxicity and the modulation of GLUT-1 expression at the BBB, coumestrol induces a reduced proliferation rate in comparison with E2 in breast cancer cells.

As previously said, coumestrol is not widely studied in the literature. However, recent studies have shown that coumestrol inhibits casein kinase 2 (CK2), a pro-proliferative protein that is overexpressed in several types of tumor, including breast cancer [386]. Thus, coumestrol promotes senescence in tumor cells [387]. This again shows that one of the main arguments against HRT, the increased risk of breast cancer, may be avoided through the use of coumestrol as the basis for that therapy.

In the opinion of the author, these are the two main technical contributions resulting from this thesis:

- A screening of selected PEs in various menopause-relevant biological models including one resulting from VCD administration.
- Isolation and characterization of BBB capillaries and the modulatory role of E2 and PEs.

Certainly that more studies need to be performed to confirm coumestrol as a valid alternative to HRT, following the results obtained, we believe that this work in complement with recent publications, points out several interesting features of this compound that make it suitable, either in treatment, or in the prevention of several pathologies and menopause associated-symptoms.

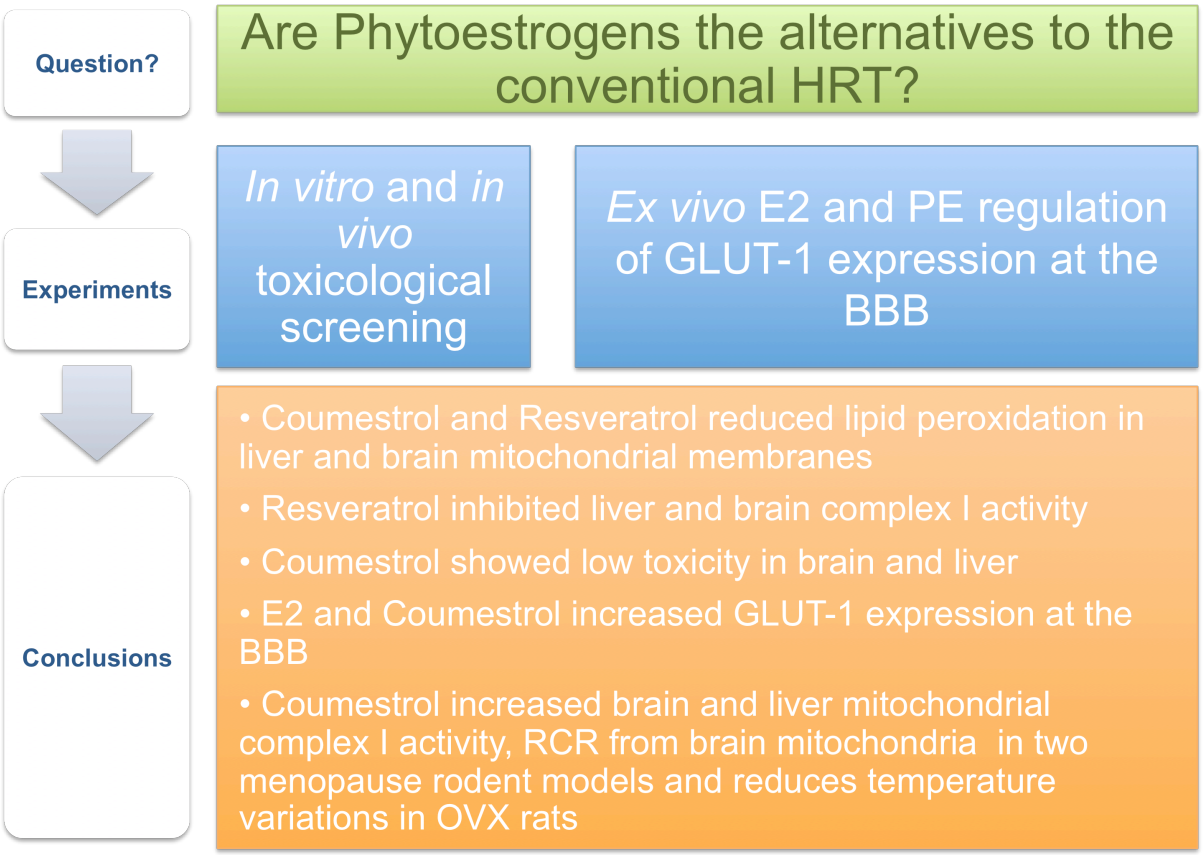

Figure 42: Summary of the main findings of this thesis.
The main conclusions of this thesis and the approaches to answer the main question of the project: Are Phytoestrogens the alternatives to the conventional HRT? The answer is that not all of the PE tested are suitable replacer, except for coumestrol which showed a large potential.

6. Future Perspectives

In the opinion of the author, this PhD thesis has clarified some cellular and mitochondrial interactions of PEs, especially in terms of their direct toxicity in brain and liver mitochondria and suggested some clues in terms of their use in HRT during menopause. However, there are still many unanswered questions.

Thus, future lines of study are proposed without any particular order:

1. Investigate the effects of coumestrol on breast cancer progression in a rat model of breast cancer following the loss of ovarian function. Even though in this thesis we showed lower proliferation of breast cells *in vitro* incubated with coumestrol in comparison with E2, its effects in breast cancer progression *in vivo* were not performed. Thus, we propose to follow the recent study of Giles *et al.* [388], although instead of studying the role of obesity, we would investigate the role of PEs in the size and characteristics of tumor in OVX rats.

2. Investigate the role of PE in the prevention of menopausal symptoms. It is generally accepted that Asian women, who consume a PE enriched diet, in comparison with Western women, have less menopausal symptoms [389]. However, these conclusions come from epidemiologic studies and several questions can be generated on these conclusions, such as: Which are the signaling pathways modified by these diets? How delayed is the menopausal symptoms onset?

3. Further analysis of the hormone levels has to be done in the VCD model, not only by measuring E2 content, but also by evaluating the levels of inibins, FSH, LH and activins. This evaluation was not performed during the experiments of this thesis due to the lack of commercially available kits.

7. References

1. Porter, T.E., et al., *Characterization of dissimilar steroid productions by granulosa, theca interna and theca externa cells during follicular maturation in the turkey (Meleagris gallopavo).* Gen Comp Endocrinol, 1991. **84**(1): p. 1-8.
2. Endo, T., et al., *Effects of estradiol and an aromatase inhibitor on progesterone production in human cultured luteal cells.* Gynecol Endocrinol, 1998. **12**(1): p. 29-34.
3. Walf, A.A., et al., *Divergent mechanisms for trophic actions of estrogens in the brain and peripheral tissues.* Brain Res, 2011. **1379**: p. 119-36.
4. Nilsson, S., et al., *Mechanisms of estrogen action.* Physiol Rev, 2001. **81**(4): p. 1535-65.
5. Moenter, S.M., et al., *Mechanisms underlying episodic gonadotropin-releasing hormone secretion.* Front Neuroendocrinol, 2003. **24**(2): p. 79-93.
6. Kumar, S., et al., *Role of estrogen receptors in pro-oxidative and anti-oxidative actions of estrogens: a perspective.* Biochim Biophys Acta, 2010. **1800**(10): p. 1127-35.
7. Welboren, W.J., et al., *Identifying estrogen receptor target genes.* Mol Oncol, 2007. **1**(2): p. 138-43.
8. Moggs, J.G. and G. Orphanides, *Estrogen receptors: orchestrators of pleiotropic cellular responses.* EMBO Rep, 2001. **2**(9): p. 775-81.
9. Gustafsson, J.A., *Novel aspects of estrogen action.* J Soc Gynecol Investig, 2000. **7**(1 Suppl): p. S8-9.
10. Vignon, F., et al., *Antiestrogenic effect of R5020, a synthetic progestin in human breast cancer cells in culture.* J Clin Endocrinol Metab, 1983. **56**(6): p. 1124-30.
11. Zheng, Z.Y. and V.C. Lin, *Anti-estrogenic effect of unliganded progesterone receptor is estrogen-selective in breast cancer cells MCF-7.* Cancer Lett, 2008. **268**(2): p. 202-11.
12. Carmeci, C., et al., *Identification of a gene (GPR30) with homology to the G-protein-coupled receptor superfamily associated with estrogen receptor expression in breast cancer.* Genomics, 1997. **45**(3): p. 607-17.
13. Filardo, E.J., et al., *Estrogen-induced activation of Erk-1 and Erk-2 requires the G protein-coupled receptor homolog, GPR30, and occurs via trans-activation of the epidermal growth factor receptor through release of HB-EGF.* Mol Endocrinol, 2000. **14**(10): p. 1649-60.
14. Pedram, A., M. Razandi, and E.R. Levin, *Nature of functional estrogen receptors at the plasma membrane.* Mol Endocrinol, 2006. **20**(9): p. 1996-2009.
15. Klinge, C.M., *Estrogenic control of mitochondrial function and biogenesis.* J Cell Biochem, 2008. **105**(6): p. 1342-51.
16. Soules, M.R., et al., *Stages of Reproductive Aging Workshop (STRAW).* J Womens Health Gend Based Med, 2001. **10**(9): p. 843-8.
17. Nelson, H.D., *Menopause.* Lancet, 2008. **371**(9614): p. 760-70.
18. Utian, W.H., *Ovarian function, therapy-oriented definition of menopause and climacteric.* Exp Gerontol, 1994. **29**(3-4): p. 245-51.
19. McKinlay, S.M., D.J. Brambilla, and J.G. Posner, *The normal menopause transition.* Maturitas, 2008. **61**(1-2): p. 4-16.
20. McKinlay, S.M., N.L. Bifano, and J.B. McKinlay, *Smoking and age at menopause in women.* Ann Intern Med, 1985. **103**(3): p. 350-6.
21. Gold, E.B., et al., *Factors associated with age at natural menopause in a multiethnic sample of midlife women.* Am J Epidemiol, 2001. **153**(9): p. 865-74.
22. Melby, M.K., M. Lock, and P. Kaufert, *Culture and symptom reporting at menopause.* Hum Reprod Update, 2005. **11**(5): p. 495-512.

23. Shifren, J.L. and N.E. Avis, *Surgical menopause: effects on psychological well-being and sexuality.* Menopause, 2007. **14**(3 Pt 2): p. 586-91.
24. Sakata, R., et al., *Effect of radiation on age at menopause among atomic bomb survivors.* Radiat Res, 2011. **176**(6): p. 787-95.
25. Knobf, M.T., *"Coming to grips" with chemotherapy-induced premature menopause.* Health Care Women Int, 2008. **29**(4): p. 384-99.
26. Burger, H.G., et al., *Cycle and hormone changes during perimenopause: the key role of ovarian function.* Menopause, 2008. **15**(4 Pt 1): p. 603-12.
27. Burger, H.G., et al., *The endocrinology of the menopausal transition: a cross-sectional study of a population-based sample.* J Clin Endocrinol Metab, 1995. **80**(12): p. 3537-45.
28. Hurwitz, J.M. and N. Santoro, *Inhibins, activins, and follistatin in the aging female and male.* Semin Reprod Med, 2004. **22**(3): p. 209-17.
29. Knight, P.G., L. Satchell, and C. Glister, *Intra-ovarian roles of activins and inhibins.* Mol Cell Endocrinol, 2012. **359**(1-2): p. 53-65.
30. *The menopausal transition.* Fertil Steril, 2008. **90**(5 Suppl): p. S61-5.
31. Oliveira, P.J., et al., *Fatty Acid Oxidation and Cardiovascular Risk during Menopause: A Mitochondrial Connection?* J Lipids, 2012. **2012**: p. 365798.
32. Nelson, H.D., et al., *Nonhormonal therapies for menopausal hot flashes: systematic review and meta-analysis.* JAMA, 2006. **295**(17): p. 2057-71.
33. Freedman, R.R., *Physiology of hot flashes.* Am J Hum Biol, 2001. **13**(4): p. 453-64.
34. Daly, E., et al., *Measuring the impact of menopausal symptoms on quality of life.* BMJ, 1993. **307**(6908): p. 836-40.
35. Shanafelt, T.D., et al., *Pathophysiology and treatment of hot flashes.* Mayo Clin Proc, 2002. **77**(11): p. 1207-18.
36. Dormire, S.L., *The potential role of glucose transport changes in hot flash physiology: a hypothesis.* Biol Res Nurs, 2009. **10**(3): p. 241-7.
37. Krychman, M.L., *Vaginal estrogens for the treatment of dyspareunia.* J Sex Med, 2011. **8**(3): p. 666-74.
38. Semmens, J.P., et al., *Effects of estrogen therapy on vaginal physiology during menopause.* Obstet Gynecol, 1985. **66**(1): p. 15-8.
39. Woods, N.F., *An overview of chronic vaginal atrophy and options for symptom management.* Nurs Womens Health, 2012. **16**(6): p. 482-94.
40. Hutter, R., et al., *Coronary artery disease in aging women: a menopause of endothelial progenitor cells?* Med Clin North Am, 2012. **96**(1): p. 93-102.
41. Crepaldi, G. and S. Maggi, *Epidemiologic link between osteoporosis and cardiovascular disease.* J Endocrinol Invest, 2009. **32**(4 Suppl): p. 2-5.
42. *Bone fractures after menopause.* Hum Reprod Update, 2010. **16**(6): p. 761-73.
43. Matthews, K.A., et al., *Influence of the perimenopause on cardiovascular risk factors and symptoms of middle-aged healthy women.* Arch Intern Med, 1994. **154**(20): p. 2349-55.
44. van Beresteijn, E.C., et al., *Perimenopausal increase in serum cholesterol: a 10-year longitudinal study.* Am J Epidemiol, 1993. **137**(4): p. 383-92.
45. Gallagher, J.C., et al., *Effect of discontinuation of estrogen, calcitriol, and the combination of both on bone density and bone markers.* J Clin Endocrinol Metab, 2002. **87**(11): p. 4914-23.
46. Hill, K., *The demography of menopause.* Maturitas, 1996. **23**(2): p. 113-27.
47. Palacios, S., *Advances in hormone replacement therapy: making the menopause manageable.* BMC Womens Health, 2008. **8**: p. 22.
48. Kopera, H. and P.A. van Keep, *Development and present state of hormone replacement therapy.* Int J Clin Pharmacol Ther Toxicol, 1991. **29**(10): p. 412-7.

49. Deady, J., *Clinical monograph: hormone replacement therapy.* J Manag Care Pharm, 2004. **10**(1): p. 33-47.
50. *Estrogen and progestogen therapy in postmenopausal women.* Fertil Steril, 2008. **90**(5 Suppl): p. S88-102.
51. Franco, H.L., et al., *Epithelial progesterone receptor exhibits pleiotropic roles in uterine development and function.* FASEB J, 2012. **26**(3): p. 1218-27.
52. Pitkin, J., et al., *Continuous combined hormone replacement therapy relieves climacteric symptoms and improves health-related quality of life in early postmenopausal women.* Menopause Int, 2007. **13**(3): p. 116-23.
53. Barrett-Connor, E., *Hormone replacement therapy.* BMJ, 1998. **317**(7156): p. 457-61.
54. Collins, P., *Clinical cardiovascular studies of hormone replacement therapy.* Am J Cardiol, 2002. **90**(1A): p. 30F-34F.
55. Lisabeth, L. and C. Bushnell, *Stroke risk in women: the role of menopause and hormone therapy.* Lancet Neurol, 2012. **11**(1): p. 82-91.
56. Palacios, S., *Current perspectives on the benefits of HRT in menopausal women.* Maturitas, 1999. **33 Suppl 1**: p. S1-13.
57. Nilsen, J., *Estradiol and neurodegenerative oxidative stress.* Front Neuroendocrinol, 2008. **29**(4): p. 463-75.
58. Gaspard, U.J., J.M. Gottal, and F.A. van den Brule, *Postmenopausal changes of lipid and glucose metabolism: a review of their main aspects.* Maturitas, 1995. **21**(3): p. 171-8.
59. Kannel, W.B., *Metabolic risk factors for coronary heart disease in women: perspective from the Framingham Study.* Am Heart J, 1987. **114**(2): p. 413-9.
60. Renoux, C., S. Dell'Aniello, and S. Suissa, *Hormone replacement therapy and the risk of venous thromboembolism: a population-based study.* J Thromb Haemost, 2010. **8**(5): p. 979-86.
61. Stevenson, J.C., *Hormone replacement therapy and cardiovascular disease revisited.* Menopause Int, 2009. **15**(2): p. 55-7.
62. Rossouw, J.E., et al., *Risks and benefits of estrogen plus progestin in healthy postmenopausal women: principal results From the Women's Health Initiative randomized controlled trial.* JAMA, 2002. **288**(3): p. 321-33.
63. Chlebowski, R.T., et al., *Breast cancer after use of estrogen plus progestin in postmenopausal women.* N Engl J Med, 2009. **360**(6): p. 573-87.
64. Dhiman, R.K. and Y.K. Chawla, *Is there a link between oestrogen therapy and gallbladder disease?* Expert Opin Drug Saf, 2006. **5**(1): p. 117-29.
65. Argento, M., P. Hoffman, and A.S. Gauchez, *Ovarian cancer detection and treatment: current situation and future prospects.* Anticancer Res, 2008. **28**(5B): p. 3135-8.
66. Mahmud, K., *Natural hormone therapy for menopause.* Gynecol Endocrinol, 2010. **26**(2): p. 81-5.
67. Patisaul, H.B. and W. Jefferson, *The pros and cons of phytoestrogens.* Front Neuroendocrinol, 2010. **31**(4): p. 400-19.
68. Coxam, V., *Phyto-oestrogens and bone health.* Proc Nutr Soc, 2008. **67**(2): p. 184-95.
69. Messina, M., *Investigating the optimal soy protein and isoflavone intakes for women: a perspective.* Womens Health (Lond Engl), 2008. **4**(4): p. 337-56.
70. Mitchell, J.H., et al., *Antioxidant efficacy of phytoestrogens in chemical and biological model systems.* Arch Biochem Biophys, 1998. **360**(1): p. 142-8.
71. Dixon, R.A., *Phytoestrogens.* Annu Rev Plant Biol, 2004. **55**: p. 225-61.

72. Bingham, S.A., et al., *Phyto-oestrogens: where are we now?* Br J Nutr, 1998. **79**(5): p. 393-406.
73. Adlercreutz, H., *Lignans and human health.* Crit Rev Clin Lab Sci, 2007. **44**(5-6): p. 483-525.
74. Clavel, T., et al., *Intestinal bacterial communities that produce active estrogen-like compounds enterodiol and enterolactone in humans.* Appl Environ Microbiol, 2005. **71**(10): p. 6077-85.
75. Jin, J.S., N. Kakiuchi, and M. Hattori, *Enantioselective oxidation of enterodiol to enterolactone by human intestinal bacteria.* Biol Pharm Bull, 2007. **30**(11): p. 2204-6.
76. Aehle, E., et al., *Lignans as food constituents with estrogen and antiestrogen activity.* Phytochemistry, 2011. **72**(18): p. 2396-405.
77. Franke, A.A., et al., *Rapid HPLC analysis of dietary phytoestrogens from legumes and from human urine.* Proc Soc Exp Biol Med, 1995. **208**(1): p. 18-26.
78. Jacob, D.A., et al., *Coumestrol antagonizes neuroendocrine actions of estrogen via the estrogen receptor alpha.* Exp Biol Med (Maywood), 2001. **226**(4): p. 301-6.
79. Walle, T., *Bioavailability of resveratrol.* Ann N Y Acad Sci, 2011. **1215**: p. 9-15.
80. Gehm, B.D., et al., *Resveratrol, a polyphenolic compound found in grapes and wine, is an agonist for the estrogen receptor.* Proc Natl Acad Sci U S A, 1997. **94**(25): p. 14138-43.
81. Setchell, K.D., *Phytoestrogens: the biochemistry, physiology, and implications for human health of soy isoflavones.* Am J Clin Nutr, 1998. **68**(6 Suppl): p. 1333S-1346S.
82. Miyazaki, K., *Novel approach for evaluation of estrogenic and anti-estrogenic activities of genistein and daidzein using B16 melanoma cells and dendricity assay.* Pigment Cell Res, 2004. **17**(4): p. 407-12.
83. Sun, Z., et al., *Concentration-dependent effects of the soy phytoestrogen genistein on the proteome of cultured cardiomyocytes.* J Proteomics, 2012. **75**(12): p. 3592-604.
84. Barone, M., et al., *Estrogens, phytoestrogens and colorectal neoproliferative lesions.* Genes Nutr, 2008. **3**(1): p. 7-13.
85. Oseni, T., et al., *Selective estrogen receptor modulators and phytoestrogens.* Planta Med, 2008. **74**(13): p. 1656-65.
86. An, J., et al., *Estrogen receptor beta-selective transcriptional activity and recruitment of coregulators by phytoestrogens.* J Biol Chem, 2001. **276**(21): p. 17808-14.
87. Lazennec, G., et al., *ER beta inhibits proliferation and invasion of breast cancer cells.* Endocrinology, 2001. **142**(9): p. 4120-30.
88. Vergara, D., et al., *Resveratrol downregulates Akt/GSK and ERK signalling pathways in OVCAR-3 ovarian cancer cells.* Mol Biosyst, 2012. **8**(4): p. 1078-87.
89. Brownson, D.M., et al., *Flavonoid effects relevant to cancer.* J Nutr, 2002. **132**(11 Suppl): p. 3482S-3489S.
90. Belcher, S.M. and A. Zsarnovszky, *Estrogenic actions in the brain: estrogen, phytoestrogens, and rapid intracellular signaling mechanisms.* J Pharmacol Exp Ther, 2001. **299**(2): p. 408-14.
91. Tinwell, H., et al., *Estradiol-type activity of coumestrol in mature and immature ovariectomized rat uterotrophic assays.* Environ Health Perspect, 2000. **108**(7): p. 631-4.
92. Bowers, J.L., et al., *Resveratrol acts as a mixed agonist/antagonist for estrogen receptors alpha and beta.* Endocrinology, 2000. **141**(10): p. 3657-67.

93. Gencel, V.B., et al., *Vascular effects of phytoestrogens and alternative menopausal hormone therapy in cardiovascular disease.* Mini Rev Med Chem, 2012. **12**(2): p. 149-74.
94. McCann, S.E., et al., *Dietary intakes of total and specific lignans are associated with clinical breast tumor characteristics.* J Nutr, 2012. **142**(1): p. 91-8.
95. Cheng, G., et al., *Isoflavone treatment for acute menopausal symptoms.* Menopause, 2007. **14**(3 Pt 1): p. 468-73.
96. Adjakly, M., et al., *Genistein and daidzein: different molecular effects on prostate cancer.* Anticancer Res, 2013. **33**(1): p. 39-44.
97. Taku, K., et al., *Extracted or synthesized soybean isoflavones reduce menopausal hot flash frequency and severity: systematic review and meta-analysis of randomized controlled trials.* Menopause, 2012.
98. Jenks, B.H., et al., *A Pilot Study on the Effects of S-Equol Compared to Soy Isoflavones on Menopausal Hot Flash Frequency and Other Menopausal Symptoms.* J Womens Health (Larchmt), 2012.
99. Bolanos-Diaz, R., et al., *Soy extracts versus hormone therapy for reduction of menopausal hot flushes: indirect comparison.* Menopause, 2011. **18**(7): p. 825-9.
100. Jacobs, A., et al., *Efficacy of isoflavones in relieving vasomotor menopausal symptoms - A systematic review.* Mol Nutr Food Res, 2009. **53**(9): p. 1084-97.
101. Castelo-Branco, C. and I. Soveral, *Phytoestrogens and bone health at different reproductive stages.* Gynecol Endocrinol, 2013. **29**(8): p. 735-43.
102. Hagen, M.K., et al., *Antioxidant characterization of soy derived products in vitro and the effect of a soy diet on peripheral markers of oxidative stress in a heart disease model.* Can J Physiol Pharmacol, 2012. **90**(8): p. 1095-103.
103. Li, J., et al., *Genistein: the potential for efficacy in rheumatoid arthritis.* Clin Rheumatol, 2013.
104. Piao, M., et al., *Inhibition of endothelial cell proliferation, in vitro angiogenesis, and the down-regulation of cell adhesion-related genes by genistein. Combined with a cDNA microarray analysis.* Endothelium, 2006. **13**(4): p. 249-66.
105. Li, Y., et al., *Epigenetic regulation of multiple tumor-related genes leads to suppression of breast tumorigenesis by dietary genistein.* PLoS One, 2013. **8**(1): p. e54369.
106. Choi, E.J. and G.H. Kim, *Antiproliferative activity of daidzein and genistein may be related to ERalpha/c-erbB-2 expression in human breast cancer cells.* Mol Med Report, 2013.
107. Ullah, M.F., et al., *Soy isoflavone genistein induces cell death in breast cancer cells through mobilization of endogenous copper ions and generation of reactive oxygen species.* Mol Nutr Food Res, 2011. **55**(4): p. 553-9.
108. van Duursen, M.B., et al., *Genistein induces breast cancer-associated aromatase and stimulates estrogen-dependent tumor cell growth in in vitro breast cancer model.* Toxicology, 2011. **289**(2-3): p. 67-73.
109. Khan, S.A., et al., *Soy isoflavone supplementation for breast cancer risk reduction: a randomized phase II trial.* Cancer Prev Res (Phila), 2012. **5**(2): p. 309-19.
110. Liu, X., et al., *Anti-breast cancer potential of daidzein in rodents.* Life Sci, 2012. **91**(11-12): p. 415-9.
111. Adlercreutz, H., *Phytoestrogens: epidemiology and a possible role in cancer protection.* Environ Health Perspect, 1995. **103 Suppl 7**: p. 103-12.
112. Guglielmini, P., A. Rubagotti, and F. Boccardo, *Serum enterolactone levels and mortality outcome in women with early breast cancer: a retrospective cohort study.* Breast Cancer Res Treat, 2012. **132**(2): p. 661-8.

113. Abarzua, S., et al., *Antiproliferative activity of lignans against the breast carcinoma cell lines MCF 7 and BT 20.* Arch Gynecol Obstet, 2012. **285**(4): p. 1145-51.
114. Notas, G., et al., *Resveratrol exerts its antiproliferative effect on HepG2 hepatocellular carcinoma cells, by inducing cell cycle arrest, and NOS activation.* Biochim Biophys Acta, 2006. **1760**(11): p. 1657-66.
115. Kim, Y.S., J.W. Sull, and H.J. Sung, *Suppressing effect of resveratrol on the migration and invasion of human metastatic lung and cervical cancer cells.* Mol Biol Rep, 2012. **39**(9): p. 8709-16.
116. Vassalle, C., A. Mercuri, and S. Maffei, *Oxidative status and cardiovascular risk in women: Keeping pink at heart.* World J Cardiol, 2009. **1**(1): p. 26-30.
117. Song, W.O., et al., *Soy isoflavones as safe functional ingredients.* J Med Food, 2007. **10**(4): p. 571-80.
118. Tissier, R., et al., *Pharmacological postconditioning with the phytoestrogen genistein.* J Mol Cell Cardiol, 2007. **42**(1): p. 79-87.
119. Carlson, S., et al., *Effects of botanical dietary supplements on cardiovascular, cognitive, and metabolic function in males and females.* Gend Med, 2008. **5 Suppl A**: p. S76-90.
120. Maulik, S.K., et al., *Genistein prevents isoproterenol-induced cardiac hypertrophy in rats.* Can J Physiol Pharmacol, 2012. **90**(8): p. 1117-25.
121. Babu, P.V., et al., *Genistein prevents hyperglycemia-induced monocyte adhesion to human aortic endothelial cells through preservation of the cAMP signaling pathway and ameliorates vascular inflammation in obese diabetic mice.* J Nutr, 2012. **142**(4): p. 724-30.
122. Hassan, H.A. and M.A. Abdel-Wahhab, *Effect of soybean oil on atherogenic metabolic risks associated with estrogen deficiency in ovariectomized rats: dietary soybean oil modulate atherogenic risks in overiectomized rats.* J Physiol Biochem, 2012. **68**(2): p. 247-53.
123. Baur, J.A., et al., *Resveratrol improves health and survival of mice on a high-calorie diet.* Nature, 2006. **444**(7117): p. 337-42.
124. Lagouge, M., et al., *Resveratrol improves mitochondrial function and protects against metabolic disease by activating SIRT1 and PGC-1alpha.* Cell, 2006. **127**(6): p. 1109-22.
125. Barron, A.M. and C.J. Pike, *Sex hormones, aging, and Alzheimer's disease.* Front Biosci (Elite Ed), 2012. **4**: p. 976-97.
126. Grimm, A., et al., *Alzheimer's disease, oestrogen and mitochondria: an ambiguous relationship.* Mol Neurobiol, 2012. **46**(1): p. 151-60.
127. Dong, Y.L., et al., *Protective effects of phytoestrogen alpha-zearalanol on beta amyloid25-35 induced oxidative damage in cultured rat hippocampal neurons.* Endocrine, 2007. **32**(2): p. 206-11.
128. Mao, Z., et al., *The anti-apoptosis effects of daidzein in the brain of D-galactose treated mice.* Molecules, 2007. **12**(7): p. 1455-70.
129. Lovekamp-Swan, T., M. Glendenning, and D.A. Schreihofer, *A high soy diet reduces programmed cell death and enhances bcl-xL expression in experimental stroke.* Neuroscience, 2007. **148**(3): p. 644-52.
130. Liu, L.X., et al., *Neuroprotective effects of genistein on dopaminergic neurons in the mice model of Parkinson's disease.* Neurosci Res, 2008. **60**(2): p. 156-61.
131. Valles, S.L., et al., *Estradiol or genistein prevent Alzheimer's disease-associated inflammation correlating with an increase PPAR gamma expression in cultured astrocytes.* Brain Res, 2010. **1312**: p. 138-44.

132. Alonso, A., et al., *Acute effects of 17 beta-estradiol and genistein on insulin sensitivity and spatial memory in aged ovariectomized female rats.* Age (Dordr), 2010. **32**(4): p. 421-34.
133. Takahashi, M., et al., *Effects of coumestrol on lipid and glucose metabolism as a farnesoid X receptor ligand.* Biochem Biophys Res Commun, 2008. **372**(3): p. 395-9.
134. Nogowski, L., *Effects of phytoestrogen-coumestrol on lipid and carbohydrate metabolism in young ovariectomized rats may be independent of its estrogenicity.* J Nutr Biochem, 1999. **10**(11): p. 664-9.
135. Wong, M.C., et al., *The cytoprotective effect of alpha-tocopherol and daidzein against d-galactosamine-induced oxidative damage in the rat liver.* Metabolism, 2007. **56**(7): p. 865-75.
136. Ae Park, S., et al., *Genistein and daidzein modulate hepatic glucose and lipid regulating enzyme activities in C57BL/KsJ-db/db mice.* Life Sci, 2006. **79**(12): p. 1207-13.
137. Grandemange, S., S. Herzig, and J.C. Martinou, *Mitochondrial dynamics and cancer.* Semin Cancer Biol, 2009. **19**(1): p. 50-6.
138. Wallace, D.C. and W. Fan, *Energetics, epigenetics, mitochondrial genetics.* Mitochondrion, 2010. **10**(1): p. 12-31.
139. Detmer, S.A. and D.C. Chan, *Functions and dysfunctions of mitochondrial dynamics.* Nat Rev Mol Cell Biol, 2007. **8**(11): p. 870-9.
140. Twig, G., et al., *Tagging and tracking individual networks within a complex mitochondrial web with photoactivatable GFP.* Am J Physiol Cell Physiol, 2006. **291**(1): p. C176-84.
141. Koopman, W.J., et al., *OXPHOS mutations and neurodegeneration.* EMBO J, 2013. **32**(1): p. 9-29.
142. Pereira, C.V., et al., *Investigating drug-induced mitochondrial toxicity: a biosensor to increase drug safety?* Curr Drug Saf, 2009. **4**(1): p. 34-54.
143. Shadel, G.S., *Mitochondrial DNA, aconitase 'wraps' it up.* Trends Biochem Sci, 2005. **30**(6): p. 294-6.
144. Vockley, J. and D.A. Whiteman, *Defects of mitochondrial beta-oxidation: a growing group of disorders.* Neuromuscul Disord, 2002. **12**(3): p. 235-46.
145. Hebert, S.L., I.R. Lanza, and K.S. Nair, *Mitochondrial DNA alterations and reduced mitochondrial function in aging.* Mech Ageing Dev, 2010. **131**(7-8): p. 451-62.
146. Zick, M., R. Rabl, and A.S. Reichert, *Cristae formation-linking ultrastructure and function of mitochondria.* Biochim Biophys Acta, 2009. **1793**(1): p. 5-19.
147. Brand, M.D. and D.G. Nicholls, *Assessing mitochondrial dysfunction in cells.* Biochem J, 2011. **435**(2): p. 297-312.
148. Nicholls, D.G., *Forty years of Mitchell's proton circuit: From little grey books to little grey cells.* Biochim Biophys Acta, 2008. **1777**(7-8): p. 550-6.
149. Brand, M.D., *The sites and topology of mitochondrial superoxide production.* Exp Gerontol, 2010. **45**(7-8): p. 466-72.
150. Sena, L.A. and N.S. Chandel, *Physiological roles of mitochondrial reactive oxygen species.* Mol Cell, 2012. **48**(2): p. 158-67.
151. Di Lisa, F., et al., *Mitochondrial pathways for ROS formation and myocardial injury: the relevance of p66(Shc) and monoamine oxidase.* Basic Res Cardiol, 2009. **104**(2): p. 131-9.
152. Adam-Vizi, V. and C. Chinopoulos, *Bioenergetics and the formation of mitochondrial reactive oxygen species.* Trends Pharmacol Sci, 2006. **27**(12): p. 639-45.

153. Solaini, G., et al., *Hypoxia and mitochondrial oxidative metabolism.* Biochim Biophys Acta, 2010. **1797**(6-7): p. 1171-7.
154. Cadenas, E., *Mitochondrial free radical production and cell signaling.* Mol Aspects Med, 2004. **25**(1-2): p. 17-26.
155. Fruehauf, J.P. and F.L. Meyskens, Jr., *Reactive oxygen species: a breath of life or death?* Clin Cancer Res, 2007. **13**(3): p. 789-94.
156. Go, Y.M., M. Orr, and D.P. Jones, *Increased nuclear thioredoxin-1 potentiates cadmium-induced cytotoxicity.* Toxicol Sci, 2013. **131**(1): p. 84-94.
157. Brandon, M., P. Baldi, and D.C. Wallace, *Mitochondrial mutations in cancer.* Oncogene, 2006. **25**(34): p. 4647-62.
158. Balaban, R.S., S. Nemoto, and T. Finkel, *Mitochondria, oxidants, and aging.* Cell, 2005. **120**(4): p. 483-95.
159. Van Houten, B., V. Woshner, and J.H. Santos, *Role of mitochondrial DNA in toxic responses to oxidative stress.* DNA Repair (Amst), 2006. **5**(2): p. 145-52.
160. Brown, G.C. and V. Borutaite, *Nitric oxide and mitochondrial respiration in the heart.* Cardiovasc Res, 2007. **75**(2): p. 283-90.
161. Poderoso, J.J., *The formation of peroxynitrite in the applied physiology of mitochondrial nitric oxide.* Arch Biochem Biophys, 2009. **484**(2): p. 214-20.
162. Bae, Y.S., et al., *Regulation of reactive oxygen species generation in cell signaling.* Mol Cells, 2011. **32**(6): p. 491-509.
163. Bolisetty, S. and E.A. Jaimes, *Mitochondria and reactive oxygen species: physiology and pathophysiology.* Int J Mol Sci, 2013. **14**(3): p. 6306-44.
164. Jezek, P. and L. Hlavata, *Mitochondria in homeostasis of reactive oxygen species in cell, tissues, and organism.* Int J Biochem Cell Biol, 2005. **37**(12): p. 2478-503.
165. Zhang, D.X. and D.D. Gutterman, *Mitochondrial reactive oxygen species-mediated signaling in endothelial cells.* Am J Physiol Heart Circ Physiol, 2007. **292**(5): p. H2023-31.
166. Giorgi, C., et al., *Ca2+ signaling, mitochondria and cell death.* Curr Mol Med, 2008. **8**(2): p. 119-30.
167. Cali, T., D. Ottolini, and M. Brini, *Mitochondrial Ca(2+) as a key regulator of mitochondrial activities.* Adv Exp Med Biol, 2012. **942**: p. 53-73.
168. Jouaville, L.S., et al., *Regulation of mitochondrial ATP synthesis by calcium: evidence for a long-term metabolic priming.* Proc Natl Acad Sci U S A, 1999. **96**(24): p. 13807-12.
169. McCormack, J.G. and R.M. Denton, *The effects of calcium ions and adenine nucleotides on the activity of pig heart 2-oxoglutarate dehydrogenase complex.* Biochem J, 1979. **180**(3): p. 533-44.
170. McCormack, J.G., A.P. Halestrap, and R.M. Denton, *Role of calcium ions in regulation of mammalian intramitochondrial metabolism.* Physiol Rev, 1990. **70**(2): p. 391-425.
171. Rizzuto, R., et al., *Mitochondria as sensors and regulators of calcium signalling.* Nat Rev Mol Cell Biol, 2012. **13**(9): p. 566-78.
172. Hunter, D.R., R.A. Haworth, and J.H. Southard, *Relationship between configuration, function, and permeability in calcium-treated mitochondria.* J Biol Chem, 1976. **251**(16): p. 5069-77.
173. Bonora, M., et al., *Role of the c subunit of the FO ATP synthase in mitochondrial permeability transition.* Cell Cycle, 2013. **12**(4): p. 674-83.
174. Krauskopf, A., et al., *Properties of the permeability transition in VDAC1(-/-) mitochondria.* Biochim Biophys Acta, 2006. **1757**(5-6): p. 590-5.
175. Siemen, D. and M. Ziemer, *What is the nature of the mitochondrial permeability transition pore and what is it not?* IUBMB Life, 2013. **65**(3): p. 255-62.

176. Tomasello, F., et al., *Outer membrane VDAC1 controls permeability transition of the inner mitochondrial membrane in cellulo during stress-induced apoptosis.* Cell Res, 2009. **19**(12): p. 1363-76.
177. Kokoszka, J.E., et al., *The ADP/ATP translocator is not essential for the mitochondrial permeability transition pore.* Nature, 2004. **427**(6973): p. 461-5.
178. Giorgio, V., et al., *Dimers of mitochondrial ATP synthase form the permeability transition pore.* Proc Natl Acad Sci U S A, 2013. **110**(15): p. 5887-92.
179. Brenner, C. and M. Moulin, *Physiological roles of the permeability transition pore.* Circ Res, 2012. **111**(9): p. 1237-47.
180. Kroemer, G., L. Galluzzi, and C. Brenner, *Mitochondrial membrane permeabilization in cell death.* Physiol Rev, 2007. **87**(1): p. 99-163.
181. Jiang, X. and X. Wang, *Cytochrome C-mediated apoptosis.* Annu Rev Biochem, 2004. **73**: p. 87-106.
182. Benard, G., et al., *Physiological diversity of mitochondrial oxidative phosphorylation.* Am J Physiol Cell Physiol, 2006. **291**(6): p. C1172-82.
183. Cocco, T., et al., *Control of OXPHOS efficiency by complex I in brain mitochondria.* Neurobiol Aging, 2009. **30**(4): p. 622-9.
184. Johnson, D.T., et al., *Tissue heterogeneity of the mammalian mitochondrial proteome.* Am J Physiol Cell Physiol, 2007. **292**(2): p. C689-97.
185. Floyd, R.A. and J.M. Carney, *Free radical damage to protein and DNA: mechanisms involved and relevant observations on brain undergoing oxidative stress.* Ann Neurol, 1992. **32 Suppl**: p. S22-7.
186. Uttara, B., et al., *Oxidative stress and neurodegenerative diseases: a review of upstream and downstream antioxidant therapeutic options.* Curr Neuropharmacol, 2009. **7**(1): p. 65-74.
187. Cunha-Oliveira, T., et al., *Mitochondrial complex I dysfunction induced by cocaine and cocaine plus morphine in brain and liver mitochondria.* Toxicol Lett, 2013.
188. Moreira, A.C., et al., *Resveratrol affects differently rat liver and brain mitochondrial bioenergetics and oxidative stress in vitro: investigation of the role of gender.* Food Chem Toxicol, 2013. **53**: p. 18-26.
189. Fernandez-Vizarra, E., et al., *Tissue-specific differences in mitochondrial activity and biogenesis.* Mitochondrion, 2011. **11**(1): p. 207-13.
190. Scatena, R., *Mitochondria and drugs.* Adv Exp Med Biol, 2012. **942**: p. 329-46.
191. Pereira, S.P., et al., *Can drug safety be predicted and animal experiments reduced by using isolated mitochondrial fractions?* Altern Lab Anim, 2009. **37**(4): p. 355-65.
192. Gerencser, A.A., et al., *Quantitative microplate-based respirometry with correction for oxygen diffusion.* Anal Chem, 2009. **81**(16): p. 6868-78.
193. Vanhees, K., et al., *Epigenetics: prenatal exposure to genistein leaves a permanent signature on the hematopoietic lineage.* FASEB J, 2011. **25**(2): p. 797-807.
194. Lehraiki, A., et al., *Genistein impairs early testosterone production in fetal mouse testis via estrogen receptor alpha.* Toxicol In Vitro, 2011. **25**(8): p. 1542-7.
195. Lee, B.J., et al., *Effects of exposure to genistein during pubertal development on the reproductive system of male mice.* J Reprod Dev, 2004. **50**(4): p. 399-409.
196. Crowell, J.A., et al., *Resveratrol-associated renal toxicity.* Toxicol Sci, 2004. **82**(2): p. 614-9.
197. Diel, P., et al., *Combinatorial effects of the phytoestrogen genistein and of estradiol in uterus and liver of female Wistar rats.* J Steroid Biochem Mol Biol, 2006. **102**(1-5): p. 60-70.
198. Marier, J.F., et al., *Metabolism and disposition of resveratrol in rats: extent of absorption, glucuronidation, and enterohepatic recirculation evidenced by a linked-rat model.* J Pharmacol Exp Ther, 2002. **302**(1): p. 369-73.

199. Salvi, M., et al., *Interaction of genistein with the mitochondrial electron transport chain results in opening of the membrane transition pore.* Biochim Biophys Acta, 2002. **1556**(2-3): p. 187-96.
200. Zheng, J. and V.D. Ramirez, *Inhibition of mitochondrial proton F0F1-ATPase/ATP synthase by polyphenolic phytochemicals.* Br J Pharmacol, 2000. **130**(5): p. 1115-23.
201. Bratic, I. and A. Trifunovic, *Mitochondrial energy metabolism and ageing.* Biochim Biophys Acta, 2010. **1797**(6-7): p. 961-7.
202. Gomez, L.A. and T.M. Hagen, *Age-related decline in mitochondrial bioenergetics: does supercomplex destabilization determine lower oxidative capacity and higher superoxide production?* Semin Cell Dev Biol, 2012. **23**(7): p. 758-67.
203. Harman, D., *Aging: a theory based on free radical and radiation chemistry.* J Gerontol, 1956. **11**(3): p. 298-300.
204. Lenaz, G., *Mitochondria and reactive oxygen species. Which role in physiology and pathology?* Adv Exp Med Biol, 2012. **942**: p. 93-136.
205. Boveris, A. and A. Navarro, *Brain mitochondrial dysfunction in aging.* IUBMB Life, 2008. **60**(5): p. 308-14.
206. Petrosillo, G., et al., *Mitochondrial dysfunction in rat brain with aging Involvement of complex I, reactive oxygen species and cardiolipin.* Neurochem Int, 2008. **53**(5): p. 126-31.
207. Petrosillo, G., et al., *Decline in cytochrome c oxidase activity in rat-brain mitochondria with aging. Role of peroxidized cardiolipin and beneficial effect of melatonin.* J Bioenerg Biomembr, 2013.
208. Lisanti, M.P., et al., *Hydrogen peroxide fuels aging, inflammation, cancer metabolism and metastasis: the seed and soil also needs "fertilizer".* Cell Cycle, 2011. **10**(15): p. 2440-9.
209. Munro, D., et al., *Low hydrogen peroxide production in mitochondria of the long-lived Arctica islandica: underlying mechanisms for slow aging.* Aging Cell, 2013.
210. Paradies, G., et al., *Changes in the mitochondrial permeability transition pore in aging and age-associated diseases.* Mech Ageing Dev, 2013. **134**(1-2): p. 1-9.
211. Lee, H.C. and Y.H. Wei, *Mitochondria and aging.* Adv Exp Med Biol, 2012. **942**: p. 311-27.
212. Wright, L.E., et al., *Comparison of skeletal effects of ovariectomy versus chemically induced ovarian failure in mice.* J Bone Miner Res, 2008. **23**(8): p. 1296-303.
213. Flaws, J.A., et al., *Destruction of preantral follicles in adult rats by 4-vinyl-1-cyclohexene diepoxide.* Reprod Toxicol, 1994. **8**(6): p. 509-14.
214. Van Kempen, T.A., T.A. Milner, and E.M. Waters, *Accelerated ovarian failure: a novel, chemically induced animal model of menopause.* Brain Res, 2011. **1379**: p. 176-87.
215. Hu, X., et al., *Expression and redistribution of cellular Bad, Bax, and Bcl-X(L) protein is associated with VCD-induced ovotoxicity in rats.* Biol Reprod, 2001. **65**(5): p. 1489-95.
216. Springer, L.N., et al., *Involvement of apoptosis in 4-vinylcyclohexene diepoxide-induced ovotoxicity in rats.* Toxicol Appl Pharmacol, 1996. **139**(2): p. 394-401.
217. Hu, X., et al., *Apoptosis induced in rats by 4-vinylcyclohexene diepoxide is associated with activation of the caspase cascades.* Biol Reprod, 2001. **65**(1): p. 87-93.
218. Frye, J.B., et al., *Modeling perimenopause in Sprague-Dawley rats by chemical manipulation of the transition to ovarian failure.* Comp Med, 2012. **62**(3): p. 193-202.

219. Lohff, J.C., et al., *Characterization of cyclicity and hormonal profile with impending ovarian failure in a novel chemical-induced mouse model of perimenopause.* Comp Med, 2005. **55**(6): p. 523-7.
220. Mayer, L.P., et al., *The follicle-deplete mouse ovary produces androgen.* Biol Reprod, 2004. **71**(1): p. 130-8.
221. Mayer, L.P., et al., *Atherosclerotic lesion development in a novel ovary-intact mouse model of perimenopause.* Arterioscler Thromb Vasc Biol, 2005. **25**(9): p. 1910-6.
222. Sanchez-Rodriguez, M.A., et al., *Menopause as risk factor for oxidative stress.* Menopause, 2012. **19**(3): p. 361-7.
223. Zitnanova, I., et al., *Oxidative stress in women with perimenopausal symptoms.* Menopause, 2011. **18**(11): p. 1249-55.
224. Randerath, K. and N. Mabon, *In vitro and in vivo (32)P-postlabeling analysis of 4-vinyl-1-cyclohexene (butadiene dimer) diepoxide-DNA adducts.* Cancer Lett, 1996. **101**(1): p. 67-72.
225. Wright, L.E., et al., *4-Vinylcyclohexene diepoxide (VCD) inhibits mammary epithelial differentiation and induces fibroadenoma formation in female Sprague Dawley rats.* Reprod Toxicol, 2011. **32**(1): p. 26-32.
226. Acosta, J.I., et al., *Transitional versus surgical menopause in a rodent model: etiology of ovarian hormone loss impacts memory and the acetylcholine system.* Endocrinology, 2009. **150**(9): p. 4248-59.
227. Tsutsui, T., et al., *Ovulation compensatory function after unilateral ovariectomy in dogs.* Reprod Domest Anim, 2012. **47 Suppl 6**: p. 43-6.
228. Lancaster, T.L., et al., *Quantitative Proteomic Analysis Reveals Novel Mitochondrial Targets of Estrogen Deficiency in the Aged Female Rat Heart.* Physiol Genomics, 2012.
229. Liou, C.M., et al., *Effects of 17beta-estradiol on cardiac apoptosis in ovariectomized rats.* Cell Biochem Funct, 2010. **28**(6): p. 521-8.
230. Lee, S.D., et al., *Cardiac Fas-dependent and mitochondria-dependent apoptosis in ovariectomized rats.* Maturitas, 2008. **61**(3): p. 268-77.
231. Tresguerres, J.A., et al., *Molecular mechanisms involved in the hormonal prevention of aging in the rat.* J Steroid Biochem Mol Biol, 2008. **108**(3-5): p. 318-26.
232. Ha, B.J., *Oxidative stress in ovariectomy menopause and role of chondroitin sulfate.* Arch Pharm Res, 2004. **27**(8): p. 867-72.
233. Brown, G.C., *Control of respiration and ATP synthesis in mammalian mitochondria and cells.* Biochem J, 1992. **284 (Pt 1)**: p. 1-13.
234. Mammucari, C. and R. Rizzuto, *Signaling pathways in mitochondrial dysfunction and aging.* Mech Ageing Dev, 2010. **131**(7-8): p. 536-43.
235. Kemper, M.F., et al., *Endogenous ovarian hormones affect mitochondrial efficiency in cerebral endothelium via distinct regulation of PGC-1 isoforms.* J Cereb Blood Flow Metab, 2013. **33**(1): p. 122-8.
236. Henderson, V.W. and R.D. Brinton, *Menopause and mitochondria: windows into estrogen effects on Alzheimer's disease risk and therapy.* Prog Brain Res, 2010. **182**: p. 77-96.
237. Tham, D.M., C.D. Gardner, and W.L. Haskell, *Clinical review 97: Potential health benefits of dietary phytoestrogens: a review of the clinical, epidemiological, and mechanistic evidence.* J Clin Endocrinol Metab, 1998. **83**(7): p. 2223-35.
238. Dykens, J.A. and Y. Will, *The significance of mitochondrial toxicity testing in drug development.* Drug Discov Today, 2007. **12**(17-18): p. 777-85.
239. Sassa, S., et al., *Drug metabolism by the human hepatoma cell, Hep G2.* Biochem Biophys Res Commun, 1987. **143**(1): p. 52-7.

240. Decaens, C., et al., *Which in vitro models could be best used to study hepatocyte polarity?* Biol Cell, 2008. **100**(7): p. 387-98.
241. Gerets, H.H., et al., *Selection of cytotoxicity markers for the screening of new chemical entities in a pharmaceutical context: a preliminary study using a multiplexing approach.* Toxicol In Vitro, 2009. **23**(2): p. 319-32.
242. Mersch-Sundermann, V., et al., *Use of a human-derived liver cell line for the detection of cytoprotective, antigenotoxic and cogenotoxic agents.* Toxicology, 2004. **198**(1-3): p. 329-40.
243. Knasmuller, S., et al., *Use of human-derived liver cell lines for the detection of environmental and dietary genotoxicants; current state of knowledge.* Toxicology, 2004. **198**(1-3): p. 315-28.
244. Dormire, S.L. and N.K. Reame, *Menopausal hot flash frequency changes in response to experimental manipulation of blood glucose.* Nurs Res, 2003. **52**(5): p. 338-43.
245. Pereira, S.P., et al., *Toxicity assessment of the herbicide metolachlor comparative effects on bacterial and mitochondrial model systems.* Toxicol In Vitro, 2009. **23**(8): p. 1585-90.
246. Moreno, A.J., et al., *Unaltered hepatic oxidative phosphorylation and mitochondrial permeability transition in wistar rats treated with nimesulide: Relevance for nimesulide toxicity characterization.* J Biochem Mol Toxicol, 2007. **21**(2): p. 53-61.
247. Moreira, P.I., et al., *Mitochondria from distinct tissues are differently affected by 17beta-estradiol and tamoxifen.* J Steroid Biochem Mol Biol, 2011. **123**(1-2): p. 8-16.
248. Moreno, A.J., et al., *Mechanism of inhibition of mitochondrial ATP synthase by 17beta-Estradiol.* J Bioenerg Biomembr, 2013. **45**(3): p. 261-70.
249. Rosenthal, R.E., et al., *Cerebral ischemia and reperfusion: prevention of brain mitochondrial injury by lidoflazine.* J Cereb Blood Flow Metab, 1987. **7**(6): p. 752-8.
250. Gornall, A.G., C.J. Bardawill, and M.M. David, *Determination of serum proteins by means of the biuret reaction.* J Biol Chem, 1949. **177**(2): p. 751-66.
251. Rasmussen, H.N. and U.F. Rasmussen, *Oxygen solubilities of media used in electrochemical respiration measurements.* Anal Biochem, 2003. **319**(1): p. 105-13.
252. Chance, B. and G.R. Williams, *Respiratory enzymes in oxidative phosphorylation. VI. The effects of adenosine diphosphate on azide-treated mitochondria.* J Biol Chem, 1956. **221**(1): p. 477-89.
253. Kamo, N., et al., *Membrane potential of mitochondria measured with an electrode sensitive to tetraphenyl phosphonium and relationship between proton electrochemical potential and phosphorylation potential in steady state.* J Membr Biol, 1979. **49**(2): p. 105-21.
254. Oliveira, P.J., et al., *Carvedilol-mediated antioxidant protection against doxorubicin-induced cardiac mitochondrial toxicity.* Toxicol Appl Pharmacol, 2004. **200**(2): p. 159-68.
255. Santos, M.S., et al., *Brain and liver mitochondria isolated from diabetic Goto-Kakizaki rats show different susceptibility to induced oxidative stress.* Diabetes Metab Res Rev, 2001. **17**(3): p. 223-30.
256. Fernandes, M.A., et al., *Tetrandrine concentrations not affecting oxidative phosphorylation protect rat liver mitochondria from oxidative stress.* Mitochondrion, 2006. **6**(4): p. 176-85.
257. Barja, G., *Mitochondrial oxygen radical generation and leak: sites of production in states 4 and 3, organ specificity, and relation to aging and longevity.* J Bioenerg Biomembr, 1999. **31**(4): p. 347-66.

258. Flohe, L. and W.A. Gunzler, *Assays of glutathione peroxidase.* Methods Enzymol, 1984. **105**: p. 114-21.
259. Santos, R.X., et al., *Food deprivation promotes oxidative imbalance in rat brain.* J Food Sci, 2009. **74**(1): p. H8-H14.
260. Cardoso, S., et al., *Doxorubicin increases the susceptibility of brain mitochondria to Ca(2+)-induced permeability transition and oxidative damage.* Free Radic Biol Med, 2008. **45**(10): p. 1395-402.
261. Long, J., et al., *Comparison of two methods for assaying complex I activity in mitochondria isolated from rat liver, brain and heart.* Life Sci, 2009. **85**(7-8): p. 276-80.
262. Welshons, W.V., et al., *Estrogenic activity of phenol red.* Mol Cell Endocrinol, 1988. **57**(3): p. 169-78.
263. Wesierska-Gadek, J., et al., *Phenol red in the culture medium strongly affects the susceptibility of human MCF-7 cells to roscovitine.* Cell Mol Biol Lett, 2007. **12**(2): p. 280-93.
264. Vichai, V. and K. Kirtikara, *Sulforhodamine B colorimetric assay for cytotoxicity screening.* Nat Protoc, 2006. **1**(3): p. 1112-6.
265. Hartz, A.M., et al., *17-beta-Estradiol: a powerful modulator of blood-brain barrier BCRP activity.* J Cereb Blood Flow Metab, 2010. **30**(10): p. 1742-55.
266. Fillebeen, C. and K. Pantopoulos, *Redox control of iron regulatory proteins.* Redox Rep, 2002. **7**(1): p. 15-22.
267. Bradford, M.M., *A rapid and sensitive method for the quantitation of microgram quantities of protein utilizing the principle of protein-dye binding.* Anal Biochem, 1976. **72**: p. 248-54.
268. Martin, H.J., F. Kornmann, and G.F. Fuhrmann, *The inhibitory effects of flavonoids and antiestrogens on the Glut1 glucose transporter in human erythrocytes.* Chem Biol Interact, 2003. **146**(3): p. 225-35.
269. Vera, J.C., et al., *Genistein is a natural inhibitor of hexose and dehydroascorbic acid transport through the glucose transporter, GLUT1.* J Biol Chem, 1996. **271**(15): p. 8719-24.
270. Adams, S.M., et al., *Soy isoflavones genistein and daidzein exert anti-apoptotic actions via a selective ER-mediated mechanism in neurons following HIV-1 Tat(1-86) exposure.* PLoS One, 2012. **7**(5): p. e37540.
271. Fan, Y., et al., *Genistein ameliorates adverse cardiac effects induced by arsenic trioxide through preventing cardiomyocytes apoptosis.* Cell Physiol Biochem, 2013. **31**(1): p. 80-91.
272. Jin, S., et al., *Daidzein induces MCF-7 breast cancer cell apoptosis via the mitochondrial pathway.* Ann Oncol, 2010. **21**(2): p. 263-8.
273. Nilsen, J. and R.D. Brinton, *Mitochondria as therapeutic targets of estrogen action in the central nervous system.* Curr Drug Targets CNS Neurol Disord, 2004. **3**(4): p. 297-313.
274. Nilsen, J. and R. Diaz Brinton, *Mechanism of estrogen-mediated neuroprotection: regulation of mitochondrial calcium and Bcl-2 expression.* Proc Natl Acad Sci U S A, 2003. **100**(5): p. 2842-7.
275. Nkandeu, D.S., et al., *In vitro changes in mitochondrial potential, aggresome formation and caspase activity by a novel 17-beta-estradiol analogue in breast adenocarcinoma cells.* Cell Biochem Funct, 2013.
276. Chen, J.Q., et al., *Mitochondrial localization of ERalpha and ERbeta in human MCF7 cells.* Am J Physiol Endocrinol Metab, 2004. **286**(6): p. E1011-22.
277. Yang, S.H., et al., *Mitochondrial localization of estrogen receptor beta.* Proc Natl Acad Sci U S A, 2004. **101**(12): p. 4130-5.

278. Silva, A.M. and P.J. Oliveira, *Evaluation of respiration with clark type electrode in isolated mitochondria and permeabilized animal cells.* Methods Mol Biol, 2012. **810**: p. 7-24.
279. Mari, M., et al., *Mitochondrial glutathione, a key survival antioxidant.* Antioxid Redox Signal, 2009. **11**(11): p. 2685-700.
280. Rahman, K., *Studies on free radicals, antioxidants, and co-factors.* Clin Interv Aging, 2007. **2**(2): p. 219-36.
281. Borras, C., et al., *Direct antioxidant and protective effect of estradiol on isolated mitochondria.* Biochim Biophys Acta, 2010. **1802**(1): p. 205-11.
282. Mobasheri, A. and M. Shakibaei, *Osteogenic effects of resveratrol in vitro: potential for the prevention and treatment of osteoporosis.* Ann N Y Acad Sci, 2013. **1290**(1): p. 59-66.
283. Saleh, M.C., B.J. Connell, and T.M. Saleh, *Resveratrol induced neuroprotection is mediated via both estrogen receptor subtypes, ERalpha and ERbeta.* Neurosci Lett, 2013. **548**: p. 217-21.
284. Durbin, S.M., et al., *Resveratrol supplementation preserves long bone mass, microstructure, and strength in hindlimb-suspended old male rats.* J Bone Miner Metab, 2013.
285. Kasiotis, K.M., et al., *Resveratrol and related stilbenes: Their anti-aging and anti-angiogenic properties.* Food Chem Toxicol, 2013.
286. Zhao, Y.N., et al., *Resveratrol improves learning and memory in normally aged mice through microRNA-CREB pathway.* Biochem Biophys Res Commun, 2013. **435**(4): p. 597-602.
287. Nonomura, S., H. Kanagawa, and A. Makimoto, *[Chemical Constituents of Polygonaceous Plants. I. Studies on the Components of Ko-J O-Kon. (Polygonum Cuspidatum Sieb. Et Zucc.)].* Yakugaku Zasshi, 1963. **83**: p. 988-90.
288. Pervaiz, S., *Resveratrol: from grapevines to mammalian biology.* FASEB J, 2003. **17**(14): p. 1975-85.
289. Fremont, L., *Biological effects of resveratrol.* Life Sci, 2000. **66**(8): p. 663-73.
290. Baur, J.A. and D.A. Sinclair, *Therapeutic potential of resveratrol: the in vivo evidence.* Nat Rev Drug Discov, 2006. **5**(6): p. 493-506.
291. Richard, J.L., *[Coronary risk factors. The French paradox].* Arch Mal Coeur Vaiss, 1987. **80 Spec No**: p. 17-21.
292. Gresele, P., et al., *Effects of resveratrol and other wine polyphenols on vascular function: an update.* J Nutr Biochem, 2011. **22**(3): p. 201-11.
293. Sebai, H., et al., *Cardioprotective effect of resveratrol on lipopolysaccharide-induced oxidative stress in rat.* Drug Chem Toxicol, 2011. **34**(2): p. 146-50.
294. Xu, X., et al., *Resveratrol attenuates doxorubicin-induced cardiomyocyte death via inhibition of p70 S6 kinase 1-mediated autophagy.* J Pharmacol Exp Ther, 2012. **341**(1): p. 183-95.
295. Wang, Q., et al., *Resveratrol protects against global cerebral ischemic injury in gerbils.* Brain Res, 2002. **958**(2): p. 439-47.
296. Dal-Pan, A., et al., *Cognitive Performances Are Selectively Enhanced during Chronic Caloric Restriction or Resveratrol Supplementation in a Primate.* PLoS One, 2011. **6**(1): p. e16581.
297. Huber, K. and G. Superti-Furga, *After the grape rush: Sirtuins as epigenetic drug targets in neurodegenerative disorders.* Bioorg Med Chem, 2011.
298. Agarwal, B. and J.A. Baur, *Resveratrol and life extension.* Ann N Y Acad Sci, 2011. **1215**(1): p. 138-43.

299. Fukui, M., H.J. Choi, and B.T. Zhu, *Mechanism for the protective effect of resveratrol against oxidative stress-induced neuronal death.* Free Radic Biol Med, 2010. **49**(5): p. 800-13.
300. Park, J.M., et al., *Role of resveratrol in FOXO1-mediated gluconeogenic gene expression in the liver.* Biochem Biophys Res Commun, 2010. **403**(3-4): p. 329-34.
301. Chan, C.C., et al., *The protective role of natural phytoalexin resveratrol on inflammation, fibrosis and regeneration in cholestatic liver injury.* Mol Nutr Food Res, 2011. **55**(12): p. 1841-9.
302. Gutierrez-Perez, A., et al., *Protective effects of resveratrol on calcium-induced oxidative stress in rat heart mitochondria.* J Bioenerg Biomembr, 2011. **43**(2): p. 101-7.
303. Valdecantos, M.P., et al., *Vitamin C, resveratrol and lipoic acid actions on isolated rat liver mitochondria: all antioxidants but different.* Redox Rep, 2010. **15**(5): p. 207-16.
304. Annabi, B., et al., *Resveratrol Targeting of Carcinogen-Induced Brain Endothelial Cell Inflammation Biomarkers MMP-9 and COX-2 is Sirt1-Independent.* Drug Target Insights, 2012. **6**: p. 1-11.
305. He, X., et al., *Resveratrol inhibits paraquat-induced oxidative stress and fibrogenic response by activating the Nrf2 pathway.* J Pharmacol Exp Ther, 2012.
306. Price, N.L., et al., *SIRT1 Is Required for AMPK Activation and the Beneficial Effects of Resveratrol on Mitochondrial Function.* Cell Metab, 2012. **15**(5): p. 675-90.
307. Leloup, C., et al., *Mitochondrial reactive oxygen species are required for hypothalamic glucose sensing.* Diabetes, 2006. **55**(7): p. 2084-90.
308. Chen, Q., et al., *Production of reactive oxygen species by mitochondria: central role of complex III.* J Biol Chem, 2003. **278**(38): p. 36027-31.
309. Moreira, P.I., et al., *Tamoxifen and estradiol interact with the flavin mononucleotide site of complex I leading to mitochondrial failure.* J Biol Chem, 2006. **281**(15): p. 10143-52.
310. Moreno, A.J., et al., *Mechanism of inhibition of mitochondrial ATP synthase by 17beta-Estradiol.* J Bioenerg Biomembr, 2012.
311. Gledhill, J.R. and J.E. Walker, *Inhibition sites in F1-ATPase from bovine heart mitochondria.* Biochem J, 2005. **386**(Pt 3): p. 591-8.
312. Gledhill, J.R., et al., *Mechanism of inhibition of bovine F1-ATPase by resveratrol and related polyphenols.* Proc Natl Acad Sci U S A, 2007. **104**(34): p. 13632-7.
313. Bickoff, E.M., et al., *Coumestrol, a new estrogen isolated from forage crops.* Science, 1957. **126**(3280): p. 969-70.
314. Carmeli, C., et al., *Glutathione precursor N-acetyl-cysteine modulates EEG synchronization in schizophrenia patients: a double-blind, randomized, placebo-controlled trial.* PLoS One, 2012. **7**(2): p. e29341.
315. Schonfeld, P. and G. Reiser, *Rotenone-like action of the branched-chain phytanic acid induces oxidative stress in mitochondria.* J Biol Chem, 2006. **281**(11): p. 7136-42.
316. Sousa, S.C., et al., *Ca2+-induced oxidative stress in brain mitochondria treated with the respiratory chain inhibitor rotenone.* FEBS Lett, 2003. **543**(1-3): p. 179-83.
317. Li, N., et al., *Mitochondrial complex I inhibitor rotenone induces apoptosis through enhancing mitochondrial reactive oxygen species production.* J Biol Chem, 2003. **278**(10): p. 8516-25.
318. Kelly, G.S., *Clinical applications of N-acetylcysteine.* Altern Med Rev, 1998. **3**(2): p. 114-27.
319. Jackson, S.E., *Hsp90: structure and function.* Top Curr Chem, 2013. **328**: p. 155-240.

320. Pratt, W.B., *The hsp90-based chaperone system: involvement in signal transduction from a variety of hormone and growth factor receptors.* Proc Soc Exp Biol Med, 1998. **217**(4): p. 420-34.
321. Beck, R., et al., *Hsp90 is cleaved by reactive oxygen species at a highly conserved N-terminal amino acid motif.* PLoS One, 2012. **7**(7): p. e40795.
322. Beck, R., et al., *Hsp90 cleavage by an oxidative stress leads to its client proteins degradation and cancer cell death.* Biochem Pharmacol, 2009. **77**(3): p. 375-83.
323. Marchese, S. and E. Silva, *Disruption of 3D MCF-12A breast cell cultures by estrogens--an in vitro model for ER-mediated changes indicative of hormonal carcinogenesis.* PLoS One, 2012. **7**(10): p. e45767.
324. Neve, R.M., et al., *A collection of breast cancer cell lines for the study of functionally distinct cancer subtypes.* Cancer Cell, 2006. **10**(6): p. 515-27.
325. Ciocca, D.R. and M.A. Fanelli, *Estrogen receptors and cell proliferation in breast cancer.* Trends Endocrinol Metab, 1997. **8**(8): p. 313-21.
326. Dang, Z.C. and C.W. Lowik, *Removal of serum factors by charcoal treatment promotes adipogenesis via a MAPK-dependent pathway.* Mol Cell Biochem, 2005. **268**(1-2): p. 159-67.
327. Delmas, D., et al., *Resveratrol as a chemopreventive agent: a promising molecule for fighting cancer.* Curr Drug Targets, 2006. **7**(4): p. 423-42.
328. Pervaiz, S. and A.L. Holme, *Resveratrol: its biologic targets and functional activity.* Antioxid Redox Signal, 2009. **11**(11): p. 2851-97.
329. Morin, C., et al., *Evidence for resveratrol-induced preservation of brain mitochondria functions after hypoxia-reoxygenation.* Drugs Exp Clin Res, 2003. **29**(5-6): p. 227-33.
330. Walle, T., *Bioavailability of resveratrol.* Ann N Y Acad Sci, 2011. **1215**(1): p. 9-15.
331. Eskes, T. and C. Haanen, *Why do women live longer than men?* Eur J Obstet Gynecol Reprod Biol, 2007. **133**(2): p. 126-33.
332. Vina, J., et al., *Females live longer than males: role of oxidative stress.* Curr Pharm Des, 2011. **17**(36): p. 3959-65.
333. Borras, C., J. Gambini, and J. Vina, *Mitochondrial oxidant generation is involved in determining why females live longer than males.* Front Biosci, 2007. **12**: p. 1008-13.
334. Guevara, R., et al., *Age and sex-related changes in rat brain mitochondrial function.* Cell Physiol Biochem, 2011. **27**(3-4): p. 201-6.
335. Borras, C., et al., *Mitochondria from females exhibit higher antioxidant gene expression and lower oxidative damage than males.* Free Radic Biol Med, 2003. **34**(5): p. 546-52.
336. Ghanim, H., et al., *A Resveratrol and Polyphenol Preparation Suppresses Oxidative and Inflammatory Stress Response to a High-Fat, High-Carbohydrate Meal.* J Clin Endocrinol Metab, 2011.
337. Kelsey, N.A., H.M. Wilkins, and D.A. Linseman, *Nutraceutical antioxidants as novel neuroprotective agents.* Molecules, 2010. **15**(11): p. 7792-814.
338. Toklu, H.Z., et al., *Resveratrol improves cardiovascular function and reduces oxidative organ damage in the renal, cardiovascular and cerebral tissues of two-kidney, one-clip hypertensive rats.* J Pharm Pharmacol, 2010. **62**(12): p. 1784-93.
339. Aftab, N., K. Likhitwitayawuid, and A. Vieira, *Comparative antioxidant activities and synergism of resveratrol and oxyresveratrol.* Nat Prod Res, 2010. **24**(18): p. 1726-33.
340. Robb, E.L., et al., *Molecular mechanisms of oxidative stress resistance induced by resveratrol: Specific and progressive induction of MnSOD.* Biochem Biophys Res Commun, 2008. **367**(2): p. 406-12.

341. Zini, R., et al., *Effects of resveratrol on the rat brain respiratory chain.* Drugs Exp Clin Res, 1999. **25**(2-3): p. 87-97.
342. Zini, R., et al., *Resveratrol-induced limitation of dysfunction of mitochondria isolated from rat brain in an anoxia-reoxygenation model.* Life Sci, 2002. **71**(26): p. 3091-108.
343. Dykens, J.A., et al., *In vitro assessment of mitochondrial dysfunction and cytotoxicity of nefazodone, trazodone, and buspirone.* Toxicol Sci, 2008. **103**(2): p. 335-45.
344. Hynes, J., et al., *A high-throughput dual parameter assay for assessing drug-induced mitochondrial dysfunction provides additional predictivity over two established mitochondrial toxicity assays.* Toxicol In Vitro, 2013. **27**(2): p. 560-9.
345. Swiss, R. and Y. Will, *Assessment of mitochondrial toxicity in HepG2 cells cultured in high-glucose- or galactose-containing media.* Curr Protoc Toxicol, 2011. **Chapter 2**: p. Unit2 20.
346. Alboni, S., et al., *N-acetyl-cysteine prevents toxic oxidative effects induced by IFN-alpha in human neurons.* Int J Neuropsychopharmacol, 2013. **16**(8): p. 1849-65.
347. Zhou, C.F., et al., *N-acetylcysteine attenuates subcutaneous administration of bleomycin-induced skin fibrosis and oxidative stress in a mouse model of scleroderma.* Clin Exp Dermatol, 2013. **38**(4): p. 403-9.
348. Pratt, W.B., et al., *Proposal for a role of the Hsp90/Hsp70-based chaperone machinery in making triage decisions when proteins undergo oxidative and toxic damage.* Exp Biol Med (Maywood), 2010. **235**(3): p. 278-89.
349. Lee, Y.H., et al., *Coumestrol induces senescence through protein kinase CKII inhibition-mediated reactive oxygen species production in human breast cancer and colon cancer cells.* Food Chem, 2013. **141**(1): p. 381-8.
350. Thurston, R.C., et al., *Improving the performance of physiologic hot flash measures with support vector machines.* Psychophysiology, 2009. **46**(2): p. 285-92.
351. Andrikoula, M. and G. Prelevic, *Menopausal hot flushes revisited.* Climacteric, 2009. **12**(1): p. 3-15.
352. Rahimy, M.H., N. Bodor, and J.W. Simpkins, *Effects of a brain-enhanced estrogen delivery system on tail-skin temperature of the rat: implications for menopausal hot flush.* Maturitas, 1991. **13**(1): p. 51-63.
353. Shi, J. and J.W. Simpkins, *17 beta-Estradiol modulation of glucose transporter 1 expression in blood-brain barrier.* Am J Physiol, 1997. **272**(6 Pt 1): p. E1016-22.
354. Shi, J., Y.Q. Zhang, and J.W. Simpkins, *Effects of 17beta-estradiol on glucose transporter 1 expression and endothelial cell survival following focal ischemia in the rats.* Exp Brain Res, 1997. **117**(2): p. 200-6.
355. Peters, A., et al., *The selfish brain: competition for energy resources.* Neurosci Biobehav Rev, 2004. **28**(2): p. 143-80.
356. Boado, R.J. and W.M. Pardridge, *The brain-type glucose transporter mRNA is specifically expressed at the blood-brain barrier.* Biochem Biophys Res Commun, 1990. **166**(1): p. 174-9.
357. Pardridge, W.M., R.J. Boado, and C.R. Farrell, *Brain-type glucose transporter (GLUT-1) is selectively localized to the blood-brain barrier. Studies with quantitative western blotting and in situ hybridization.* J Biol Chem, 1990. **265**(29): p. 18035-40.
358. Farrell, C.L. and W.M. Pardridge, *Blood-brain barrier glucose transporter is asymmetrically distributed on brain capillary endothelial lumenal and ablumenal membranes: an electron microscopic immunogold study.* Proc Natl Acad Sci U S A, 1991. **88**(13): p. 5779-83.
359. Ratka, A., *Menopausal hot flashes and development of cognitive impairment.* Ann N Y Acad Sci, 2005. **1052**: p. 11-26.

360. Simpson, I.A., et al., *Glucose transporter asymmetries in the bovine blood-brain barrier.* J Biol Chem, 2001. **276**(16): p. 12725-9.
361. Devraj, K., et al., *GLUT-1 glucose transporters in the blood-brain barrier: differential phosphorylation.* J Neurosci Res, 2011. **89**(12): p. 1913-25.
362. Irwin, R.W., et al., *Selective oestrogen receptor modulators differentially potentiate brain mitochondrial function.* J Neuroendocrinol, 2012. **24**(1): p. 236-48.
363. Dormire, S. and C. Howharn, *The effect of dietary intake on hot flashes in menopausal women.* J Obstet Gynecol Neonatal Nurs, 2007. **36**(3): p. 255-62.
364. Hedelin, M., et al., *Dietary phytoestrogens are not associated with risk of overall breast cancer but diets rich in coumestrol are inversely associated with risk of estrogen receptor and progesterone receptor negative breast tumors in Swedish women.* J Nutr, 2008. **138**(5): p. 938-45.
365. Magee, P.J., H. McGlynn, and I.R. Rowland, *Differential effects of isoflavones and lignans on invasiveness of MDA-MB-231 breast cancer cells in vitro.* Cancer Lett, 2004. **208**(1): p. 35-41.
366. Blok, J., et al., *Insulin-induced translocation of glucose transporters from post-Golgi compartments to the plasma membrane of 3T3-L1 adipocytes.* J Cell Biol, 1988. **106**(1): p. 69-76.
367. Klip, A. and M.R. Paquet, *Glucose transport and glucose transporters in muscle and their metabolic regulation.* Diabetes Care, 1990. **13**(3): p. 228-43.
368. Hartz, A.M., et al., *Estrogen receptor beta signaling through phosphatase and tensin homolog/phosphoinositide 3-kinase/Akt/glycogen synthase kinase 3 down-regulates blood-brain barrier breast cancer resistance protein.* J Pharmacol Exp Ther, 2010. **334**(2): p. 467-76.
369. Welch, R.D. and J. Gorski, *Regulation of glucose transporters by estradiol in the immature rat uterus.* Endocrinology, 1999. **140**(8): p. 3602-8.
370. Behrooz, A. and F. Ismail-Beigi, *Dual control of glut1 glucose transporter gene expression by hypoxia and by inhibition of oxidative phosphorylation.* J Biol Chem, 1997. **272**(9): p. 5555-62.
371. Ososki, A.L. and E.J. Kennelly, *Phytoestrogens: a review of the present state of research.* Phytother Res, 2003. **17**(8): p. 845-69.
372. Nilsen, J., et al., *Estradiol in vivo regulation of brain mitochondrial proteome.* J Neurosci, 2007. **27**(51): p. 14069-77.
373. Robb, E.L. and J.A. Stuart, *Multiple Phytoestrogens Inhibit Cell Growth and Confer Cytoprotection By Inducing Manganese Superoxide Dismutase Expression.* Phytother Res, 2013.
374. Diaz Brinton, R., *Minireview: translational animal models of human menopause: challenges and emerging opportunities.* Endocrinology, 2012. **153**(8): p. 3571-8.
375. Gordon, C.J., E. Puckett, and B. Padnos, *Rat tail skin temperature monitored noninvasively by radiotelemetry: characterization by examination of vasomotor responses to thermomodulatory agents.* J Pharmacol Toxicol Methods, 2002. **47**(2): p. 107-14.
376. Williams, H., P.A. Dacks, and N.E. Rance, *An improved method for recording tail skin temperature in the rat reveals changes during the estrous cycle and effects of ovarian steroids.* Endocrinology, 2010. **151**(11): p. 5389-94.
377. Berendsen, H.H. and H.J. Kloosterboer, *Oestradiol and mirtazapine restore the disturbed tail-temperature of oestrogen-deficient rats.* Eur J Pharmacol, 2003. **482**(1-3): p. 329-33.
378. Cosmi, S., et al., *Simultaneous telemetric monitoring of tail-skin and core body temperature in a rat model of thermoregulatory dysfunction.* J Neurosci Methods, 2009. **178**(2): p. 270-5.

379. Opas, E.E., et al., *Rat tail skin temperature regulation by estrogen, phytoestrogens and tamoxifen.* Maturitas, 2004. **48**(4): p. 463-71.
380. Irwin, R.W., et al., *Progesterone and estrogen regulate oxidative metabolism in brain mitochondria.* Endocrinology, 2008. **149**(6): p. 3167-75.
381. La Colla, A., A. Vasconsuelo, and R. Boland, *Estradiol exerts antiapoptotic effects in skeletal myoblasts via mitochondrial PTP and MnSOD.* J Endocrinol, 2013. **216**(3): p. 331-41.
382. Solakidi, S., A.M. Psarra, and C.E. Sekeris, *Differential subcellular distribution of estrogen receptor isoforms: localization of ERalpha in the nucleoli and ERbeta in the mitochondria of human osteosarcoma SaOS-2 and hepatocarcinoma HepG2 cell lines.* Biochim Biophys Acta, 2005. **1745**(3): p. 382-92.
383. Mittelman-Smith, M.A., et al., *Role for kisspeptin/neurokinin B/dynorphin (KNDy) neurons in cutaneous vasodilatation and the estrogen modulation of body temperature.* Proc Natl Acad Sci U S A, 2012. **109**(48): p. 19846-51.
384. Duarte, F.V., et al., *Exposure to dibenzofuran affects lung mitochondrial function in vitro.* Toxicol Mech Methods, 2011. **21**(8): p. 571-6.
385. Mota, P.C., et al., *Differential effects of p,p'-DDE on testis and liver mitochondria: implications for reproductive toxicology.* Reprod Toxicol, 2011. **31**(1): p. 80-5.
386. Tapia, J.C., et al., *Casein kinase 2 (CK2) increases survivin expression via enhanced beta-catenin-T cell factor/lymphoid enhancer binding factor-dependent transcription.* Proc Natl Acad Sci U S A, 2006. **103**(41): p. 15079-84.
387. Liu, S., et al., *Coumestrol from the national cancer Institute's natural product library is a novel inhibitor of protein kinase CK2.* BMC Pharmacol Toxicol, 2013. **14**(1): p. 36.
388. Giles, E.D., et al., *Obesity and overfeeding affecting both tumor and systemic metabolism activates the progesterone receptor to contribute to postmenopausal breast cancer.* Cancer Res, 2012. **72**(24): p. 6490-501.
389. Reed, S.D., et al., *Premenopausal vasomotor symptoms in an ethnically diverse population.* Menopause, 2013.